Torbjørn Vegard Løkken

Comparison of Hygrometers for Monitoring of Water Vapour in Natural Gas

Thesis for the degree of Philosophiae Doctor

Trondheim, January 2015

Norwegian University of Science and Technology
Faculty of Natural Sciences and Technology
Department of Chemistry

NTNU – Trondheim
Norwegian University of
Science and Technology

NTNU
Norwegian University of Science and Technology

Thesis for the degree of Philosophiae Doctor

Faculty of Natural Sciences and Technology
Department of Chemistry

ISBN 978-82-326-0712-9 (printed ver.)
ISBN 978-82-326-0713-6 (electronic ver.)
ISSN 1503-8181

Doctoral theses at NTNU, 2015:21

Printed by NTNU-trykk

Summary

To be able to maintain a safe, regular and economic production and transportation of natural gases, it is crucial to be able to accurately quantify the water vapour concentration in the gas. Underestimation of the water vapour concentration will increase the risk of undesirable corrosion and gas hydrate formation. The importance of water vapour measurements in various industries has inspired the development of many measuring techniques during the last 50 years. The high adsorptivity of water and its abundance in the atmosphere are major reasons why trace analysis of gaseous water is challenging. Traditional thermodynamic models also have demonstrated their insufficiency when it comes to calculations involving phase distribution of water and other polar components.

Despite some scientific papers on the subject of water vapour measurements in gases, there is a limited amount of information dealing with the specific measuring challenges for the natural gas industry. These challenges are high pressure sampling, potential presence of liquids and particles, interferences from both the hydrocarbon components and traces of production chemicals.

In this work various techniques for monitoring of water vapour in gases, relevant for the natural gas industry, were compared. Through laboratory experiments parameters such as accuracy, stability, speed of response and influence from polar production chemicals have been compared for the techniques. To perform these experiments a test rig for generation of water vapour and vaporous trace chemicals in gas was established. The water vapour concentration was varied between 20 and 120 parts per million (μmol/mol) during the experiments.

Additionally results from the test rig and chosen reference techniques have been used for the generation of equilibrium data for water in methane and natural gas. A thermodynamic model, the Cubic Plus Association Equation of state (CPA EoS), optimised for accurate calculations on water and other polar compounds, was validated with these data.

The experiments clearly showed that the various measuring techniques behave differently with respect to the parameters studied. Some of the parameters seem to be closely connected to sorption phenomena and equilibrium conditions for water. This indicates that miniaturised sensors at elevated temperatures or non-equilibrium techniques will be advantageous for general performance of the hygrometers. During exposure to methanol or ethylene glycol, step changes, upward drift and downward drift were observed for some of the tested techniques. Exposure to higher parts per million concentration levels of methanol interfered with some of the techniques. Low parts per million concentration levels of methanol did not exhibit any significant effects. Ethylene glycol exhibited effects on some of the techniques even at parts per billion concentration levels.

In general the results from this work demonstrate the need for careful evaluation of the individual moisture monitoring application, before choosing a measuring technique. This evaluation should be made with special attention to the presence of polar chemicals. A well-considered strategy for quality control of the moisture monitoring is of utmost importance to establish a moisture monitoring system with high accuracy. This is regardless of the chosen measuring technique.

Contents

Acknowledgements

The work presented in this doctoral thesis was carried out at the Department of Chemistry at the Norwegian University of Science and Technology (NTNU) between 2005 and 2013. Financial support has been provided from Gassco ASA and Statoil ASA, and is gratefully acknowledged.

I would like to thank my supervisors, Dr Rudolf Schmid and Prof. Arne Olav Fredheim, playing crucial roles in guiding me steadily through the various phases of the PhD project.

Many colleagues at Statoils research centre have played their roles as discussion partners and motivators. Especially I would like to thank Dr Nina Aas for always believing in me, motivating me and helping me through some tough periods in my journey. Trond Kirkerød, Gas Solutions AS, has also been an important support during the PhD, with his extreme enthusiasm during discussions within the field of analysis, sampling and moisture measurements in special.

I would like to thank Trine, my supporting wife, and Vilja, Tiril and Vegard, my three children, who mean everything to me. Without their encouragement and patience I would never be able to finish this work. Attention to my children's daily activities has been important for my energy situation and gave me positive recreation and inspiration when needed.

Finally I would like to thank all my sporty friends, especially Finn, Geir and Lars, for keeping my endorphin production stable and high, through frequent training sessions and liberating discussions about everything else than moisture measurements.

List of papers

The thesis is based on the following four published papers:

I. **Løkken, T.V.**, 2012. Comparison of hygrometers for monitoring of water vapour in natural gas. Journal of Natural Gas Science and Engineering 6, 24-36.

II. **Løkken, T.V.**, 2012. Water vapour monitoring in natural gas in the presence of methanol. Journal of Natural Gas Science and Engineering 7, 7-15.

III. **Løkken, T.V.**, 2013. Water vapour measurements in natural gas in the presence of ethylene glycol. Journal of Natural Gas Science and Engineering 12, 13-21.

IV. **Løkken, T.V.**, Bersås, A., Christensen, K.O., Nygaard, C.F., Solbraa, E., 2008. Water content of high pressure natural gas: data, prediction and experience from field. International Gas Research Conference. Curran Associates Inc., Paris.

Author contribution: I am the main author of this conference paper. I made major contributions to the experimental part of the work, preparation of experimental results and the writing of the paper.

Nomenclature

Abbreviations

AC	alternating current
CaC_2-GC	hygrometer based on a calcium carbide reactor and gas chromatographic analysis
CPA	Cubic-Plus-Association, an equation of state
DEG	diethylene glycol
EoS	equation of state
LED	light emitting diode
LNG	liquefied natural gas
m/z	molecular mass to charge ratio of an ion, a term used in mass spectrometry
MEG	(mono) ethylene glycol
NGL	natural gas liquids
NIST	National Institute of Standards and Technology
NPL	National Physical Laboratory
PR	Peng-Robinson
QCM	quartz crystal microbalance
SRK	Soave Redlich Kwong
TD-GC/MS	thermal desorption combined with gas chromatographic separation and mass spectrometric detection.
TEG	triethylene glycol
TREG	tetraethylene glycol
UKAS	United Kingdom Accreditation Service

List of symbols

α	significance level
A_c	area of parallel conducting plates
A_p	piezoelectric active surface area
C	capacitance
C_m	constant dependent on type of piezoelectric crystal
c_w	concentration (µmol/mol)
ε	permittivity of dielectric
ε_0	permittivity of vacuum = 8.85×10^{-12} F/m
Δf	change of crystal resonance frequency
Δm	mass change
d	distance between parallel conducting plates
$e_i(T_K)$	saturation pressure (hectopascal)
f_0	fundamental resonance frequency
K	dielectric constant of dielectric material
μ	shear modulus of quartz ($2{,}947 \times 10^{11}$ g/(cm s^2))
n	number of measurements
n_h	order of harmonic

ρ	density of quartz
TC	temperature (°C)
TK	temperature (K)

1 Introduction

1.1 Background

Accurate determination of water vapour, often referred to as moisture, is crucial for maintaining a stable and safe processing and transport of natural gas. Underestimated moisture concentration in the natural gas can lead to condensation of liquid water in process equipment or pipelines. Liquids can reduce the volumetric capacity of the system, increase the pipeline pressure drop and interfere with or damage process equipment (Gandhidasan, 2003). When combined with hydrogen sulphide and carbon dioxide, condensed water will increase the corrosion potential (Mychajliw, 2002). Accurate moisture monitoring is also important to avoid the formation of gas hydrates (Jamieson and Sikkenga, 1986). Gas hydrates, having a consistency similar to ice, are being formed from water and low molecular weight compounds in natural gases (e.g. methane) at certain temperature and pressure conditions (Sloan, 2003; Sloan and Koh, 2007). The hydrate will deposit and build up on solid surfaces, and can plug valves and equipment, resulting in loss of production or obstructed transportation of natural gas. In extreme cases the hydrate can totally block the gas flow of a pipeline (Manning and Wood, 1993). Such situations are highly undesirable as the loss of production is very expensive and the removal of a hydrate plug could be a hazardous operation. To prevent operational problems, restrictions are imposed on the gas quality, such as moisture concentration limits, frequently expressed as a “water dew point”. To meet the restrictions the natural gas has to be dehydrated by means of some kind of selective and economically method.

Even though analysis of moisture in various gases has been performed for more than 50 years, this is still regarded as one of the most challenging type of trace gas analyses. One important reason for this is the high polarity of water making it extremely adsorptive. Thus surfaces regarded as dry are usually coated with a thin film of moisture (Carr-Brion, 1986; Knight and Weiss, 1962). The abundance of water in the atmosphere also makes trace analysis challenging, with high potential for background moisture interference.

Trace moisture measurements are important in many disciplines and instrumentation or measuring techniques are often tailor made for these disciplines. As a consequence moisture measurements excellently fitted for the semiconductor industry do not necessarily fit the natural gas industry at all. In the literature there already exist a few review articles and books on the subject of moisture measurements in gases (Carr-Brion, 1986; Funke et al., 2003; McAndrew and Boucheron, 1992; McAndrew, 1997; Wiederhold, 1997a), but these are not dealing with the special challenges for the natural gas industry. These challenges are for instance high pressure sampling (could be more than 200 bar), numerous potential

interferences from the hydrocarbon components, traces of production chemicals (e.g. glycols and alcohols), mists or liquids and particles (Lurvey, 1977).

1.2 Use of chemicals in the natural gas industry

Chemical and physical changes, during processing and transportation of the hydrocarbon fluids, generate a variety of production chemistry issues (Kelland, 2009). As the fluids undergo significant pressure changes, temperature changes and considerable agitation, both predictable and unpredictable changes in states will occur. This will have impacts on the efficiency of the overall operation. Some of the major production chemistry issues are various fouling phenomena (e.g. scale and gas hydrates), separation challenges (e.g. foaming) and corrosion related issues. Even though several nonchemical techniques, such as heating and insulation, can prevent or solve many problems, the use of chemicals is often essential for an effective operation.

Methanol is a popular hydrate inhibitor in addition to being used for dehydration, removal of hydrogen sulphide and carbon dioxide and for recovery of heavy hydrocarbons (Esteban et al., 2000; Kohl and Nielsen, 1997). The higher vapour pressure of methanol, compared to many other chemicals used in processing hydrocarbons, can lead to significant concentrations of methanol in the natural gas. In the case of continuous use of methanol the natural gas will always contain some methanol, the concentration being dependent on the process conditions and the concentration of methanol in the injected aqueous phase. More widespread is the intermittent use of methanol, e.g. as a hydrate inhibitor during process start-up or shutdown (Bahadori and Vuthaluru, 2010). In this case the concentration of methanol will vary, from no detectable methanol at all to high concentrations (several thousand parts per million).

Ethylene glycol is a preferred hydrate inhibitor in many multiphase systems, where the inhibitor is regenerated and recirculated. Ethylene glycol is also occasionally used for dehydration of natural gas. Despite having a relative low vapour pressure, some of the ethylene glycol will be lost to the gas phase. The resulting concentration in natural gas will be dependent on process conditions, but often concentrations of gaseous ethylene glycol are less than 1 μmol/mol.

Moisture monitors, herein called hygrometers, used in these hydrocarbon systems will be exposed to methanol and ethylene glycol. Like water, ethylene glycol and methanol are relatively polar molecules and especially ethylene glycol adsorbs easily to surfaces. These similarities make ethylene glycol and methanol suspect when it comes to interference with moisture monitoring. A literature study did not reveal any specific information describing the influence from these chemicals on the measurement of moisture, neither theoretically nor experimentally.

1.3 Dehydration of natural gas

Unprocessed natural gas is saturated with water vapour, originating from the reservoir. Several methods can be utilised to remove water from the natural gas (Grosso et al., 1980; Hubbard, 1991):

- absorption by liquid desiccants (glycols, glycerol, calcium chloride)
- adsorption by solid desiccants (molecular sieves, alumina, silica gel)
- absorption and hydrate inhibition by injection of hydrate point depressants (methanol, ethylene glycol)
- dehydration by expansion refrigeration

The history of natural gas dehydration is thoroughly cited e.g. by Hubbard and Campbell (Hubbard, 1991). Table 1 shows an overview of existing dehydrating technologies.

From these methods, the absorption with liquid desiccants is the far most popular one. Ethylene glycol (MEG), diethylene glycol (DEG) and triethylene glycol (TEG) are the commonly used liquid desiccants, due to exceptionally high hygroscopicity, excellent heat stability, low level of decomposition, low vapour pressures and ready availability at moderate cost. TEG is normally the preferred choice, mainly for following reasons (Rihani and Prasad, 1999):

- lower vaporisation loss
- higher decomposition temperature
- easier to regenerate to higher concentration

Tetraethylene glycol (TREG) is only occasionally used, e.g. to prevent loss in the vapour phase when the dehydration is performed at high temperatures (> 50 °C) (Betts and Lay, 1996; Graham et al., 1994).

Adsorption by solid desiccants is used when high dew point depressions are needed, such as in cryogenic natural gas liquids (NGL) plants, and liquefied natural gas (LNG) plants. Today molecular sieves are almost exclusively the adsorbent of choice, while alumina and silica gel are less popular.

Table 1: An overview of available technology for dehydration of natural gas (based on Graham et al., 1994).

Technology	Type	Process	Applications	Dew Point reduction	Glycol conc. [1)]	Capital expenditures	Operating expenses	Comments
LIQUID DESICCANT								
EG	Injection/ Contact	Continuous	Wellhead	55 °C	95.8 %	Low	High	Mostly used on small wells
DEG	Liquid contact	Continuous	Wellhead	60 °C	97.0 %	Low	Low	Popular many years ago. Problems with DEG degradation.
TEG	Liquid contact	Continuous	Wellhead	85 °C	98.7 %	Low	Low	Most popular type. Hard to use at low temperatures.
TREG	Liquid contact	Continuous	Wellhead	95 °C	99.3 %	Low	Low	Seldom used. High BTEX emissions.
Stripping gas	Liquid contact	Continuous	Wellhead	> 100 °C	99.5 %	Moderate	Moderate	Seldom used, higher costs.
Vacuum Pressure	Liquid contact	Continuous	Wellhead	> 100 °C	99.5 %	Moderate	Moderate	Seldom used, higher costs.
DRIZO	Liquid contact	Continuous	All	> 150 °C	99.999 %	Moderate	Moderate	High purity glycol via solvent. About 50 units installed.
Methanol	Injection	Continuous	Cold, Deep water	Varies		Low	High	Used mainly for production and storage.
IFPEXOL	Methanol Stripping	Continuous	NGL Plant, Offshore	> 150 °C		Moderate	Low	New technology only 2 plants.
SOLID DESICCANT								
Molecular Sieve	Solid	Batch	NGL Plant	>200 °C		Highest	High	Most expensive. Used almost exclusively for NGL plants.
Silica Gel	Solid	Batch	NGL Plant	125 °C		High	High	Not very popular.
Activated Alumina	Solid	Batch	NGL Plant, Others	>150 °C		Moderate	Moderate	Not very popular.
OTHER								
Calcium Chloride	Chemical	Batch	Wellhead, Gathering	80 °C		Lowest	Low	Used in remote gathering systems with small volumes.
Membrane	Barrier	Continuous	Mostly off-shore and small field	< 100 °C		Moderate	Moderate	Safe, environmentally friendly units.

1) Typical concentration of so-called lean glycol entering drying tower, after regeneration of used (rich) glycol.

1.4 Interpretation of moisture measurements

The amount of moisture in a natural gas can either be expressed as concentration (e.g. µmol/mol or mg/Sm^3 at some defined standard temperature and pressure) or as dew or frost point temperature. The dew point is the highest temperature, at a specified pressure and moisture concentration, where water can condense from the gas. The frost point is the highest temperature, at a specified pressure and moisture concentration, where ice can precipitate from the gas (Løkken et al., 2008). In the temperature region between 0 °C and -20 °C it is difficult to predict whether the moisture will condense as dew or precipitate as ice. It is necessary to distinguish between the dew point and the frost point, as these could deviate with several kelvin for the same moisture concentration. Several accurate formulas for conversion between dew or frost point at atmospheric pressure and concentration (via saturation vapour pressure) are reviewed in the literature (Murphy and Koop, 2005). The following formulas, published by Sonntag (Sonntag, 1990; Sonntag, 1994), are used in this work for conversions between frost point and saturation vapour pressure:

For the given temperature range
$173.15K \le T_K \le 273.16K \quad (-100°C \le T_C \le 0.01°C)$

$$\begin{aligned}\ln e_i(T_K) = {} & -6024.5282 T_K^{-1} + 24.7219 + 1.0613868 \times 10^{-2} T_K \\ & - 1.3198825 \times 10^{-5} T_K^{\,2} - 0.49382577 \ln T_K,\end{aligned} \tag{1}$$

$e_i(T_K)$ is the saturation vapour pressure with respect to ice in hPa (hectopascal), T_K is frost point temperature in K.

Saturation vapour pressure can be converted to frost point by formula (2), which is derived from equation (1):

$$\begin{aligned}T_K = {} & 12.1197 y + 5.25112 \times 10^{-1} y^2 + 1.92206 \times 10^{-2} y^3 \\ & + 3.84403 \times 10^{-4} y^4 + 273.15\end{aligned} \tag{2}$$

In the conversion formula (2)

$$y = \ln(e_i(T_K) / 6.11153) \tag{3}$$

For conversions between saturation vapour pressure and concentration the following formula can be used:

$$c_w = \frac{e_i(T_K) \times 10^6}{1013.26} \tag{4}$$

c_w is concentration in µmol/mol. At elevated pressures the formulas of Sonntag are not applicable because of increasing non ideal behaviour of gases.

Conversion between moisture concentration and dew point or frost point at elevated pressure has traditionally been performed by use of the correlation charts from McKetta and Wehe (McKetta and Wehe, 1958) or by the formulas of Bukacek (Bukacek, 1955). The methods are based on empirical data produced between the years of 1927 and 1955, the most important publications being Dodson and Standing (Dodson and Standing, 1944), Skinner (Skinner, 1948) and Hammerschmidt (Hammerschmidt, 1933). Bukacek and McKetta and Wehe extended the older data with their own experimental work. These conversions always relate the moisture concentration to condensed water (dew), despite the fact that the thermodynamically most stable phases in the lower temperature regions are gas hydrates or ice (dependent of the pressure and temperature). The methods have gained widespread use when it comes to calculations of the moisture concentration or the dew point of unprocessed natural gas, and they have been important for design of dehydration processes. The chart of McKetta and Wehe, shown in figure 1, seems to be the most popular correlation and is for the time being used in gas processing handbooks published by GPSA (GPSA, 2012) J.M. Campbell (Campbell, 1994) and Kohl and Nielsen (Kohl and Nielsen, 1997).

Thermodynamic modelling is often a preferred alternative for calculating equilibrium water content of natural gas. In contrast to charts and simple formulas thermodynamic models usually have the possibilities of covering broad ranges of compositions, pressures and temperatures. The equations of state (EoS) traditionally used in the oil and natural gas industry, like the SRK- and PR-EoS, have shown severe limitations for description of aqueous systems and polar substances in general (Folas et al., 2007; Løkken et al., 2008). More than 10 years ago, the European gas research group (GERG) proposed a modified PR-EoS, tailor-made for the modelling of water in gas with a primary working range of 5 bar to100 bar and -5 °C to 15 °C (Althaus, 1999; Oellrich and Althaus, 2001). The model has been published in the form of an ISO standard (ISO, 2004). The CPA-EoS (Cubic Plus Association) is another thermodynamic model proven to accurately calculate equilibrium concentration of water as well as other polar substances in hydrocarbon systems (Folas et al., 2007). This comprehensive model covers wider pressure and temperature ranges compared to the "GERG-Water-EoS", in addition to being able to model all phases (liquid, ice and hydrate), both stable and metastable ones (e.g. super-cooled dew).

Hygrometers returning dew or frost points as their primary unit of measurement are usually calibrated at ambient pressure using a high precision chilled mirror as the reference. The calibration process will start at the lowest moisture concentration, typically cooling the mirror to well below -40 °C, to make sure the temperature reading relates to ice. When ice is formed on the mirror surface, the water phase will remain as ice until the mirror temperature increases to 0 °C again. As a consequence these hygrometers will return frost points for negative temperatures and dew points for positive temperatures. Converting frost points or dew points to concentration at atmospheric pressure is easy e.g. using Sonntag's formulas ((1) – (3)). Traditionally, hygrometers have been installed in the natural gas stream at line pressure (typically between 50 and 150 bar), alternatively at an intermediate pressure (e.g. specified pressure corresponding to the dew point transport specification). Conversion methods, provided by the suppliers, typically convert the raw signals (frost points) to dew points at some specified or measured pressure. These methods usually relies on the original atmospheric frost point calibration combined with the use of the formulas of Bukacek (Bukacek, 1955) for calculation of dew points at defined pressures. Conversions utilising the chart of McKetta and Wehe or the formulas of Bukacek, should only be performed on dew points (≥ 0 °C). The errors involved using these methods directly on frost points (< 0 °C) will increase as the temperature decrease, and the use the GERG EoS for water or CPA EoS is regarded as a more accurate approach.

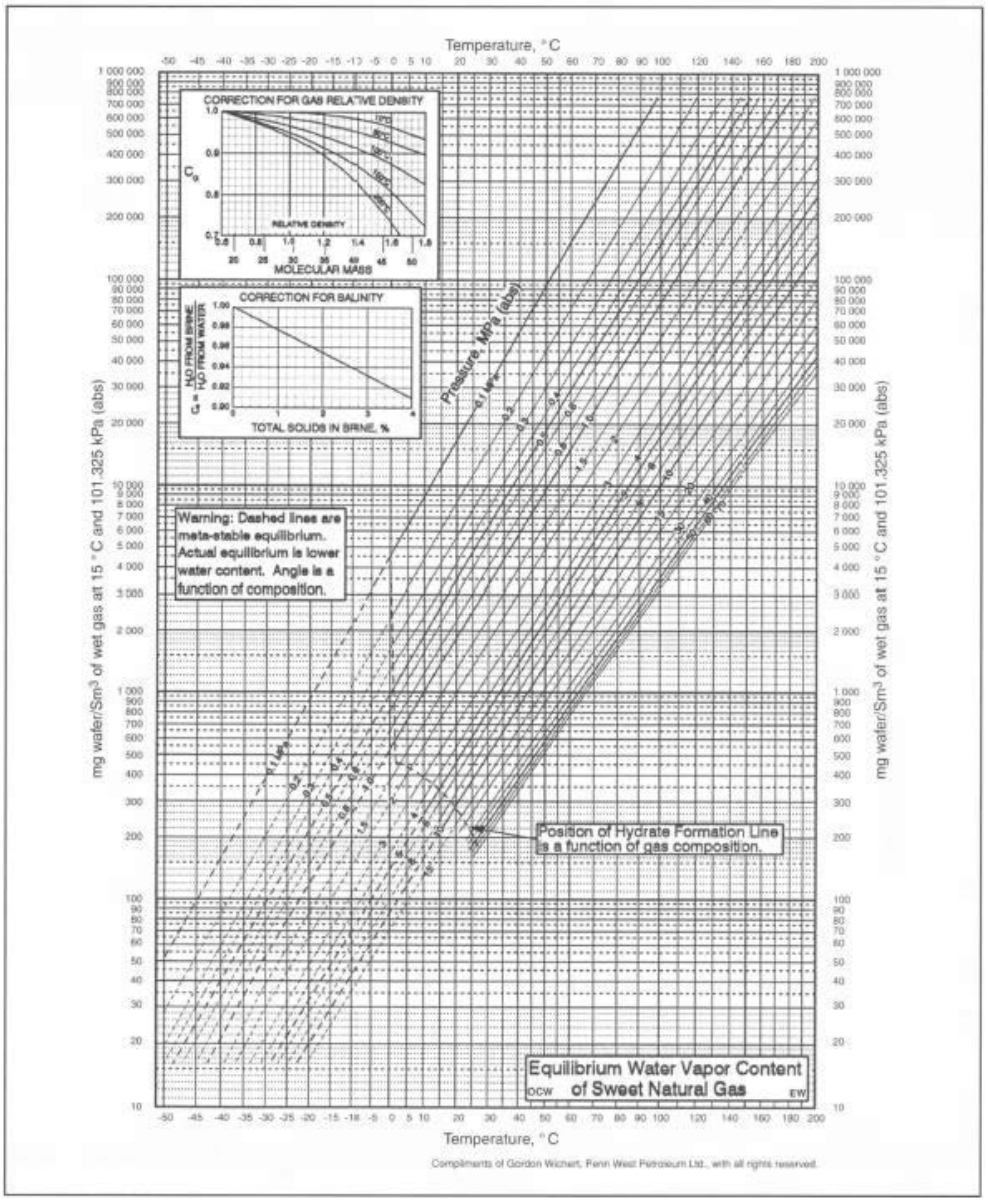

Figure 1: Water content of sweet natural gas (GPSA, 2012; McKetta and Wehe, 1958).

1.5 Objective of this work

In this work several devices more or less frequently used in the natural gas industry for monitoring of moisture in gases were compared. The devices are referred to as hygrometers, The comparison was performed through several laboratory experiments. The overall scope of work has been to evaluate different instrument types and moisture measuring techniques regarding suitability for use in the natural gas industry, for applications involving moisture concentrations between 20 and 120 μmol/mol. Consequently, a suitable test rig for generation of moisture in gases was established. In addition to comparing general parameters such as accuracy, robustness, long term stability and speed of response there has been focus on how methanol and glycols affect the performance of the hygrometers. For practical and safety reasons, the long term (approximately one month) comparison measurements were performed in the laboratory at ambient conditions using nitrogen as the matrix gas. Another goal of this work has been to demonstrate the use of the test rig and reference hygrometers to produce reliable data on equilibrium moisture concentration in methane and natural gas at high pressures.

Many users in the natural gas industry already have a chosen instrument type for their moisture monitoring. For various reasons they often would, if possible, prefer to keep these in use instead of purchasing a new and perhaps more suitable instrument type for their application. Hence it has been a goal for this work to find ways to overcome instrument specific challenges, as well as the more general challenges within the field of trace moisture analysis in high pressure natural gas.

From this work users of instruments for water vapour measurements in natural gas should be able to:

- given a chosen instrument type, establish reasonable routines that ensure trace moisture measurements in natural gas with adequate accuracy and regularity
- given a well-defined application, choose between relevant instrument types and establish reasonable routines that ensure trace moisture measurements with optimised quality

For any situation trace moisture measurements are extremely sensitive to the performance of the sampling system. It has not been a scope of this work to study this topic in any detail. On the other side numerous discussions with users and suppliers of trace moisture instruments as well as with suppliers of sampling systems, have made it possible to give some general recommendations within the field of sampling systems.

1.6 Structure of the thesis

This thesis is an integration of 4 published papers. The thesis elaborates some relevant topics, which were only briefly discussed in the papers, and links the individual papers together.

The thesis is organised as follows:

- Chapter 1: gives an introduction to the topic of moisture measurements in natural gas, and presents the objective to this work.
- Chapter 2: gives information on the individual techniques and working principles for moisture measurements, supplementing the brief introductions provided in the papers.
- Chapter 3: reviews the experimental setup for the experiments briefly, however the same information is provided with high degree of details in the papers.
- Chapter 4: summarises the results from the experimental work, as published in the 4 individual papers.
- Chapter 5: interprets the overall significance of the results to the natural gas industry.
- Chapter 6: discusses some future aspects of moisture measurements.
- Chapter 7: provides final conclusions.

2 Description of techniques for moisture analysis

2.1 Review of applied techniques

Throughout the years numerous methods or techniques for moisture measurements in gases have been developed and established. Most of them are thoroughly described in published literature (Blakemore et al., 1986; Bruttel and Regina, 2006; Carr-Brion, 1986; Funke et al., 2003; ISO, 1993a; ISO, 1993b; Keidel, 1959; Knight and Weiss, 1962; McAndrew and Boucheron, 1992; McAndrew, 1997; Monroe, 1998; Wiederhold, 1997a; Wiederhold, 2000; Willsch et al., 2005). In this work hygrometers based on capacitor sensor, quartz crystal microbalance (QCM), electrolytic cell, fibre-optic sensor, reaction GC (CaC_2-GC), chilled mirror and Karl Fischer titration have been investigated. These methods were chosen mainly based on their frequency of use in the natural gas industry and their availability for tests in this work. The basic principles of the methods are briefly summarised in Table 2, and more information is given in subsequent chapters.

Chilled mirror hygrometry and Karl Fischer titration are usually regarded as absolute or fundamental methods, as they utilise a direct relationship between the measured quantity and the amount of moisture. Hence they often are preferred as reference methods.

Table 2: Summary of methods for moisture measurements in gases.

Method	Typical uncertainty	Working principle
Capacitor sensor	(1 to 3) °C	Capacitance or impedance measured as a function of water molecules adsorbed to the porous dielectric (usually metal oxides like Al_2O_3 or SiO_2) of a capacitor. (Carr-Brion, 1986; Funke et al., 2003; McAndrew and Boucheron, 1992; McAndrew, 1997; Wiederhold, 1997a)
Quartz crystal microbalance (QCM)	±10 %	Measures the resonance frequency of an oscillating quartz crystal (piezoelectric) coated with a hygroscopic polymer. The frequency changes with mass as water molecules adsorb on the quartz crystal. (Blakemore et al., 1986; Carr-Brion, 1986; Funke et al., 2003; McAndrew and Boucheron, 1992; McAndrew, 1997; Wiederhold, 1997a)
Electrolytic cell	±10 %	Measures current generated from electrolytic decomposition of water adsorbed in strongly hygroscopic P_2O_5. (Keidel, 1959)
CaC_2-GC	±10 %	Water and calcium carbide (CaC_2) react to form ethyne: $2H_2O + CaC_2 \rightarrow C_2H_2 + Ca(OH)_2$. Quantification of ethyne by gas chromatographic (GC) separation and detection e.g. with a thermal conductivity or a flame ionisation detector. (Knight and Weiss, 1962; Monroe, 1998)
Fibre-optic sensor	±2 °C	Measures a shift in reflection spectrum dependent on the amount of adsorbed water in a hygroscopic Fabry-Perot filter. “Fibre-optic” in the sense that light is emitted and reflected via fibre-optic cables. (Rittersma, 2002; Willsch et al., 2005)
Karl Fischer titration	±10 %	The Karl Fischer reaction: $ROH + SO_2 + R'N \rightarrow (R'NH)SO_3R$ $(R'NH)SO_3R + 2R'N + I_2 + H_2O \rightarrow (R'NH)SO_4R + 2(R'NH)I$ ROH = alcohol, R'N = basic nitrogen compound For coulometric titration the amount of water is calculated by measuring the current needed for the electrochemical generation of iodine (I_2) from iodide (I^-). (Bruttel and Regina, 2006; ISO, 1993a; ISO, 1993b)
Chilled mirror	±0.2 °C	Measures the temperature at which water molecules condense from the gas to form dew or frost on a reflective surface (mirror). The dew or frost is detected optically on the surface by an electro-optic detector. (Wiederhold, 1997a; Wiederhold, 2000)

2.2 Reference techniques

2.2.1 Chilled mirror hygrometers

Moisture measurements using the chilled mirror technique involve determining the dew point or the frost point of a gas. As dew and frost points are thermodynamic properties, the chilled mirror technique is considered an absolute or fundamental method (Funke et al., 2003). This, in addition to the high accuracy (e.g. ± 0.1 °C) and reliability, has made chilled mirror hygrometry a preferred choice for secondary standard applications, e.g. by national measuring institutions such as the National Institute of Standards and Technology (NIST) (McAndrew and Boucheron, 1992). There is a direct correlation between the dew point or frost point temperature and the water vapour partial pressure, which in turn defines the concentration of water vapour (Dalton's law).

Continuous condensation chilled mirror hygrometers
Most chilled mirror hygrometers today have an automatic reading of the dew or frost point, and belong to the family of so called "continuous condensation chilled mirror hygrometers", as illustrated in Figure 2. The reading is based on an electro-optic controller system. A collimated light source, such as a high intensity light emitting diode (LED), illuminates the mirror, and a photodetector produce a photocurrent proportional to the amount of reflected light. The photocurrent is compared to a reference photocurrent from another set of LED and photodetector (without a mirror) in a bridge circuit. An adjustable balance on this bridge circuit controls the current to the thermoelectric mirror cooler (Peltier heat pump), and this way the mirror temperature is controlled (McAndrew and Boucheron, 1992).

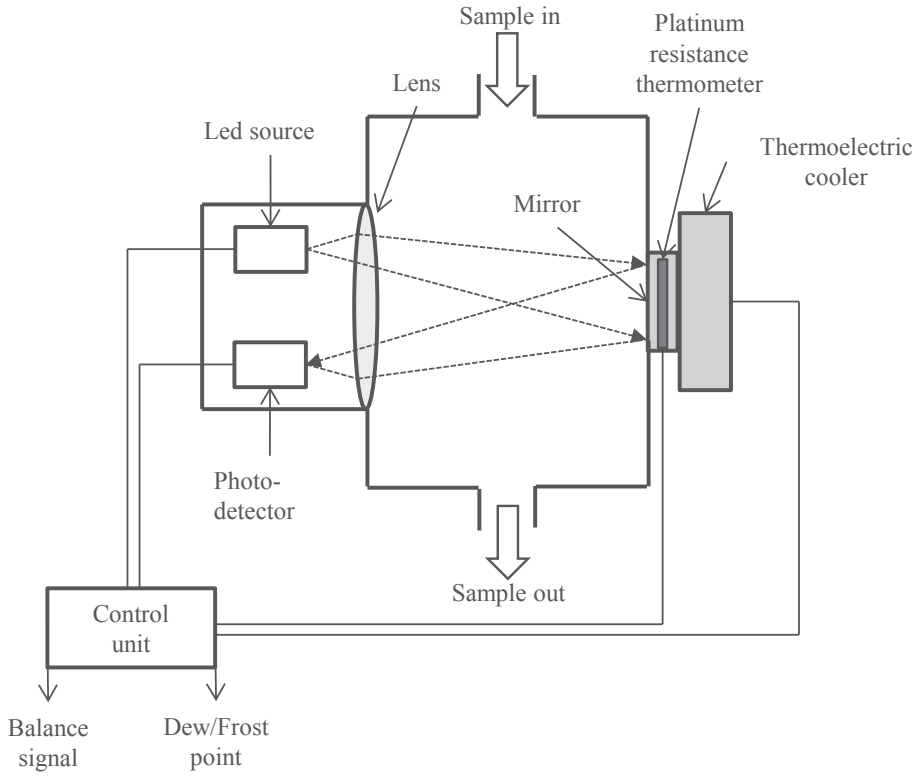

Figure 2: Schematic of a continuous condensation chilled mirror hygrometer.

As water condenses or precipitates on the surface of the mirror during the chilling process, more of the incident light is scattered, and thereby the amount of light received by the photodetectors is reduced. The control unit then responds by heating up the mirror until evaporation exceeds the condensation and the thickness of the condensed layer decreases. The control unit will repeat cooling and heating cycles of the mirror until the system reaches equilibrium, i.e. the condensation equals the evaporation, so that a predefined thickness of the dew or frost on the mirror is maintained. Under these equilibrium conditions, the surface temperature is precisely at the dew or frost point of the gas passing by the mirror (Mehrhoff, 1985; Wiederhold, 1997a).

Provided the mirror surface is regulated at the true dew or frost point temperature, the accuracy of the measurement is assumed to be limited by the quality of the temperature sensor. The sensor of choice is usually a precision NIST-traceable platinum resistant thermometer or equivalent thermistors that are embedded within the mirror surface to accurately measure the surface temperature. The accuracy of 0.1 °C, which usually is the highest accuracy claimed by the manufacturers, correspond to about ± 0.3 µmol/mol at the 20 µmol/mol level of moisture concentration. The lowest detectable level of dew or frost point is determined by

the lowest mirror temperature that the cooling system can achieve and maintain for sufficient amount of time.

Sources of error for chilled mirror hygrometers
The literature suggests accumulation of particulate or volatile contaminants on the mirror surface, disturbing the optical detection of the dew or frost layer, as the major source of error for chilled mirrors (Fenner and Zdankiewicz, 2001; Funke et al., 2003; Wiederhold, 2000). The presence of soluble contaminants, such as salts, on the mirror surface decreases the vapour pressure at the mirror surface for a given temperature (Raoult effect). Hence, the sensor will be controlled at a temperature above the dew or frost point temperature. Hygroscopic impurities may reduce the vapour pressure of water, and lower the apparent dew or frost point. Accumulation of contaminants is prevented by cycling the mirror temperature to high temperatures with some adequate frequency (application dependent). The challenge with contaminants is low for applications involving clean gases (e.g. semiconductor gases and calibration gases).

2.2.2 Karl Fischer titration

The Karl Fischer titration is a widely used titrimetric method for water determination in various substances, including gases. The German chemist Karl Fischer developed the method in 1935, when he needed a method for moisture determination in sulphur dioxide. The starting point was the well-known Bunsen reaction (1), used for determination of sulphur dioxide in aqueous solutions:

$$2H_2O + I_2 + SO_2 \rightarrow H_2SO_4 + 2HI \quad (1)$$

The idea was that water would be determined if sulphur dioxide was present in excess, and the produced acid was neutralized by a base. The original Karl Fischer reagent contained iodine, sulphur dioxide, anhydrous pyridine (base) and anhydrous methanol (protic solvent), and the following equation (2) was proposed by Karl Fischer:

$$2H_2O + I_2 + SO_2 * 2C_5H_5N + 2C_5H_5N \rightarrow (C_5H_5N)_2H_2SO_4 + 2C_5H_5NHI \quad (2)$$

The end point of the reaction was indicated by a change of the colour of the reaction solution.

The Karl Fischer titration has been extensively reviewed since 1935, and different reactions have been proposed (MacLeod, 1991). It was demonstrated that pyridine does not take part in the reaction, but rather acts as a buffer (Cedergren, 1974; Verhoef and Barendrecht, 1976). Today equation (3) and (4) are widely accepted as the best representative for the Karl Fischer reaction (ISO, 1993a):

Step 1:

$$CH_3OH + SO_2 * R_3N \rightarrow [R_3NH]SO_3CH_3 \quad (3)$$

Step 2:

$$H_2O + I_2 + [R_3NH]SO_3CH_3 + 2R_3N \rightarrow [R_3NH]SO_4CH_3 + 2[R_3NH]I \quad (4)$$

In equation (3) and (4) methanol is used as a protic solvent and R_3N represents a base such as imidazole. Other examples of protic solvents which have been in use are 2-metoxyethanol and ethylene glycol. The original base, pyridine, is not preferred because of its bad odour. Use of the odourless imidazole led to a higher speed and more stable endpoints compared to the use of pyridine (MacLeod, 1991).

Volumetric titration and coulometric titration are two main methods for Karl Fischer titrations (Figure 3). For both methods the end point is defined by excess iodine detected by an indicator electrode, once all present water is consumed. For volumetric titration an iodine-containing solution in a burette serves as the titrating agent. The water content of the sample is calculated using the titration volume and the mass of water titrated pr. mL of titrating agent (titer). For coulometric titration the iodine (I_2) is generated electrochemically by anodic oxidation of iodide (I^-) present in the titration cell (MacLeod, 1991). The amount of water in the sample is calculated from the number of moles of electrons used in the iodine generation. For higher water contents (i.e. 1 to 100 mg) the volumetric titration method is preferred (Althaus, 1999). For lower water contents (i.e. 10 µg to 10 mg) coulometric titration is the method of choice. In modern Karl Fischer titrators the end point is determined by the help of a pair of Pt-electrodes, either as biamperometric indication or as bivoltametric indication (Bruttel and Regina, 2006; MacLeod, 1991).

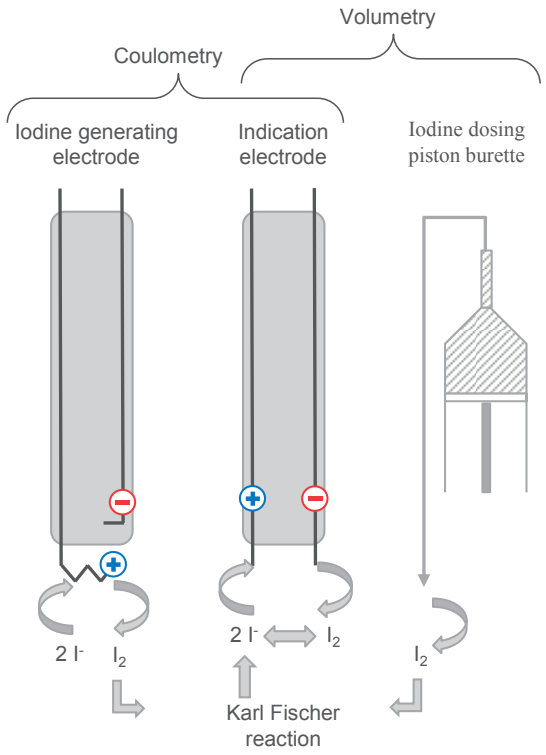

Figure 3: Coulometric and volumetric Karl Fischer titration; iodine being provided for the Karl Fischer reaction (equation (4)) from an iodine generating electrode or iodine dosing piston burette, respectively. The indication electrode detects an excess of iodine when all water is consumed, defining the endpoint of the reaction.

For acceptable accuracy of Karl Fischer titrations it is absolutely essential that no significant amounts of iodine are consumed by side reactions. For natural gas applications sulphur compounds are the most relevant compounds involved in such side reactions. H_2S will cause false high moisture concentration when determined with Karl Fischer titrations. For H_2S concentrations less than 20 % of the moisture concentration the latter can be adjusted (ISO, 1993b). Karl Fischer titration is not recommended for gases containing H_2S corresponding to more than 20 % of the moisture concentration. Correct subtraction of response from background moisture, diffusing into the titration cell through various connections, is generally one of the major challenges when using Karl Fischer for determination of trace amounts of moisture in gas (Dong et al., 2005). Accurate measurement of the titrated gas volume and accurate end point determination are other challenges. These are all determining factors for the accuracy and precision obtainable for moisture measurements using the Karl Fischer technique.

2.3 Online hygrometers

2.3.1 General set up

Online hygrometers are connected directly to the gas stream of interest, and monitor the moisture concentration or the dew/frost point continuously at some given frequency, as illustrated in Figure 4. Traditionally the sensors of the hygrometers have been installed in a bypass stream of the gas at pipeline pressure, with some necessary sample conditioning upstream the sensor. Alternatively the sample pressure is reduced to ambient pressure upstream the sensor. Both alternatives are shown in Figure 4, though usually the sensor is located either at high or at low pressure, dependent on the hygrometer of choice.

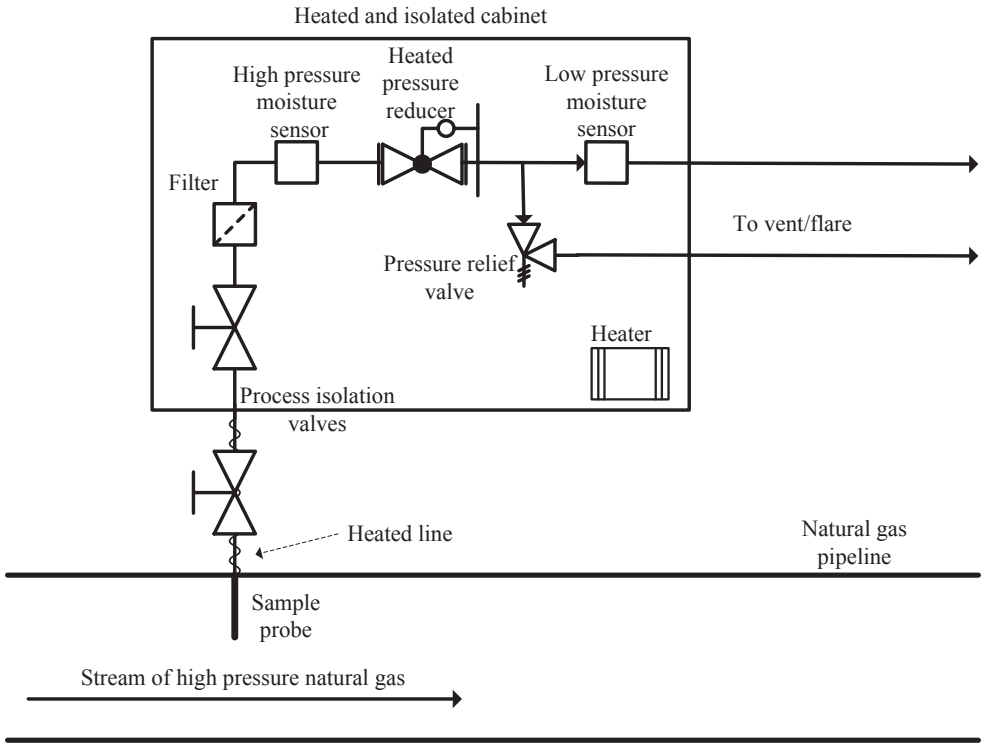

Figure 4: Illustration of an online moisture monitoring system. The moisture sensor is located at high or low pressure gas, dependent of the hygrometer of choice. The moisture sensor is connected to a processing unit, for data treatment and reporting (not shown).

2.3.2 Capacitor based hygrometers

Hygrometers based on capacitive properties have enjoyed widespread use for online moisture monitoring in process gases. Reasons for their popularity are easiness of use, flexibility regarding temperature, flow, pressure and moisture level

of the process gases, low price and rugged design. (Funke et al., 2003; Mermoud et al., 1989)

A capacitor is basically a component in an electrical circuit that stores energy as an accumulation of electrical charge. A parallel-plate capacitor consists of two parallel conducting plates, each with area A_c, separated by a distance d (Figure 5). If they are separated by vacuum, the capacitance C depends only on A_c and d (Young and Freedman, 2004):

$$C = \varepsilon_0 A_c / d \tag{5}$$

C = capacitance
ε_0 = permittivity of vacuum = 8.85 x 10^{-12} F/m
A_c = area of the parallel conducting plates
d = distance between the parallel conducting plates

When the space between the conductors is filled with an insulating layer of a dielectric material, the capacitance increases by a factor K, called the dielectric constant of the material, leading to the expression (Larson, 2003; Young and Freedman, 2004):

$$C = \varepsilon_0 K A_c / d = \varepsilon A_c / d \tag{6}$$

K = dielectric constant of dielectric material
$\varepsilon = \varepsilon_0 K$ = permittivity of the dielectric

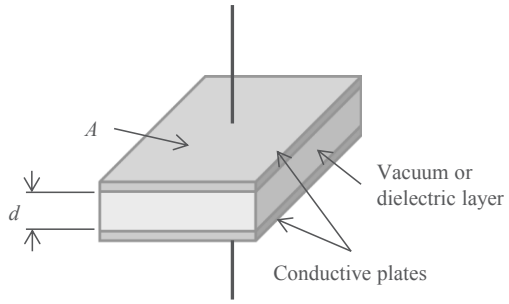

Figure 5: Schematic showing of a parallel-plate capacitor, with conducting plate area A and distance d between the plates.

The dielectric layer in a capacitor based moisture sensor adsorbs water molecules and achieves an equilibrium condition dependent on the partial pressure of the water vapour in the sample gas (Mychajliw, 2002). As the dielectric constant of the dielectric material is low (approx. 9.3 for aluminium oxide) and the dielectric constant of water is high (80.4), even small amounts of moisture results in a detectable change of capacitance of the capacitor (Funke et al., 2003). Resistive components of the capacitor are also affected by water adsorption. Most

commercial instrumentation therefore measure the impedance (resistive, capacitive and inductive component in an AC circuit) of the sensor assembly (Funke et al., 2003), as shown in Figure 6. Calibration of a capacitor based sensor is usually done by comparing impedance related signals to a series of known dew points and frost points in nitrogen or air, at ambient conditions.

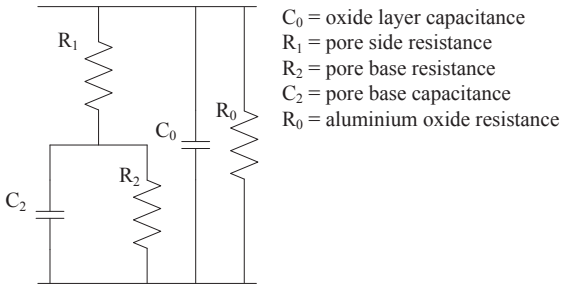

Figure 6: Electronic of an aluminium oxide capacitor.

The most commonly used capacitor based hygrometers for natural gas applications are based on a metal oxide like aluminium oxide. The aluminium oxide sensors consist of anodized aluminium strips, providing a porous oxide layer. A very thin metal layer (e.g. gold) is deposited over this structure. The aluminium base and the metal layer form the two electrodes of the resulting aluminium oxide capacitor, as illustrated in Figure 7 (McAndrew and Boucheron, 1992; Mehrhoff, 1985; Mermoud et al., 1989). Capacitor based hygrometers are regarded as low accuracy hygrometers, mainly caused by their challenges with hysteresis effects (Funke et al., 2003).

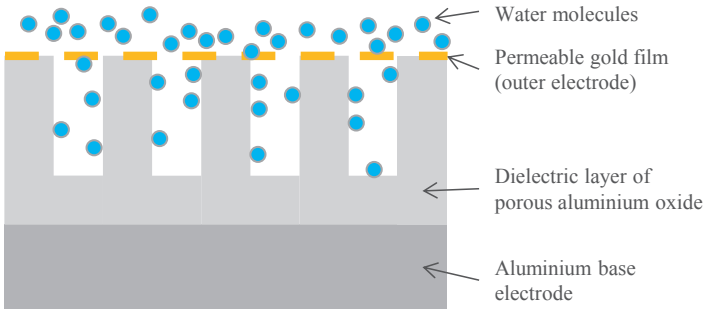

Figure 7: Schematic of an aluminium oxide capacitor.

2.3.3 Quartz crystal microbalance

Piezoelectric sensors are commonly referred to as oscillating (vibrating) quartz crystal microbalances (QCM sensor) and have increasingly been used in the field of analytical chemistry. The technology has been reviewed in several publications

(Guilbault et al., 1988; O'Sullivan and Guilbault, 1999). When utilised for moisture measurements, both faces of the quartz crystal are coated with a thin film of a hygroscopic material in order to enhance the selective adsorption of water molecules (Figure 8).

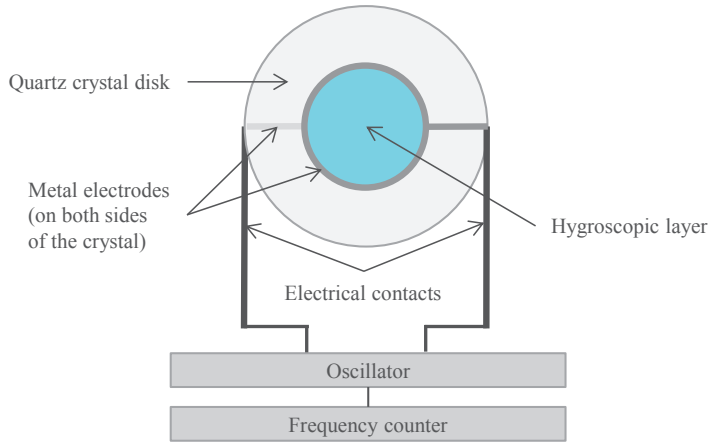

Figure 8: Schematic of a quartz crystal microbalance.

The principle of the QCM sensor can be expressed by the following equations: (Funke et al., 2003; Rittersma, 2002)

$$\Delta f = -C_m \Delta m \tag{7}$$

where Δf is the change of the crystal resonance frequency resulting from a change in mass (Δm) per unit surface area and the constant C_m is a property of the crystal used:

$$C_m = \frac{2f_0^2}{n_h A_p \sqrt{\mu\rho}} \tag{8}$$

Where f_0 is the fundamental resonance frequency, n_h is the order of the harmonic, A_p is the piezoelectric active surface area, μ is the shear modulus of quartz (2.947×10^{11} g/(cm s^2)) and ρ is the density of quartz (2.648 g/cm^3). For a 5 MHz crystal operating in the fundamental mode (n = 1), mass sensitivity is approximately 18 ng/(cm^2 Hz).

The QCM sensor is exposed to moisture containing (wet) and dry process gas in an alternating manner, at some fixed continuous cycling intervals (e.g. 30 s). An adsorbent bed, typically a molecular sieve, provides the dry process gas. Water molecules in the wet process gas accumulate selectively on the surface of the QCM sensor, increasing its mass. This mass of water decreases the crystal resonance frequency of the sensor. The difference between wet and dry frequency is directly proportional to moisture content in the process gas. This continuous cycling

between wet and dried process gas also means that the sensor never achieves a physical equilibrium with moisture in the process gas. As a consequence the QCM sensor is regarded as a fast responding sensor. Commercially available QCM devices, are usually equipped with an internal moisture generator based on a permeation tube, as illustrated in Figure 9. This can be used for periodical checks or adjustments of the instruments factory calibration (Funke et al., 2003).

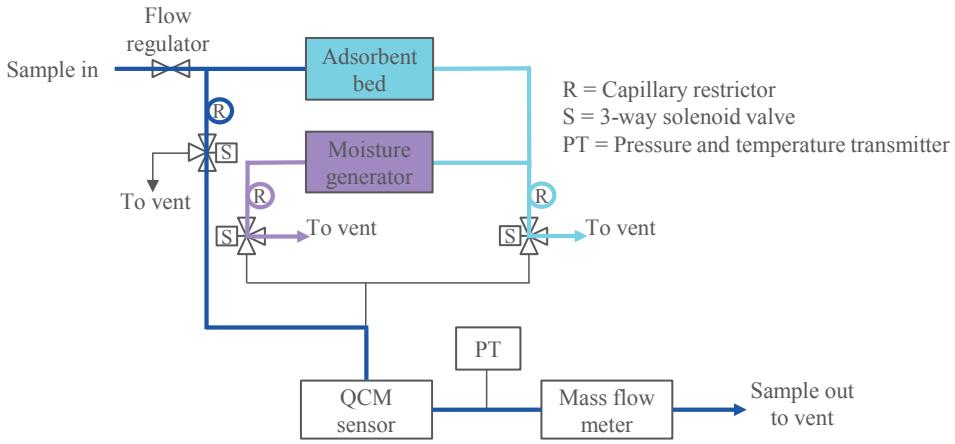

Figure 9: Schematic of a QCM device, measuring in wet sample gas mode.

For the QCM hygrometers to maintain a high level of accuracy, it is important that the adsorbent bed is replaced before it is saturated with water and that the permeation tube is replaced before the water inside the tube is consumed. These replacements are typically needed annually. Dependent of the level of contaminants in the process gas, the sensor also has to be replaced with some frequency. (e.g. annually or biannually). Hence, good routines for quality control and preventive maintenance will be necessary for QCM hygrometers.

2.3.4 Fibre-optic hygrometers

With the development of optical fibre technology, a considerable level of research has been focused on fibre optic based techniques for moisture measurements. Small size, immunity to electromagnetic interference, multiplexing and remote sensing capabilities are properties that have made fibre optic hygrometers attractive (Wang and Wolfbeis, 2012; Yeo et al., 2008).

Several sensing techniques are available such as direct spectroscopic, evanescent wave, in-fibre grating and interferometric methods. For moisture in natural gas applications, interferometric techniques have been utilised for some years. This hygrometer consist of a sensor that is an optical filter according to the Fabry-Pérot interference principle, and fibre-optic in the sense that signal transmission is done

with the help of fibre-optic cables. Its sensor consists of a pile of thin dielectric metal oxide layers, with alternately high and low refraction indexes, as illustrated in Figure 10 (Willsch et al., 2005). The sensors are produced with micro pores running through the complete layer package. The pores are less than 0.4 nm in diameter, allowing permeation of water (effective diameter of 0.28 nm) in to the sensor. Increased water vapour pressure in the sample gas will increase the equilibrium level of adsorbed water molecules in the pore structure of the sensor. The adsorbed water will change the refraction indexes of the individual layers, leading to a reflection spectrum that is shifted towards larger wavelengths. The moisture concentration in the gas is directly proportional to the shift in wavelength of the reflected light. The measuring principle is independent of the intensity of the reflected light, and the sensor can be installed up to 800 meters from the evaluation device.

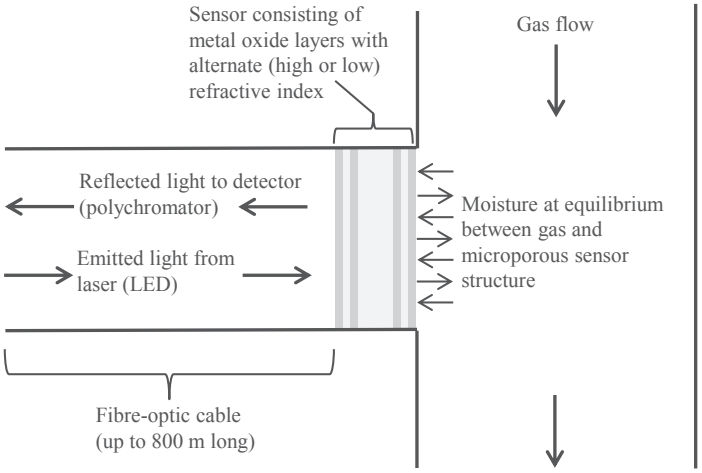

Figure 10: Schematic representation of a microporous Fabry-Pérot interferometric moisture sensor.

2.3.5 Electrolytic cell hygrometers

Electrolytic hygrometers represent one of the most widely established methods for trace moisture determination, first described by Keidel in the 1950's (Keidel, 1956; Keidel, 1959). They are relatively inexpensive and convenient compared to many other types of hygrometers and offer some of the lowest detection limits available. At the same time electrolytic hygrometers are prone to give erroneous measurements in the presence of alcohols, glycols and ammonia or amines (Galloway, 1989; Laughlin, 1976; Lechner-Fish, 1997).

The typical electrolytic sensor consists of two precious metal electrodes (typically platinum or rhodium) helically wound around a support mandrel or imbedded in a hollow glass tube (Figure 11). The electrodes are coated with a thin layer of the strongly hydroscopic phosphorus pentoxide (P_2O_5), serving as the electrolyte.

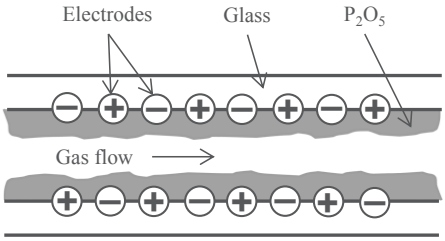

Figure 11: Schematic of an electrolytic cell hygrometer, with two wounded electrodes coated by phosphorus pentoxide (P_2O_5).

During operation a controlled amount of gas is allowed to flow through or across the electrodes, and all the moisture will absorb in the electrolyte. A voltage potential is applied across the electrodes, electrolysing the water molecules that have been absorbed in the P_2O_5 according to:

Cathode reaction:	$2H_2O + 2e^- \rightarrow 2OH^- + H_2$	(9)
Anode reaction:	$H_2O \rightarrow 1/2O_2 + 2H^+ + 2e^-$	(10)
Net reaction:	$2H_2O \rightarrow 2H_2 + O_2$	(11)

Each electrolysed water molecule causes two electrons to be displaced from the anode to the cathode. The steady state current created by these electrons can be related to the moisture concentration in the incoming sample stream using Faraday's law and the sample flow rate (Coulometric operation) (Black, 1979; McAndrew, 1997; Mychajliw, 2002). Hence the electrolytic hygrometers are regarded as absolute in principle. In practice, instrument specific effects and different modes of operation result in measurement errors that require calibrations (Funke et al., 2003). The main source of errors are ohmic (nonelectrolytic) current between the electrodes, catalytic recombination of hydrogen and oxygen and moisture outgassing in the cell itself (McAndrew and Boucheron, 1992).

2.3.6 Reaction GC

Some gas chromatographic (GC) applications can benefit from a conversion of the analyte to an alternative compound. Reaction GC is a term often used for such applications. The conversion can be thermally based or facilitated by one or several reactive substances. The motivation for using reaction GC could be primary analytes which give low detector sensitivity, give difficult chromatographic separation or are thermally too labile for avoiding decomposition during traditional GC analysis.

Direct analysis of traces of moisture in gases by GC methods is challenging, mainly caused by the high adsorptivity of water to surfaces and problems with

keeping moisture from surrounding atmosphere out of the general purpose GCs. Several authors have described the reaction GC method involving conversion of water (H_2O) to ethyne (C_2H_2) with calcium carbide (CaC_2), according to the following reaction (Goldup and Westaway, 1966; Knight and Weiss, 1962; Latif et al., 1983; Lindblom et al., 1992; Monroe, 1998):

$$CaC_2\,(s) + 2H_2O\,(g) \rightarrow Ca\,(OH)_2\,(s) + C_2H_2\,(g) \qquad (12)$$

From this reaction (12) the gaseous ethyne can easily be detected by a sensitive thermal conductivity detector (TCD) or an even more sensitive flame ionisation detector (FID), after chromatographic separation on e.g. a porous polymer column. The GC detector has to be calibrated with respect to etyne, by the help of gravimetric gaseous reference standards. The application is typically set up, as shown in figure 11, with the gas stream of interest passing through a small vertical placed reactor filled with ground calcium carbide, placed in front of the injection loop of a GC. Stainless steel pipes of dimensions down to 18 cm x 0,64 cm have been used as reactor, filled approximately 3 g grounded calcium carbide (Monroe, 1998).

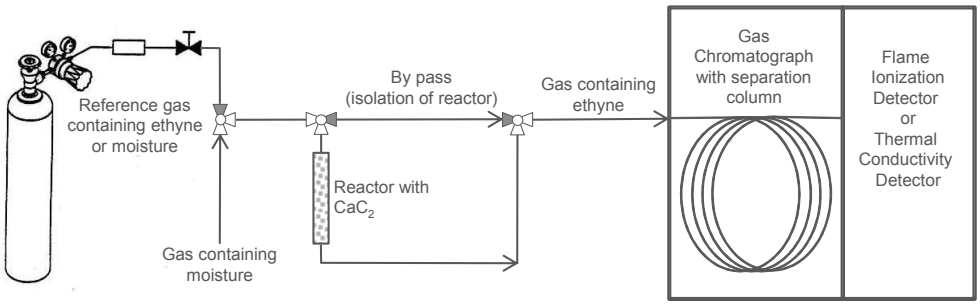

Figure 12: Schematic of a reaction GC application, based on conversion of water to ethyne with calcium carbide.

Published data indicate that the conversion of water to ethyne is stoichiometric according to the reaction equation (12) (Knight and Weiss, 1962; Lindblom et al., 1992). Monroe (1998) and Lindblom et al. (1992) pointed out that the formation of ethyne is enhanced by low temperatures. This means that the molar moisture concentration will correspond to twice the ethyne concentration returned from the reaction GC application.

2.3.7 Other techniques

There exist several methods or technologies capable of monitoring moisture in gases, which are not covered in this work. Most of them are not very relevant for the natural gas industry for reasons such as: lack of sensitivity, lack of resistance to

harsh process environment, problems with interferences from other natural gas constituents or high level of required maintenance.

In addition to fibre-optic hygrometers (chapter 2.2.3), various other optical techniques can be applied for moisture monitoring. Tuneable diode laser absorption spectroscopy (TDLAS), cavity ringdown spectroscopy (CRDS), intracavity laser spectroscopy (ILS) and Fourier transform infrared spectroscopy (FTIR) are examples of such optical or spectroscopic methods. From these examples especially the TDLAS has increasingly been used for moisture monitoring in natural gases the last years. Hence, this technique will be briefly explained here, even though TDLAS was not tested in this work.

Absorption spectroscopy using diode lasers has been used for determination of gas temperatures and concentrations of various chemical compounds for at least 25 years (Lackner, 2007). During the last decade maturation and improvements of the method have made it popular in numerous applications in industrial process plants. As for most spectroscopic hygrometers, quantitative detection using TDLAS is made possible by the light absorption, at selected wave numbers, as a function of concentration of absorbing species (e.g. water). This can be described by Beer-Lambert's law (Funke et al., 2003):

$$I(v) = I_0(v)e^{-\sigma(v)\cdot N\cdot L} \tag{13}$$

where $I(v)$ represents the intensity of the transmitted light, through the sample, at a frequency v, $I_0(v)$ is the intensity of the incident light, $\sigma(v)$ is the absorption cross section of the light absorbing molecule at frequency v, N is the number of molecules per unit volume in the beam path and L is the path length of the light travelling through the sample.

The relation of Beer-Lambert can be further refined to express proportionality between the concentration and absorbed light:

$$\ln\frac{I_0(v)}{I(v)} = A(v) = \varepsilon(v)Lc \tag{14}$$

where $A(v)$ is the absorbance, $\varepsilon(v)$ is the molar absorption coefficient (molecule specific), L is the path length and c is the concentration of the absorbing species.

The Beer-Lambert relations show that an increase of the optical path length (L) will increase the absorbance and hence the sensitivity of the measurements. For practical reasons the length of a measuring cell is usually limited to a few meters. Various dual-pass or multi-pass cells have been proposed, such as the Herriot cell and the White cell, to increase the path length at the same time as retaining a compact size of the measuring cell. Figure 13 illustrates Beer-Lambert's relation in TDLAS for a dual-pass measuring cell.

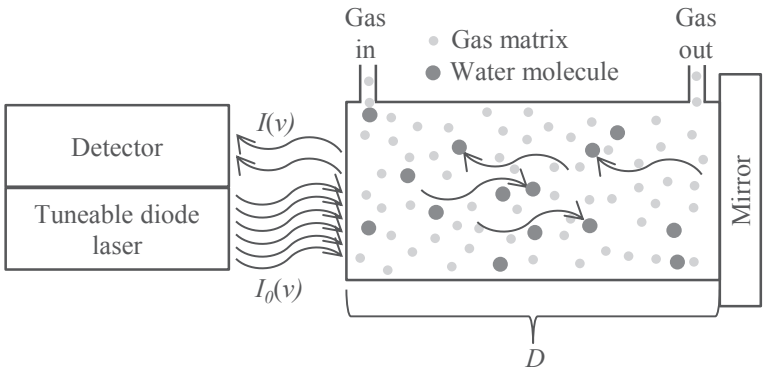

Figure 13: Illustration of Beer-Lambert's law in TDLAS for a dual-pass measuring cell of cell length *D* (path length *L* = 2 x *D*).

Compared to the broadband IR sources for FTIR, the emitted light from diode lasers has an extremely narrow line width, in the order of 10^{-4} cm^{-1}. This enables the resolution of the relevant absorption signals even in the presence of interferences at nearby wavelengths. The simplest approach to TDLAS is direct absorption measurement where the absorption at the line centre is compared with the absorption slightly to the side of the line. This technique is not very much used as measuring a small difference in two large signals gives a rather low detection sensitivity (Linnerud et al., 1998). The use of harmonic detection, the second harmonic usually being the most favourable, with modulation techniques such as wavelength modulation spectroscopy (WMS) significantly enhances the sensitivity of TDLAS. Limitations on detection limits are background moisture levels of the analytical system and interfering species in the gas matrix (Inman and McAndrew, 1994).

3 Experimental set up

3.1 Moisture generator

Several methods for the generation of moisture in gases are described in the literature, such as the two-pressure, two-flow or two-temperature generator (Funke et al., 2003; Hasegava and Little, 1977; Sonntag, 1994; Wiederhold, 1997a). A lot of effort can be made with the aim of producing a stream of gas with a very accurate moisture concentration. Such equipment is often found at national measurement institutes (NMI), such as NPL (National Physical Laboratory, United Kingdom) and NIST (National Institute of Standards and Technology, USA), PTB (Physikalisch-Technische Bundesanstalt, Germany) and NMIJ (National Metrology Institute of Japan). Several publications are published, describing the moisture generators at NIST (Meyer et al., 2010; Meyer et al., 2008; Scace et al., 1997), in addition to a publication describing a gravimetrical reference hygrometer at NIST (Meyer et al., 2010; Meyer et al., 2008; Scace et al., 1997). Recently EURAMET (European association of national metrology institutes) reported a comparison of a number of trace moisture generation facilities at several NMIs (Brewer et al., 2011).

In this work a much simpler moisture generator was established, with the option to mix in a volatile or semivolatile chemical. The equipment is well suited for comparison of hygrometers rather than calibrating them accurately. Having applications for moisture in natural gas in mind, the main focus was to produce a gas with sufficient long term, drift-free and controllable concentrations of both moisture and a volatile chemical. A special version of the test rig was set up for production of equilibrium data for moisture in methane at high pressures.

3.2 Test rig for comparison of hygrometers

A test rig for generation of moisture, alone or in combination with a volatile chemical was established as shown in Figure 14 and Table 2. The test rig was able to generate a stream of nitrogen gas with drift-free concentrations of moisture and methanol or ethylene glycol. The generated gas stream was split up and distributed to a set of hygrometers, denoted as H-1 to H-8 in the Figure 14 and Table 3. Nitrogen gas (> 99.999 % purity) was fed to the test rig at about 4 bar through a pressure regulator (V-1). The gas flow was split in three lines: one line for generation of dry gas for dilution (T-2) and two lines for generation of gas saturated with moisture and methanol or ethylene glycol respectively (T-3 and T-4). Details about the test rig and its operation can be found in papers 1 to 3 (Løkken, 2012a; Løkken, 2012b; Løkken, 2013).

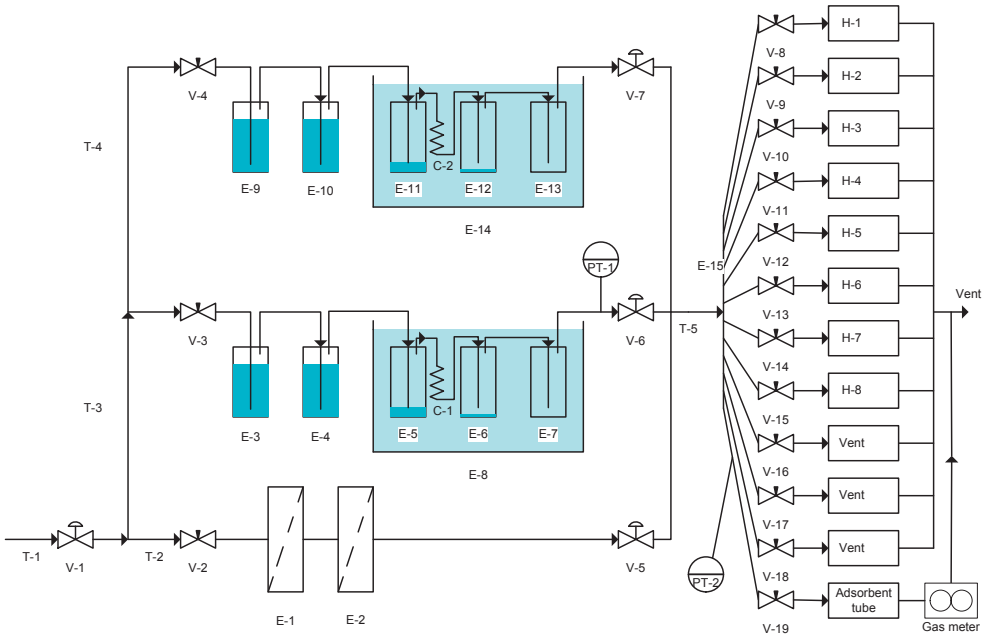

Figure 14: Schematic representation of the test rig. Component identifications and descriptions are found in Table 2.

Table 3: Equipment description, the codes refers to Figure 14.

Code		Description	Model	Manufacturer
V-1		Single stage pressure regulator	SI15	SMT S.A.S., France
V-2 to V-4		Needle valves	3812F4Y	Hoke, USA
V-5		Flow controller	PC 8942	Brooks Instrument, USA
V-6 and V-7		Flow controller	FMC-2000	FlowMatrix Inc., USA
V-8 to V19		Fine metering valve	SS-2MG	Swagelok, USA
E-1 and E-2		Molecular sieves		Ametek, USA
E-3, E-4, E-9 and E-10		Modified filter housings, saturators	Model 122	Headline Filters, UK
E-5 to E-7 and E-11 to E-13		Modified filter housings, condensers	Model 122	Headline Filters, UK
E-8 and E-14		Cooling bath	FP-45	Julabo Labortechnik GmbH, Germany
E-15		Gas manifold	Z12M2	Vici AG International, Switzerland
PT-1		Pressure transmitter	PA-55X	Keller AG, Switzerland
PT-2		Pressure transducer	Model SA	Honeywell, USA
H-1		Capacitor A		
H-2		Capacitor B		
H-3		QCM		
H-4		CaC_2-GC		
	H-4.1	Reactor with grinded calcium carbide	Particles with diameter from 0.3mm to 1mm	Merck KGaA, Germany
	H-4.2	Gas Chromatograph	CP4900 Micro-GC	Varian Inc., USA
	H-4.3	GC separation column	CP-PoraPlot Q, 10 m long, 0.25 mm i.d.	Varian Inc., USA
H-5		Fibre-optic		
H-6		Karl Fischer Titrator	Model 831	Metrohm AG, Switzerland
	H-6.1	Gas meter	TG 1 Mod. 5-8	Ritter, Germany
H-7		Chilled mirror	S4000 Integrale	Michell Instruments ltd., UK
H-8		Electrolytic		
C-1		1 m coil made of 1/8 x 0.035 inch, SS 316L tubing	Sandvik 3R60	AB Sandvik Materials Technology, Sweden
T-1 to T-4		1/8 x 0.035 inch, SS 316L tubing	Sandvik 3R60	AB Sandvik Materials Technology, Sweden
T-5		Treated 1/8 x 0.035 inch SS 316L tubing	Siltek™	Restek Corporation, USA

3.3 Hygrometers

Eight hygrometers, based on capacitor sensor (two different brands), quartz crystal microbalance (QCM), electrolytic cell, CaC_2-GC, fibre-optic sensor, Karl Fischer titration and chilled mirror (continuously operated), have been investigated in the experiments.

The hygrometers were equipped with control units for communication with the probes or sensors and transfer of data to a computer for storage. Data points were stored every 5 minutes. The CaC_2-GC hygrometer consisted of a calcium carbide reactor (H-4.1) for conversion of moisture to ethyne and a micro gas chromatograph (H-4.2) for quantification of ethyne. The micro gas chromatograph was equipped with a separation column (H-4.3) and a micro thermal conductivity detector and was controlled by chromatography software (CP Maitre Elite) on the computer. The processed data from CP Maitre Elite was collected approximately every 10 minutes.

Two direct methods were utilised for reference measurements, not being of interest with respect of continuous online process monitoring. These were a chilled mirror hygrometer (H-7) and a Karl Fischer titrator (H-6). The volume of the titrated gas was measured by a drum-type gas meter (H-6.1). The chilled mirror hygrometer was set up to perform continuous measurements, with storage of data every 5 minutes. The Karl Fischer titrations (between 3 and 9 parallels) were performed manually on weekdays during the experiments.

3.4 Operation of moisture generator

The mixing ratio of the three gas streams (T-2, T-3 and T-4) was controlled by three manually operated flow controllers (V-5, V-6 and V-7). The two gas streams, saturated with moisture and methanol or ethylene glycol respectively, were controlled between 0 and 300 cm^3/min (ambient conditions) with flow controllers (V-6 and V-7), while the dry dilution gas was adjusted to about 6 dm^3/min (ambient conditions) with another flow controller (V-5). The temperature in the cooling bath for line 2 (moisture) was set to 10 °C (±0.01 °C) and the pressure in the condensers was controlled at approximately 4 bar and monitored with a pressure transmitter (PT-1). The temperature in the cooling bath for line 3 (methanol or ethylene glycol) was initially set to -10 °C (±0.01 °C). By changing the settings on the three flow controllers, and eventually changing the temperature in the cooling baths, different concentrations of moisture and methanol or ethylene glycol could be produced and changed quickly. The pressure upstream the metering valves (V-8 to V-19) was about 2 bar, monitored by a pressure transducer (PT-2). The QCM had internal mass flow controllers which needed a sample pressure slightly elevated from atmospheric pressure. The other hygrometers were fed with test gas at ambient pressure. The flow rates to the different hygrometers were controlled in agreement with the recommendations made by the manufacturers. Excess test gas was distributed to vent through 1/8 inch stainless steel tubing

connected to the spare ports on the compact gas manifold (E-15). Fine metering valves (V-15 to V19) were used to control the flow rates also on these gas streams.

The gas upstream V6 and V7 was expected to be saturated with respect to water and methanol or ethylene glycol respectively. The gas temperature decrease due to Joule Thomson cooling, when reducing the pressure from 4 to 2 bar, was compensated with a temperature increase in the system from 10 °C (water) and -10 °C (methanol or ethylene glycol) towards 25 °C (room temperature) prior to pressure reduction. This temperature increase, combined with dilution with dry nitrogen, prevented condensation of water and methanol or ethylene glycol associated with the pressure reduction step.

3.5 Test rig for production of equilibrium data at high pressures for moisture in methane and natural gas

To be able to generate high pressure gas saturated with water vapour, the test rig used for comparison of hygrometers was slightly modified. Only one of the saturation lines was used, and the flow controller (V6/V7) was replaced by an electrical heated high pressure regulator (HPR-2 series from GO regulators, USA). Safety valves were installed to reduce risks involved with high pressure experiments. Details about this rig can be found in paper 4 (Løkken et al., 2008).

4 Summary of the included papers

4.1 Paper I

Comparison of hygrometers for monitoring of water vapour in natural gas

In this paper a collection of hygrometers, relevant for the natural gas industry, were compared with respect to accuracy, long term stability and response time. The hygrometers were based on capacitor sensor, quartz crystal microbalance (QCM), electrolytic cell, fibre-optic sensor and reaction GC (CaC_2-GC), respectively. Monitoring of moisture concentrations between 20 µmol/mol and 120 µmol/mol was carried out in the laboratory, using nitrogen as the matrix gas. The chosen concentration range is typical for many natural gases after dehydration at gas production platforms in the North Sea and the Norwegian Sea.

In Figure 15 the overall results from the experiments, performed over 39 days, are shown. The moisture concentration levels, expressed as frost points in Figure 15, were step changed four times during the experiments (on day 16, 23, 35 and 36).

The capacitor hygrometers and the electrolytic cell hygrometer showed a tendency to drift, which reduced their accuracy. The QCM, fibre-optic and CaC_2-GC hygrometer showed good accuracy and long term stability. The QCM hygrometer had the overall shortest response times, as illustrated in Figure 16 and Figure 17. The fact that this hygrometer is based on a non-equilibrium sensor is believed to be one explanation for the superiority of this hygrometer with regards to speed of response. For the capacitor, the CaC2-GC and the fibre-optic hygrometers, porous micro structures with given adsorption, desorption and diffusion kinetics are involved. Hence it is expected that performance depends on parameters like chemical composition, thickness and pore size distribution of the porous micro structure. Also the operating temperature will presumably play an important role. With this in mind one would expect to find different performances among hygrometers, even if they are based on the same technology.

The results generally demonstrated the need for careful quality control of the hygrometers, and monitoring systems which are thoroughly adapted to meet the requirements of individual natural gas applications.

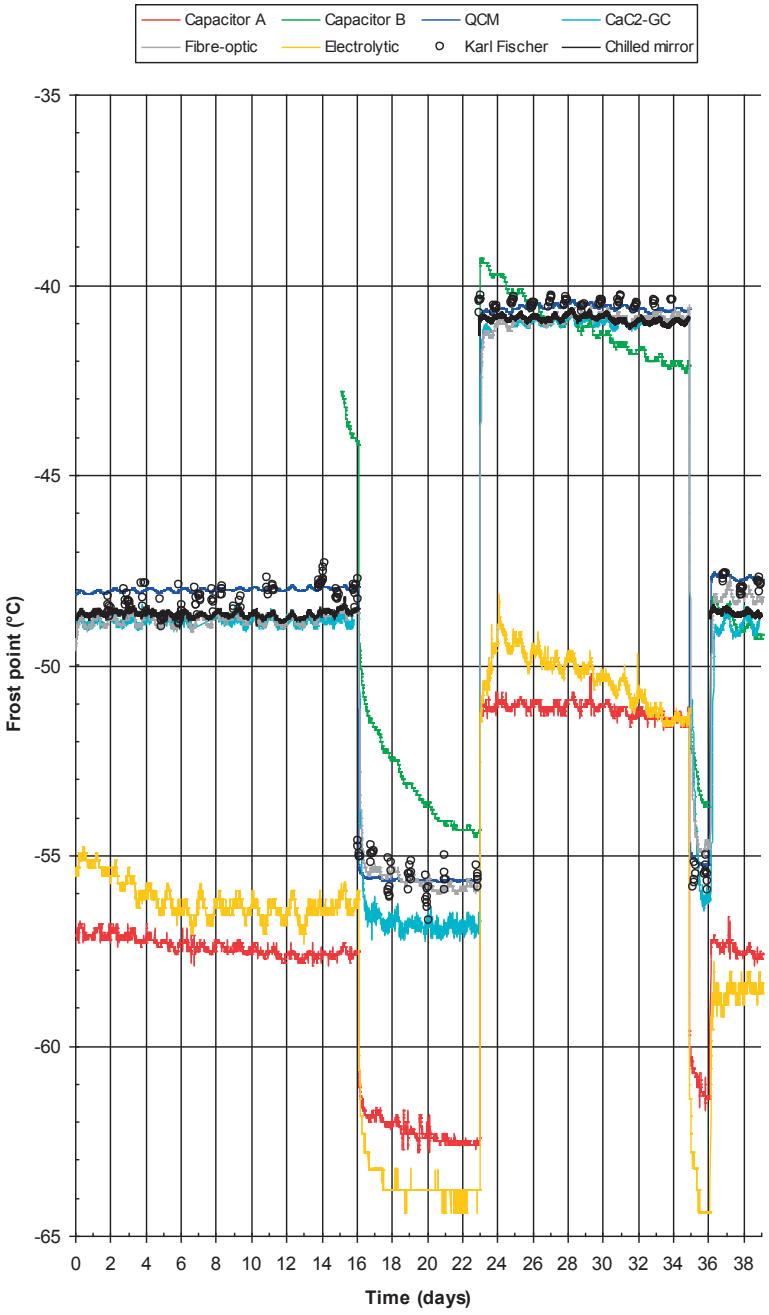

Figure 15: Readings from the moisture monitors during 39 days of experiments, moisture content expressed as frost point (°C). The chilled mirror was unable to cool the mirror sufficiently to produce data at the lowest frost point regions. A new capacitor sensor of brand B replaced a malfunctioning one on day 15.

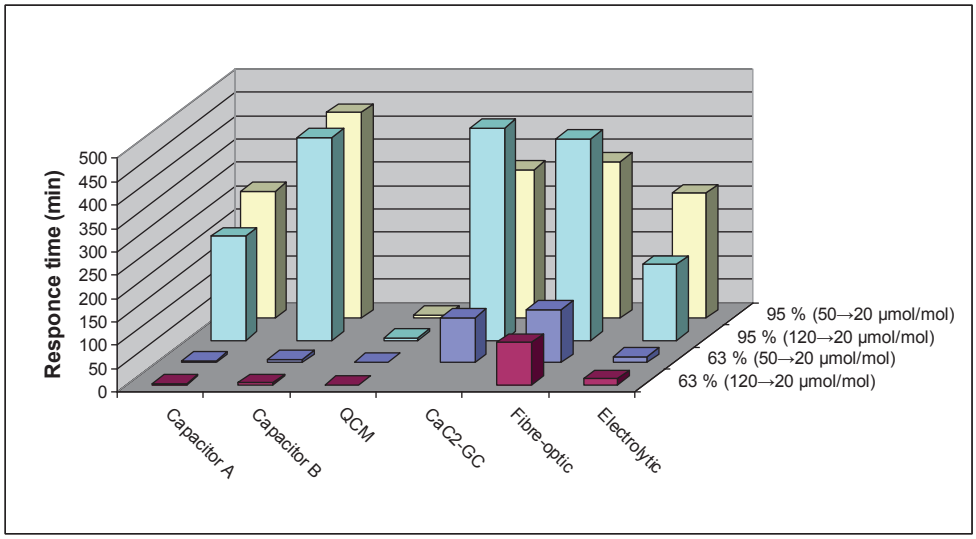

Figure 16: Response times for decreasing moisture concentrations for changes of 63 % and 95 % of the step changes.

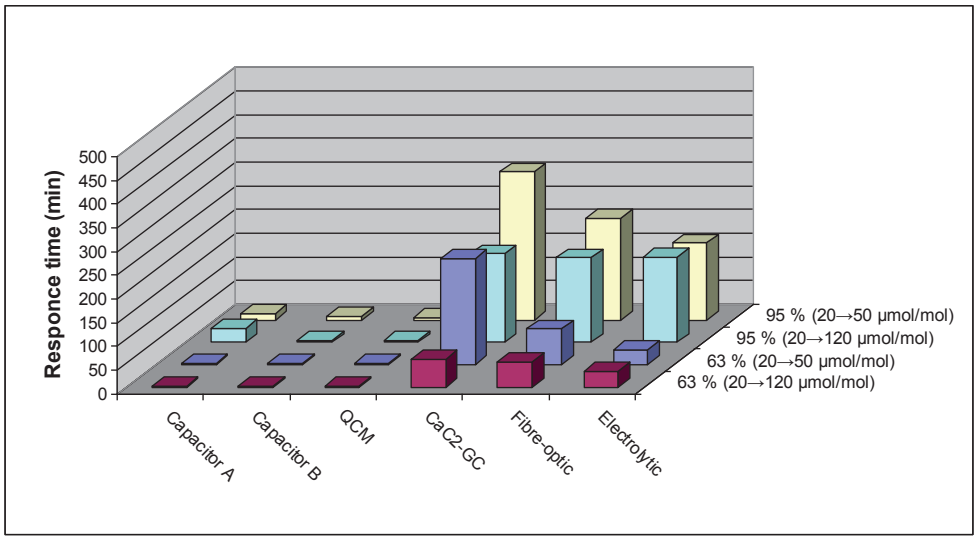

Figure 17: Response times for increasing moisture concentrations for changes of 63 % and 95 % of the step changes.

4.2 Paper II

Water vapour monitoring in natural gas in the presence of methanol

In paper II the same collection of hygrometers, as for paper I, was compared for monitoring of moisture with co-exposure of methanol. While monitoring moisture

at the level of 45 µmol/mol, the hygrometers were exposed to approximately 10, 170 and 750 µmol/mol gaseous methanol respectively. The experiments were performed in the laboratory, using nitrogen as the matrix gas.

The overall results of 34 days of experiments are demonstrated in Figure 18 and Figure 19. Figure 18 includes results from the hygrometers originally returning frost point readings, while Figure 19 includes results from the hygrometers originally returning concentration readings. Results from the reference techniques are included in both figures, using the formulas published by Sonntag (Sonntag, 1990; Sonntag, 1994) for conversions between frost point and concentration. The methanol concentration level, quantified by gas chromatography, was increased from 10 to 170 µmol/mol after 6 days and further increased to 750 µmol/mol on day 13. From day 14 the methanol concentration decreased, reaching a level of less than 10 µmol/mol after day 22. The decreasing methanol concentration from day 14 was caused by reduced level of methanol in the saturator (consumption) leading to insufficient saturation of methanol in the saturator.

Stable readings from the chilled mirror hygrometer were not obtained during exposure to methanol concentrations at 170 and 750 µmol/mol. For this reason data from the chilled mirror is left out from Figure 18 and Figure 19, during this exposure to medium and high concentrations of methanol.

Exposure to approximately 10 µmol/mol methanol demonstrated no clear effect on the tested hygrometers. At the higher levels of 170 µmol/mol and 750 µmol/mol methanol, the readings from several hygrometers were affected. Taken into account the specified uncertainty of the hygrometers, only the electrolytic cell and one of the two tested capacitor sensors (Capacitor B) were significantly affected during the test period. These two hygrometers demonstrated severe misreading as a result of methanol exposure. The readings from the fibre-optic sensor drifted slowly upwards during exposure to the higher methanol levels. The drift speed increased with increasing methanol concentration. However, despite the drift, the readings from the fibre-optic sensor stayed within its specified uncertainty (± 2 °C) during the test period. The QCM made a minor shift to higher readings when exposed to 750 µmol/mol methanol. Similar shifts were noticed for the two different brands of capacitor sensors tested. Both capacitor sensors also demonstrated a permanent downward drift during the experiments, one of them increasing the drift speed upon increased methanol concentration. The CaC2-GC did not show any clear influence from methanol.

The results imply that methanol exposure should be taken into consideration when choosing equipment for moisture monitoring and when determining a quality control strategy for the monitoring.

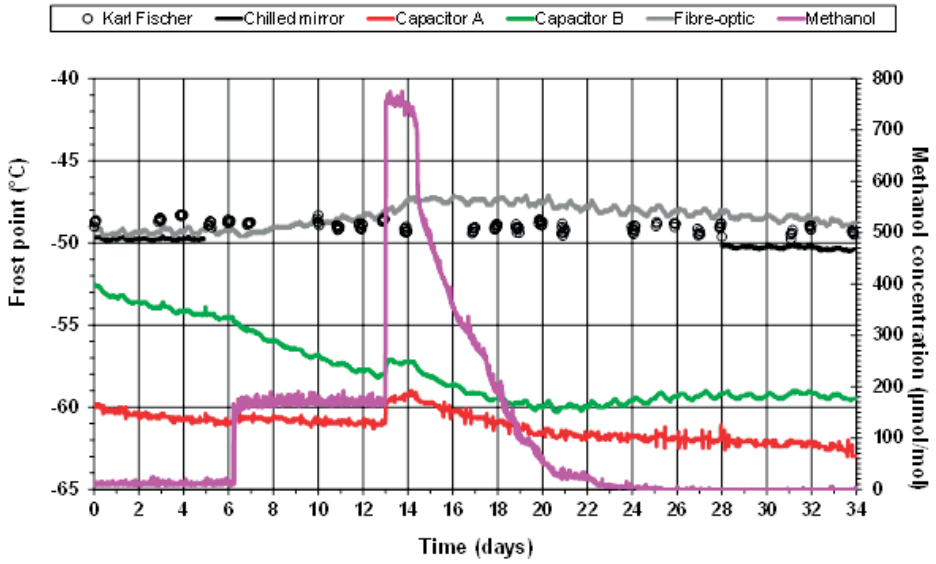

Figure 18: Frost point readings from Capacitor A, Capacitor B and Fibre-optic, at a moisture concentration level of 45 µmol/mol during variable methanol exposure, together with readings from the reference hygrometers (Karl Fischer and Chilled mirror). The methanol concentration is plotted against the secondary y-axis. The chilled mirror readings are plotted only at the lowest methanol exposures due to interferences at the higher methanol concentrations.

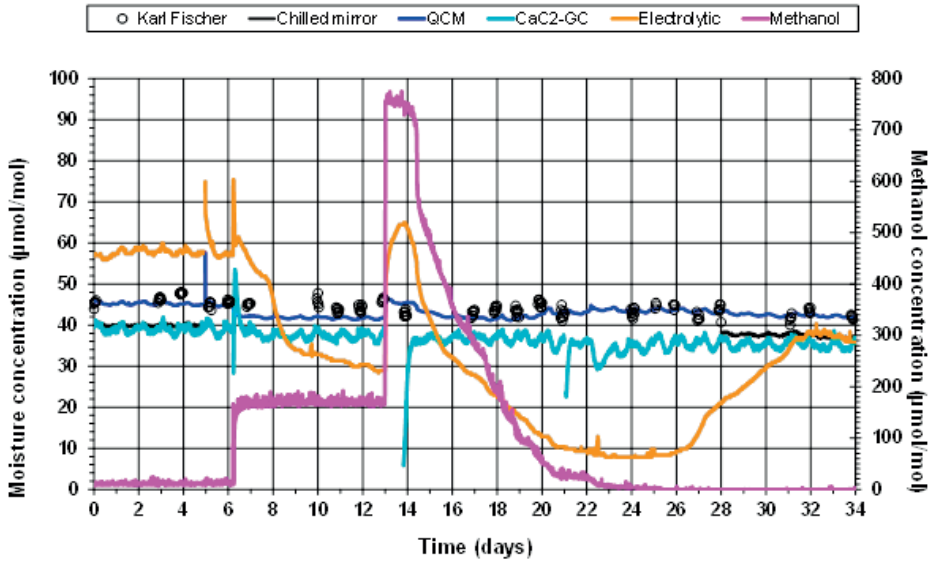

Figure 19: Moisture concentration readings from QCM, CaC2-GC and Electrolytic, at a moisture concentration level of 45 µmol/mol during variable methanol exposure, together with readings from the reference hygrometers (Karl Fischer and Chilled mirror). The methanol concentration is plotted against the secondary y-axis. The chilled mirror readings are plotted only at the lowest methanol exposures due to interferences at the higher methanol concentrations.

4.3 Paper III

Water vapour measurements in natural gas in the presence of ethylene glycol

In paper III, an investigation of hygrometers for monitoring of moisture in natural gas has been performed, with respect to response on ethylene glycol co-exposure. The tested hygrometers are based on capacitor sensor, quartz crystal microbalance (QCM), fibre-optic sensor and reaction GC (CaC_2-GC). The electrolytic cell hygrometer (available for paper 2 and 3), was not available during this investigation, due to severe technical problems. The moisture concentration level in the test gas was 50 µmol/mol during the experiments, corresponding to a frost point of approximately -48 °C (atmospheric pressure). The experiments were performed in the laboratory, using nitrogen as matrix gas.

The overall results of 33 days of experiments are demonstrated in Figure 20. On day 6, ethylene glycol at a level of 0.25 µmol/mol was introduced to the test gas. On day 20 the ethylene glycol concentration was increased to 0.65 µmol/mol. The ethylene glycol exposure was terminated from day 26. An analytical system based on thermal desorption, gas chromatographic separation and mass spectrometric detection (TD-GC/MS) was used for the quantification of ethylene glycol.

The QCM hygrometer responded with a downward drift of the frost point readings in the presence of ethylene glycol. The drift increased when the ethylene glycol concentration increased from 0.25 µmol/mol to 0.65 µmol/mol, and the frost point readings from the QCM hygrometer decreased close to 5 °C during a total of 20 days of ethylene glycol exposure. The QCM hygrometer seemed to recover slowly from the ethylene glycol exposure, indicated by a decreasing upward drift as soon as the ethylene glycol exposure terminated.

Both tested capacitor hygrometers responded significantly to ethylene glycol exposure. The responses were not uniform, though, with one performing considerably better than the other one.

The experiments also demonstrated the insufficiency of chilled mirror techniques for interpreting water frost points or water dew points, with subsequent moisture concentration calculation, in the presence of ethylene glycol. The chilled mirror frost point readings increased with approximately 20 and 27 °C during exposure to 0.25 and 0.65 µmol/mol ethylene glycol, respectively (not shown in Figure 20). This made the chilled mirror technique totally unsuitable for reference measurements after the introduction of even sub ppm levels of ethylene glycol to the test gas.

The fibre-optic sensor hygrometer and the CaC2-GC hygrometer showed minor response for ethylene glycol.

In general the results from this work demonstrate the need for careful evaluation of individual moisture monitoring applications, before choosing a hygrometer. A well-considered strategy for quality control of the moisture monitoring, regardless of the chosen hygrometer, is of utmost importance to establish a moisture monitoring system with high accuracy.

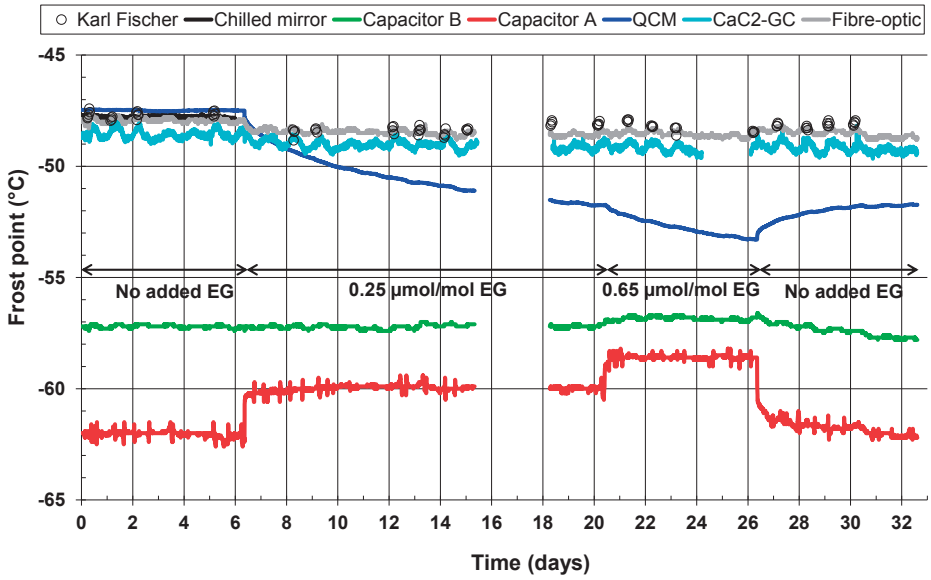

Figure 20: Frost point readings of the tested hygrometers during co-exposure to ethylene glycol, at a moisture concentration level of 50 µmol/mol (corresponding to a frost point of approximately -48 °C).

4.4 Paper IV

Water content of high pressure natural gas: Data, prediction and experience from field

This conference paper presents phase behaviour of natural gases with focus on saturation points and phase behaviour for water and selected trace components, such as glycols. Included is also a discussion on various methods for water dew point control (dehydration and analysis) and a review of published methods (graphical-, empirical- and thermodynamic models) for the calculation of equilibrium water concentration or water dew point in natural gas. Phase behaviour is related to the various dehydration processes used for dew point control of natural gases and the paper describes why various water related saturation points have to be considered in the design and operation of gas production and transport systems. The thermodynamic model discussed in this work is based on the Cubic Plus

Association Equation of State (CPA-EoS) combined with thermodynamic models for the ice and gas hydrate phase.

Experiences from selected gas processing plants in operation related to the formation of liquid water, an aqueous phase, natural gas hydrate or ice in process equipment and pipelines are presented and discussed. The experiences from these situations are compared to results from experimental and modelling work.

New experimental data for water concentration in methane and natural gas, in stable equilibrium with liquid water, ice and natural gas hydrate are presented, for the temperature range of -20 to 20 °C, and pressures of 50, 100 and 150 bar. The data are summarised in Table 4 for the methane and Table 5 for a rich natural gas. An evaluation of conventional methods for calculation of equilibrium water vapour concentration and water dew point is presented and these methods are compared with calculations performed with the CPA-EoS.

Table 4: Measured gas phase water concentration (µmol/mol) for the binary system water – methane, at various temperatures and pressures.

T/ºC	50 bar	100 bar	150 bar
-20	31	19	19
-10	73	40	35
0	172	80	82
10	273	168	151
20	483	320	297

Table 5: Measured gas phase water concentration (µmol/mol) for the water - natural gas system, at various temperatures and pressures.

T/ºC	100 bar	150 bar
-20	22	19
-10	41	37
0	86	72
10	178	150
20	341	291

The CPA-EoS is shown to give excellent result, both for the calculation of equilibrium water content of natural gas, water dew point-, natural gas hydrate- and ice precipitation temperature as well as the aqueous dew points. The model is compared to the ISO 18453 (GERG-water-EoS) developed for water dew point calculation of natural gas, with a primary working range of 5 bar to 100 bar and -5 °C to 15 °C. Within this working range CPA-EoS and ISO 18453 generally agree

well, as illustrated in Figure 21. Outside the working range for ISO 18453, calculated data from CPA-EoS are superior, as illustrated in Figure 22. An accurate chart for graphical reading of water content of a sweet natural gas is presented. The method and data presented in this paper can be used in design of water removal processes.

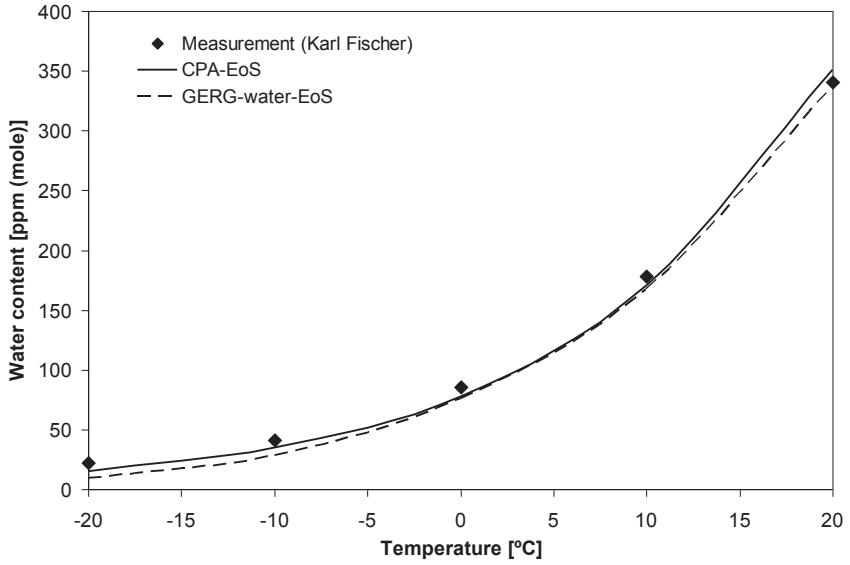

Figure 21: CPA-EoS and ISO 18453 (GERG-water-EoS) compared for calculation of gas phase moisture concentration in natural gas at 100 bar.

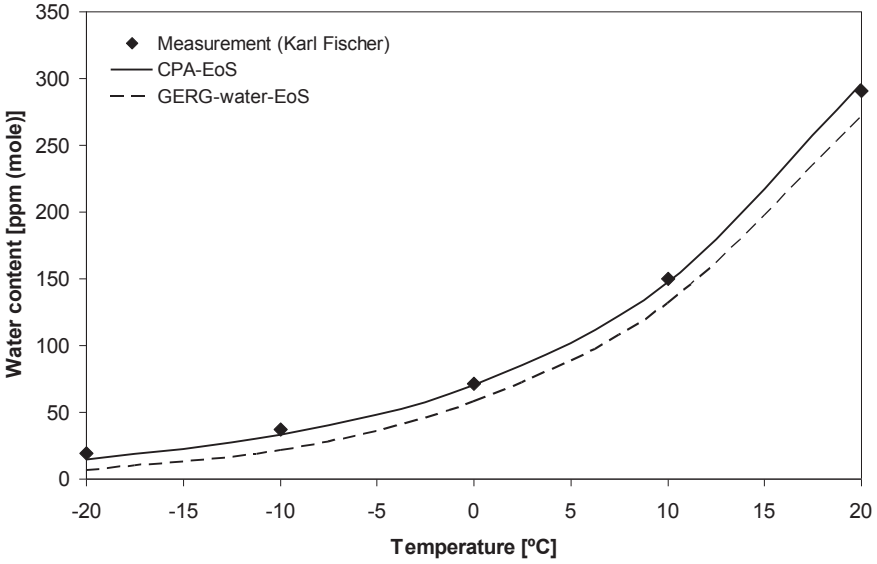

Figure 22: CPA-EoS and ISO 18453 (GERG-water-EoS) compared for gas phase moisture concentration in natural gas at 150 bar.

5 Application of results for natural gas industry

5.1 Nitrogen versus natural gas as gas matrix

A general rule of thumb when it comes to analytical chemistry is to use a test matrix (gas or liquid) as similar as possible to the real samples. For various reasons experimental work often has to be performed using simplifications. The parameters studied in this work, and the working principles of the hygrometers included in the experiments, were evaluated to be rather unaffected by the choice of matrix gases. Moreover the main focus for this work has been comparisons of the hygrometers rather than determining absolute values representing the test parameters. Hence nitrogen was chosen as the matrix gas, as this increased the feasibility and safety of performing controlled long term experiments in a multiuse laboratory. Even though similar experiments should ideally have been performed using real natural gases, the findings using nitrogen are regarded as highly relevant for natural gas applications.

5.2 Sampling of natural gas for moisture monitoring

ISO 10715:2001, GPA 2166-05 and API MPMS 14.1 (API, 2006; GPA, 2005; ISO, 2001) are industry standards which all describe how to do sampling of high pressure natural gas in a proper manner. The standards focus on the protection of the measuring devices as well as assuring a representative sample from the main gas stream. Sampling of gas close to or at their dew point, with respect of hydrocarbons or aqueous phase, should be avoided to prevent liquids from entering the sampling system. It should be strived to follow the guidelines described in these standards, as a first step in designing an adequate sampling system for moisture measurements.

As water is very adsorptive, the response time of moisture measurements will benefit greatly from the use of electropolished and heated surfaces in contact with the gas sample. Vendor information available at the internet (http://www.silcotek.com/silcod-technologies/coating-technical-literature) suggest that silica treated surfaces, such as the tubing used upstream of the hygrometers in these experiments (Siltek™, Restek Corporation, USA), will decrease the response time even more compared to electropolished tubing. A shortest possible, low volume sample pathway, especially for the high pressure sections of moisture monitoring systems, is also a very important measure, to reduce both response time and uncertainty in moisture measurements. In addition a geometry preventing liquid accumulation and minimal use of components introducing dead ends and highly adsorptive surfaces is beneficial. For moisture monitors performing their measurements at reduced pressure, the pressure reduction step is critical. Due to the

Joule Thomsen cooling of the gas, enough heat must be provided to maintain the gas at temperatures well above the dew point temperatures. For large pressure drops usually more than one heated pressure reduction step will be necessary. Keeping the entire measuring and sampling system heated at a stable temperature will provide more stable measurements, as even small temperature variations will tend to disturb the equilibrium of water, which will be monitored by the hygrometer.

At natural gas processing plants at least two types of sampling points are frequently found. One is just downstream of the dehydration units, typically triethylene glycol (TEG) contactors, and one is at the point of gas export. Moisture monitoring just downstream TEG contactors is often problematic, due to the fact that this gas will be saturated with TEG. Any pressure or temperature drop for this gas will lead to the condensation of highly concentrated TEG (containing small amounts of water), which will generate great challenges to the sampling system. In addition to the equilibrium concentration of TEG in the gas, entrained liquid TEG also might be present in this gas, depending on the operation conditions and design of the TEG contactor. A comprehensive sampling system which can deal with liquid TEG is an absolute necessity in this case, to avoid low accuracy or even malfunction of the hygrometers. Ideally liquid TEG should be prevented from entering the sampling system, which can be achieved by the use of a sampling probe with a membrane filter. If a traditional sampling probe without a membrane is used, the temperature and the pressure of the sample stream must be kept at process conditions, to prevent the gas composition to be changed due to condensation or vaporisation of TEG. A liquid filter (e.g. a membrane filter) has to be used before the sample is introduced to the sensor of the hygrometer or the pressure reducer. Lack of such filtering will lead to severe contamination of the sensor and the sample will lose its representativeness. A gas scrubber and a compression stage is commonly utilised upstream the point of gas export. The separation of liquids in addition to the provided heat and pressure during compression will move the gas away from its dew point line for TEG, and sampling of a one phase gas can be obtained. These are the reasons why accurate moisture monitoring is achieved more easily for the export gas.

When setting up a moisture monitoring application it is important that the sampling is discussed and if possible agreed upon with the supplier of the hygrometer. Often the supplier of the sampling system is not the same as the supplier of the hygrometer. This focus on the sampling system, in addition to the hygrometer, will generally result in an increased accuracy of the moisture monitoring. It will also prevent the supplier of the hygrometer from blaming issues with the moisture measurements on the sampling system.

5.3 Quality control strategy for moisture measurements

Claimed uncertainties of hygrometers
Throughout this work it soon became very clear that a carefully prepared quality control strategy is crucial for accurate moisture monitoring. All hygrometers have their uncertainties defined by their suppliers, but care must be taken to keep the hygrometers within these uncertainties. Also, dependent of the application, the recommended frequency of maintenance and recalibration is generally too low, to allow the hygrometers to stay within specification when it comes to accuracy.

Quality control with portable hygrometers
Today there is a widespread use of portable hygrometers for spot checks of online hygrometers. For this strategy to work adequately, the portable hygrometers must be under strict quality control. This is usually achieved by the means of a certified moisture standard and a dried (with respect to water) gas representing the "zero point". The certified moisture standard is usually chosen at a moisture concentration close to some specified limited moisture concentration (e.g. transport specification). In case of significant deviations between the moisture concentrations read by the online hygrometer and the portable hygrometer, the calibration of the online hygrometer has to be adjusted to fit the reading of the portable hygrometer. The frequency of the spot checks with the portable hygrometer is typically dictated by the performance of the online hygrometer and the need for accuracy of the moisture measurements.

Automated calibration verification
Some of the commercially available hygrometers today have some way of automatically checking the validity of their calibration. This is usually achieved by utilising one or several certified calibration gases, or using a permeation tube device, which can generate a certified concentration of moisture. Some hygrometers can also be equipped with an adsorption unit to produce a gas virtually free of water, to provide a "zero point" check of the hygrometer. At some user set frequency, the calibration can be adjusted to fit, either one or both of, this certified concentration of moisture and the "zero point", respectively. During long term use, calibration gases are consumed, the permeation tubes are depleted, and driers become saturated. Hence, good routines are needed to assure change of these components before they become exhausted and introduce errors to the moisture monitoring. The quality of certified calibration gases, for highly adsorptive components like moisture, is easily degraded by improper use. The precautions described for the sampling of natural gas is more or less valid also for the calibration gases (short sample pathway, electropolished tubing, temperature control etc.). The investment costs of a hygrometer with automated calibration verification will be higher compared to a hygrometer without such an option. On the other hand a strategy with use of portable spot checking will introduce extra man hours and the need of additional equipment in a local laboratory. Sufficiently trained and dedicated operators will be needed, assuring that both the portable

equipment is accurate at all times and that the spot checks are performed in a proper manner.

Moisture monitoring at high versus low pressure
Moisture monitoring at high sample pressures has traditionally been a widespread practice in the natural gas industry. To maintain the sample integrity, measurements are performed at sample line pressure or at some intermediate pressure as specified by a dew point or frost point sales or transport specification. Hygrometers for high pressure measurements are typically calibrated at ambient pressure to provide traceability to national or international standards. High pressure measurements will break this traceability chain and increase the uncertainty of the measurements. Quality control is often performed by use of portable hygrometers operating at ambient pressure. This practice usually generates the need for conversions of frost points (sub-zero temperatures) at one pressure to a corresponding frost point at another pressure, eventually combined with conversion of units (e.g. between °C and µmol/mol). The conversions can be subject to large uncertainties and errors, as available conversion tools are generally unsuited for calculations at elevated pressures involving frost points. At ambient pressure the conversions between different units can be performed with reliable conversion methods (e.g. formulas of Sonntag (Sonntag, 1990; Sonntag, 1994)), and the measurements can be related to certified standards (e.g. reference gas standards or permeation tubes). Hence, presumed that the sampling system is adequate, moisture monitoring at ambient pressure will make quality control easier and generally reduce the measurement uncertainty.

Focus on the application
A good quality control strategy for moisture monitoring should always be adapted to the application. Hence, the users will have to evaluate their specific needs of measuring range and accuracy, as well as potential contaminants, before choosing a suitable hygrometer and preparing a quality control strategy for the moisture monitoring. The sampling system must also be taken into account, as there is little use for a highly accurate hygrometer if it is fed with a non-representative gas sample.

6 Future aspects of moisture monitoring

In this work the focus has been on moisture measurement and monitoring in natural gases for applications involving moisture concentrations in low to medium parts per million levels. Typical relevant applications are moisture monitoring of rich natural gases, processed for pipeline transport to onshore process plants, and moisture monitoring of dry sales gases, processed for pipeline export and household usage. Such production sites are found both onshore and offshore. Suppliers of hygrometers are still developing new hygrometers and try to improve existing versions. Recently, users' consciousness with respect to accuracy and quality control of hygrometers has improved, which has influenced the suppliers of hygrometers and sampling systems. Suppliers have increasingly focused on automated quality control of hygrometers, which will be appreciated by many users.

Some process plants will have to dehydrate the natural gas to generate moisture concentrations at parts per billion levels. This is necessary for LNG production and other processes involving very low temperatures. For this dehydration various molecular sieves are usually utilised, and the downstream low temperature process steps will be very sensitive to moisture. This introduces moisture monitoring applications which reach even higher levels of complexity than applications dealt with in this work.

Many of the measuring techniques used in this work are also able to detect moisture at parts per billion moisture levels, but often the suppliers have special versions of their hygrometers meant to be fitted for these low moisture levels. Such applications are extremely sensitive to the sampling systems, and more than ever prone to erroneous measurements and long response times caused by adsorption along the sample pathway.

The high expenses of process upsets caused by moisture leading to ice or hydrate formation in such cold processes, will motivate both users and suppliers to improve the accuracy of these hygrometers. In addition there is a high potential for savings when prolonging the cycles between regeneration of molecular sieve units, this way extending the lifetime of these units. This can be achieved by using reliable moisture monitors to determine when to perform regenerations, instead of using fixed time intervals. Improvement of accessibility of reliable methods for verifying the calibration of hygrometers, together with stringent quality control routines, will be crucial for success in these extremely demanding applications.

7 Summary conclusions

Moisture monitoring in natural gas is an important task in the natural gas industry. There is a great variety of applications, with different demands for sensitivity, regularity, accuracy and response time. Common for these applications is that they all aim to maintain a safe, stable and economic production and transportation of hydrocarbon products. Detailed knowledge about various measurement techniques is needed, to be able to design appropriate measurement or monitoring systems, adapted to the individual applications. The same knowledge is also needed to diagnose, evaluate and improve the accuracy of existing monitoring systems.

If estimation of moisture concentration in the absence of moisture measurements is needed, accurate thermodynamic models are required. Such thermodynamic models have to be verified with experimental equilibrium data. Accurate moisture measurements are necessary to facilitate the generation of such equilibrium data from laboratory experiments.

A collection of hygrometers relevant for the natural gas industry is tested. The tested hygrometers are based on capacitor sensor, quartz crystal microbalance (QCM), electrolytic cell, fibre-optic sensor and reaction GC (CaC_2-GC), respectively. In the latter technique ethyne (converted from water) is quantified by a gas chromatograph (GC). Karl Fischer titration and chilled mirror hygrometry are utilised as reference measurements. Three series of long term (> 30 days) laboratory experiments have been performed, comparing the hygrometers:

1) Monitoring of moisture in nitrogen at concentration between 20 and 120 parts per million (µmol/mol), comparing the hygrometers with respect to accuracy, long term stability and response time.
2) Monitoring of moisture in nitrogen at the concentration level of 45 parts per million (µmol/mol), in the presence of methanol at 10, 170 and 750 parts per million (µmol/mol) levels respectively.
3) Monitoring of moisture in nitrogen at the concentration level of 45 parts per million (µmol/mol), in the presence of ethylene glycol at 250 and 660 parts per billion (nmol/mol) levels respectively.

The results from this work demonstrate that various hygrometers perform very differently with respect to accuracy, stability and response time. Moreover, methanol and ethylene glycol exposure is shown to have the potential of interfering with moisture monitoring.

The capacitor hygrometers showed a general tendency to drift, which reduced their accuracy. The drift decreased with time, which implies that it would be better to adjust the calibration of capacitor sensors after some period of time in operation, compared to exchanging to new sensors. The response times of the capacitor hygrometers were quite low for increasing moisture concentration, but high for

decreasing moisture concentrations. One of the two tested capacitor sensors (Capacitor B) demonstrated severe moisture misreading as a result of methanol exposure at 170 and 750 parts per million. Minor shifts to higher moisture readings when exposed to 750 µmol/mol methanol were observed for the two different brands of capacitor sensors tested. Both capacitor sensors also demonstrated a permanent downward drift during exposure to methanol, one of them increasing the drift upon increased methanol concentration. To ethylene glycol exposure, both tested capacitor hygrometers responded significantly. The responses were not uniform, though, with one performing considerably better than the other one.

The QCM hygrometer showed good accuracy and long term stability. This hygrometer also demonstrated the overall shortest response times. The fact that this hygrometer is based on a non-equilibrium sensor is believed to be one explanation for the superiority of this hygrometer with regard to speed of response. A minor shift to higher moisture readings was observed when exposed to 750 parts per million methanol. In the presence of traces of ethylene glycol a downward drift was seen. The drift increased initially when the ethylene glycol concentration increased from 250 to 660 parts per billion. The drift was estimated to 5 °C (frost point) during a total of 20 days of ethylene glycol exposure. The QCM hygrometer seemed to recover slowly from the ethylene glycol exposure, indicated by a decreasing upward drift as soon as the ethylene glycol exposure ended.

The electrolytic cell hygrometer tested in this work showed a tendency to drift, reducing its accuracy. Its response times were also generally high, both for increasing and decreasing moisture concentrations. Serious misreading as a result of methanol exposure was demonstrated for this hygrometer. Prior to the experiments with ethylene glycol co-exposure the electrolytic cell hygrometer broke down and was excluded from the last series of experiments.

The fibre-optic hygrometer generally proved good accuracy and long term stability. At the same time this hygrometer was one of the slowest responding hygrometers, with long response times for both increasing and decreasing moisture concentrations. Though staying within its specified uncertainty, the readings from the fibre-optic sensor drifted slowly upwards during exposure to the higher methanol levels. The drift increased with increasing methanol concentration. The fibre-optic sensor hygrometer showed no significant response for ethylene glycol.

The reaction GC hygrometer generally demonstrated good accuracy and long term stability. This was overall the slowest responding hygrometer in the performed experiments. Neither methanol nor ethylene glycol exposure provoked any significant response on the moisture readings for the reaction GC hygrometer.

The reference techniques, revealed some limitations during the experiments. The chilled mirror, which performed generally best with regards to accuracy, did not have enough cooling power for the lowest moisture concentrations. There are chilled mirror instruments on the marked being able to cool down to -100 °C, but

such an instrument was not available for these experiments. As expected, the chilled mirror technique was unable to return reliable frost points during co-exposure to methanol and ethylene glycol. These polar compounds condense or precipitate together with water on the mirror surface, at temperatures not representative for the pure water dew or frost point. The Karl Fisher technique was not affected by methanol or ethylene glycol. Hence, this technique could be used for reference measurements during all of the performed experiments. On the other hand, Karl Fischer titrations have more steps contributing with measurement uncertainties, generally reducing the accuracy and the precision of this technique compared to the chilled mirror technique.

The experiments indicate that properties of hygrometers are closely connected to sorption phenomena and equilibrium conditions of water. The relatively small molecular size and high adsorptivity of water, cause water to migrate into porous micro structures and stick to surfaces. Hence, it is believed that increased working temperature and miniaturisation of available surface areas for both sensors and other components of the hygrometer, sampling system included, will improve the general performance of hygrometers.

A modified version of the test rig was used to produce a hydrocarbon gas saturated with water at high pressures. New data for the equilibrium water concentration in methane and a natural gas were produced, for the temperature range of -20 to 20 ºC and for pressures up to 150 bar. The data were used to verify the Cubic Plus Association Equation of State (CPA-EoS). When compared with conventional methods (graphical-, empirical- and thermodynamic models) for determination of equilibrium water vapour concentrations and water dew, frost or hydrate points, the CPA-EoS demonstrated excellent results. The CPA-EoS model was also compared to the ISO 18453 developed for water dew point calculation of natural gas. The CPA-EoS demonstrated good agreement with ISO 18453, but was applicable to wider ranges of pressure, temperature and gas composition. An accurate chart for graphical reading of water content of a sweet natural gas was presented. The methods and data presented in this paper can be helpful in the design of water removal processes.

In general the results from this work demonstrate the need for careful evaluation of individual moisture monitoring applications, before choosing a hygrometer. This evaluation should be made with special attention to the presence of polar chemicals. A well-considered strategy for quality control of the moisture monitoring, regardless of the chosen hygrometer, is of utmost importance, to establish a moisture monitoring system with high accuracy.

8 Literature

Althaus, K., 1999. Messung und Berechnung von Wassergehalten kohlenwasserstoffhaltiger Gasgemische. Fortschritt-Berichte VDI, Row 3, no. 590. VDI Verlag GmbH, Düsseldorf, 193 pp.

API, 2006. API MPMS 14.1: Collecting and Handling of Natural Gas Samples for Custody Transfer. American Petroleum Institute, Washington, DC.

Bahadori, A. and Vuthaluru, H.B., 2010. Prediction of methanol loss in vapor phase during gas hydrate inhibition using Arrhenius-type functions. J Loss Prevent Proc, 23(3): 379-384.

Betts, F.C.J. and Lay, A.G., 1996. Sour Gas Dehydration In Mobile Bay, Annual Offshore Technology Conference. Offshore Technology Conference, Houston, Texas, pp. 419-426.

Black, S.D., 1979. Piezoelectric and electrolytic methods of moisture measurement in gases, Measurement technology for the 80's. Analysis Instrumentation. ISA, Newark, Delaware, pp. 187-190.

Blakemore, C.B., Steichen, J.C., Dallas, G. and Rossum, G.J.v., 1986. Continuous trace moisture analysis. In: G.J.v. Rossum (Editor), Gas Quality. Elsevier Science Publishers B.V., Groningen, pp. 327-335.

Brewer, P.J. et al., 2011. EURAMET 1002: International comparability in measurements of trace water vapour. NPL Report AS 59, National Physical Laboratory, Teddington, Middlesex.

Bruttel, P.A. and Regina, S., 2006. Water determination by Karl Fischer Titration. Monograph 8.026.5003, Metrohm Ltd., Herisau.

Bukacek, R.F., 1955. Equilibrium Moisture Content of Natural Gases. Research Bulletin 8, Institute of gas technology, Chicago.

Campbell, J.M., 1994. The Equipment Modules. Gas conditioning and processing, 2. Campbell Petroleum Series, Norman, Oklahoma, 444 pp.

Carr-Brion, K., 1986. Moisture sensors in process control. Elsevier Applied Science publishers, London and New York, 122 pp.

Cedergren, A., 1974. Reaction rates between water and the Karl Fischer reagent. Talanta, 21(4): 265-271.

Dodson, C.R. and Standing, M.B., 1944. Pressure-Volume -Temperature and Solubility Relations for Natural-Gas-Water Mixtures. API Drilling and Production Practice: 173-179.

Dong, H., Bi, P., Cao, J. and Zhao, S., 2005. Determination of Trace Water in Gas Samples by an Improved Karl Fischer Coulometer. Analytical Sciences, 21(4): 421-423.

Esteban, A., Hernandez, V. and Lunsford, K., 2000. Exploit the benefits of methanol, 79th Annual GPA Convention. Gas Processors Association, Atlanta, Georgia.

Fenner, R. and Zdankiewicz, E., 2001. Micromachined water vapor sensors: A review of sensing technologies. IEEE Sens. J., 1(4): 309-317.

Folas, G.K., Froyna, E.W., Lovland, J., Kontogeorgis, G.M. and Solbraa, E., 2007. Data and prediction of water content of high pressure nitrogen, methane and natural gas. Fluid Phase Equilib., 252(1-2): 162-174.

Funke, H.H., Grissom, B.L., McGrew, C.E. and Raynor, M.W., 2003. Techniques for the measurement of trace moisture in high-purity electronic specialty gases. Rev. Sci. Instrum., 74(9): 3909-3933.

Galloway, M., 1989. Devices for moisture measurement in natural gas, 64th International School of Hydrocarbon Measurement. International School of Hydrocarbon Measurement, Norman, Oklahoma, pp. 520-522.

Gandhidasan, P., 2003. Parametric analysis of natural gas dehydration by a triethylene glycol solution. Energy sources, 25: 189-201.

Goldup, A. and Westaway, M.T., 1966. Determination of trace quantities of water in hydrocarbons. Application of the calcium carbide - gas chromatographic method to streams containing methanol. Analytical Chemistry, 38(12): 1657-1661.

GPA, 2005. GPA 2166-05: Obtaining Natural Gas Samples for Analysis by Gas Chromatography. Gas Processors Association, Tulsa, Oklahoma.

GPSA, 2012. Engineering data book, 2. Gas Processors Suppliers Association, Tulsa, Oklahoma.

Graham, J.F., Krenek, M.R., Maxson, D.J., Pierson, J.A. and Thompson, J.L., 1994. Natural Gas Dehydration: Status And Trends: Final Report (March - October 1993). GRI-94/0099.

Grosso, S., Fowler, A.E. and Pearce, R.L., 1980. Dehydration Of Natural And Industrial Gas Streams With Liquid Desiccants. In: A.S. Mujumdar (Editor), Drying '80 - Developments in Drying. Hemisphere publishing corporation, McGraw-Hill international book company, Montreal, pp. 468-475.

Guilbault, G.G., Jordan, J.M. and Scheide, E., 1988. Analytical Uses of Piezoelectric Crystals: A Review. C R C Critical Reviews in Analytical Chemistry, 19(1): 1-28.

Hammerschmidt, E.G., 1933. Calculation and Determination of Moisture Content of Compressed Natural Gas. Western Gas, 9(9-11): 29.

Hasegava, S. and Little, J.W., 1977. The NBS two-pressure humidity generator, mark 2. J. res. Nat. Bur. Stand. Sect. A. Phys. chem., 81A(1): 81-88.

Hubbard, R.A., 1991. Recent Developments In Gas Dehydration And Hydrate Inhibition, SPE Gas Technology Symposium. Society of Petroleum Engineers, Houston, Texas, pp. 263-276.

Inman, R.S. and McAndrew, J.J.F., 1994. Application of Tunable Diode Laser Absorption Spectroscopy To Trace Moisture Measurements in Gases. Analytical Chemistry, 66(15): 2471-2479.

ISO, 1993a. ISO 10101-1:1993: Natural gas - Determination of water by the Karl Fischer method - Part 1: Introduction. International Organization for Standardization, Genève.

ISO, 1993b. ISO 10101-3:1993: Natural gas - Determination of water by the Karl Fischer method - Part 3: Coulometric procedure. International Organization for Standardization, Genève.

ISO, 2001. ISO 10715:2001: Natural gas - Sampling guidelines. International Organization for Standardization, Genève.
ISO, 2004. ISO 18453:2004 Natural gas - Correlation between water content and water dew point. International Organization for Standardization, Genève.
Jamieson, A.W. and Sikkenga, H.J., 1986. On-Line Water Dewpoint Measurement in Natural Gas. In: G.J.v. Rossum (Editor), Gas Quality. Elsevier Science Publishers B.V., Groningen, pp. 289-299.
Keidel, F.A., 1956. A Novel, Inexpensive Instrument for Accurate Analysis for Traces of Water, Pittsburgh Conference on on Analytical Chemistry and Applied Spectroscopy, Pittsburg, Pennsylvania
Keidel, F.A., 1959. Determination of water by direct amperometric measurement. Anal. Chem., 31(12): 2043-2048.
Kelland, M.A., 2009. Production chemicals for the oil and gas industry. CRC Press, Boca Raton.
Knight, H.S. and Weiss, F.T., 1962. Determination of Traces of Water in Hydrocarbons - A Calcium Carbide-Gas Liquid Chromatography Method. Anal. Chem., 34(7): 749-751.
Kohl, A.L. and Nielsen, R.B., 1997. Gas purification. Gulf Publishing Company, Houston, Texas, 1395 pp.
Lackner, M., 2007. Tunable diode laser absorption spectroscopy (TDLAS) in the process industries – a review. Reviews in Chemical Engineering, 23(2): 65-147.
Larson, B., 2003. Fields tests of conductive polymer moisture sensor in natural gas. Tech. Pap. ISA, 444: 39-48.
Latif, S., Haken, J.K. and Wainwright, M.S., 1983. Trace water analysis in gases using Reaction gas chromatography. Journal of Chromatography A, 258: 233-237.
Laughlin, A.R., 1976. Determination of Water Vapor Content and Hydrocarbon Dew Point in Natural Gas, 51th International School of Hydrocarbon Measurement. International School of Hydrocarbon Measurement, Norman, Oklahoma, pp. 95-98.
Lechner-Fish, T.J., 1997. Electrolytic Measurement of Moisture in Natural Gas. Sensors, September 1997: 58-65.
Lindblom, M., Andersson, L.A. and Bjerle, I., 1992. Water determination in pyrolysis gases using calcium carbide. Chem. Eng. Technol., 15: 99-102.
Linnerud, I., Kaspersen, P. and Jaeger, T., 1998. Gas monitoring in the process industry using diode laser spectroscopy. Applied Physics B, 67(3): 297-305.
Løkken, T.V., 2012a. Comparison of hygrometers for monitoring of water vapour in natural gas. Journal of Natural Gas Science and Engineering, 6: 24-36.
Løkken, T.V., 2012b. Water vapour monitoring in natural gas in the presence of methanol. Journal of Natural Gas Science and Engineering, 7: 7-15.
Løkken, T.V., 2013. Water vapour measurements in natural gas in the presence of ethylene glycol. Journal of Natural Gas Science and Engineering, 12: 13-21.
Løkken, T.V., Bersås, A., Christensen, K.O., Nygaard, C.F. and Solbraa, E., 2008. Water content of high pressure natural gas: Data, prediction and experience from field, International Gas Research Conference. Curran Associates Inc., Paris.

Lurvey, D.T., 1977. Determination of Water Vapor Content of Natural Gas, Am. Gas Assoc. Transm. Conf., St. Louis, pp. 191.
MacLeod, S.K., 1991. Moisture Determination Using Karl Fischer Titrations. Analytical Chemistry, 63(10): 557A-566A.
Manning, W.P. and Wood, H.S., 1993. Guidelines for glycol dehydrator design: I. Hydrocarbon processing, 72: 106.
McAndrew, J.J. and Boucheron, D., 1992. Moisture analysis in process gas streams. Solid State Technol., 35(2): 52-60.
McAndrew, J.J.F., 1997. Humidity measurement in gases for semiconductor processing. In: J.D. Hogan (Editor), Speciality gas analysis: A practical guidebook. Wiley-VCH, New York, pp. 21-42.
McKetta, J.J. and Wehe, A.H., 1958. Use This Chart for Water Content of Natural Gases. Petrol. Ref., 37(8): 153-154.
Mehrhoff, T.K., 1985. Comparison of continuous moisture monitors in the range 1 to 15 ppm. Rev. Sci. Instrum., 56(10): 1930-1933.
Mermoud, F., MBrandt, M.D. and Weinstein, B.L., 1989. Recalibration of capacitive-type moisture sensors. Solid State Technol., 32(5): 59-61.
Meyer, C.W. et al., 2010. The second-generation NIST standard hygrometer. Metrologia, 47: 192-207.
Meyer, C.W., Miller, W.W., Ripple, D.C. and Scace, G.E., 2008. Design and performance of the new NIST hybrid humidity generator, NCSLI 2008 Workshop and Symposium. NCSLI, Orlando, Forida.
Monroe, S., 1998. Trace moisture in ammonia: Gas chromatography using calcium carbide. J. IEST., 41(1): 21-25.
Murphy, D.M. and Koop, T., 2005. Review of the vapour pressures of ice and supercooled water for atmospheric applications. Quarterly Journal of the Royal Meteorological Society, 131(608): 1539-1565.
Mychajliw, B.J., 2002. Determination of water vapor and hydrocarbon dew point in gas, 77th International School of Hydrocarbon Measurement. International School of Hydrocarbon Measurement, Oklahoma City, Oklahoma, pp. 507-510.
O'Sullivan, C.K. and Guilbault, G.G., 1999. Commercial quartz crystal microbalances – theory and applications. Biosensors and Bioelectronics, 14(8–9): 663-670.
Oellrich, L.R. and Althaus, K., 2001. Relationship between water content and water dew point keeping in consideration the gas composition in the field of natural gas. GERG Technical Monograph TM14, Fortschritt-Berichte VDI, Row 3, no. 679. VDI Verlag GmbH, Düsseldorf.
Rihani, D.N. and Prasad, M.K.E., 1999. Process considerations in the design of natural gas glycol dehydration units. Hydrocarbon Asia, 9(1): 52.
Rittersma, Z.M., 2002. Recent achievements in miniaturised humidity sensors--a review of transduction techniques. Sensors and Actuators A: Physical, 96(2-3): 196.
Scace, G.E., Huang, P.H., Hodges, J.T., Olson, D.A. and Whetstone, J.R., 1997. The new NIST low frost-point humidity generator, NCSL Workshop and Symposium. NIST, Atlanta, Georgia.

Skinner, W., 1948. The Water Content of Natural Gas at Low Temperatures, University of Oklahoma, Norman, Oklahoma, 58 pp.
Sloan, E.D., 2003. Fundamental principles and applications of natural gas hydrates. Nature, 426(6964): 353-363.
Sloan, E.D. and Koh, C.A., 2007. Clathrate Hydrates of Natural Gases. Chemical industries. CRC Press, Boca Raton, 721 pp.
Sonntag, D., 1990. Important new values of the physical constants of 1986, vapor pressure formulations based on the ITS-90, and psychrometer formulae. Z. Meteorol., 40(5): 340-344.
Sonntag, D., 1994. Advancements in the field of hygrometry. Meteorol. Z., 3(2): 51-66.
Verhoef, J. and Barendrecht, E., 1976. Mechanism and reaction rate of the karl-fischer titration reaction: Part I. Potentiometric measurements. Journal of Electroanalytical Chemistry and Interfacial Electrochemistry, 71(3): 305-315.
Wang, X.-D. and Wolfbeis, O.S., 2012. Fiber-Optic Chemical Sensors and Biosensors (2008–2012). Analytical Chemistry, 85(2): 487-508.
Wiederhold, P.R., 1997a. Water Vapor Measurement. Marcel Dekker Inc., New York, 357 pp.
Wiederhold, P.R., 2000. The principles of chilled mirror hygrometry. Sensors, 17(7): 46-51.
Willsch, R., Ecke, W. and Schwotzer, G., 2005. Spectrally encoded optical fibre sensor systems and their application in process control, environmental and structural monitoring. In: L.R. Jaroszewicz, B. Culshaw and A.G. Mignani (Editors), Congress on Optics and Optoelectronics. SPIE, Warsaw, pp. 59520I-1 - 59520I-14.
Yeo, T.L., Sun, T. and Grattan, K.T.V., 2008. Fibre-optic sensor technologies for humidity and moisture measurement. Sensors and Actuators A: Physical, 144(2): 280-295.
Young, H.D. and Freedman, R.A., 2004. Sears and Zemansky's university physics with modern physics, 11. Pearson Addison-Wesley, Boston, Massachusetts, 1550 pp.

Paper I

Journal of Natural Gas Science and Engineering 6 (2012) 24–36

Contents lists available at SciVerse ScienceDirect

Journal of Natural Gas Science and Engineering

journal homepage: www.elsevier.com/locate/jngse

Comparison of hygrometers for monitoring of water vapour in natural gas

T.V. Løkken

Statoil ASA, Research and Development, Arkitekt Ebbels veg 10, N-7005 Trondheim, Norway

ARTICLE INFO

Article history:
Received 29 September 2011
Received in revised form
27 January 2012
Accepted 1 February 2012
Available online 3 March 2012

Keywords:
Water dew point
Capacitor sensor
Quartz crystal microbalance
Electrolytic cell
Fibre-optic sensor
Calcium carbide

ABSTRACT

Hygrometers for monitoring of water vapour (moisture) in natural gases were compared with respect to accuracy, long term stability and response time. The hygrometers were based on capacitor sensor, quartz crystal microbalance (QCM), electrolytic cell, fibre-optic sensor and conversion of water to ethyne with calcium carbide (CaC_2-GC), respectively. In the latter technique, ethyne was quantified by a gas chromatograph (GC). Monitoring of water vapour concentrations between 20 μmol/mol and 120 μmol/mol was carried out in the laboratory, using nitrogen as the matrix gas. The capacitor hygrometers and the electrolytic cell hygrometer tested in this work showed a tendency to drift, which reduced their accuracy. The QCM, fibre-optic and CaC_2-GC hygrometer showed good accuracy and long term stability. The QCM hygrometer had the overall shortest response times. The results demonstrated the need for careful quality control of the hygrometers, and monitoring systems which are thoroughly fitted to the requirements of individual natural gas applications.

1. Introduction

1.1. Background

Accurate determination of water vapour in natural gases, often referred to as moisture, is crucial for maintaining a stable and safe processing and transport of natural gas. These are important reasons why natural gas producers have a defined moisture specification in their sales contracts. The moisture specification is often expressed as a water dew point. Underestimating the moisture concentration in the natural gas can lead to condensation of liquid water in process equipment or pipelines. Condensed water will increase the corrosion potential when combined with compounds such as hydrogen sulphide and carbon dioxide (Mychajliw, 2002). Another possible consequence of underestimation of moisture is the formation of gas hydrates (Jamieson and Sikkenga, 1986). Gas hydrates can plug pipelines or process units, resulting in loss of production or obstructed transportation of natural gas.

Even though analysis of moisture in various gases has been performed for more than 50 years, this is still regarded as one of the most challenging trace gas analyses. One important reason for this is the high polarity of water making it extremely adsorptive. Consequently surfaces regarded as dry are usually coated with a thin film of moisture (Carr-Brion, 1986; Knight and Weiss, 1962). The abundance of water in the atmosphere also makes trace analysis challenging, with high potential for background moisture interference.

In this work several devices for monitoring of moisture in gases, referred to as hygrometers, more or less frequently used in natural gas business were compared. The focus was to investigate and compare the performance of the hygrometers, mainly with respect to accuracy, long term stability and response time. The range of moisture concentration examined was (20–120) μmol/mol, which is a relevant range for many natural gas applications. For practical and safety reasons, the measurements were performed in the laboratory at ambient conditions using nitrogen as the matrix gas.

1.2. Measuring techniques

Throughout the years numerous methods for moisture measurements in gases have been developed and established. Most of them are thoroughly described in published literature (Blakemore et al., 1986; Bruttel and Regina, 2006; Carr-Brion, 1986; Funke et al., 2003; ISO, 1993a,b; Keidel, 1959; Knight and Weiss, 1962; McAndrew and Boucheron, 1992; McAndrew, 1997; Monroe, 1998; Wiederhold, 1997, 2000; Willsch et al., 2005). Hygrometers based on capacitor sensor, quartz crystal microbalance (QCM), electrolytic cell, fibre-optic sensor, CaC_2-GC, chilled mirror and Karl Fischer titration have been investigated in this work. The basic principles for these methods are briefly summarised in Table 1. Karl Fischer titration and chilled mirror hygrometry

E-mail address: tvl@statoil.com.

1875-5100/$ – see front matter © 2012 Elsevier B.V. All rights reserved.
doi:10.1016/j.jngse.2012.02.001

Table 1
Summary of methods for moisture measurements in gases.

Method	Typical uncertainty	Working principle
Capacitor sensor	(1–3) °C	Capacitance or impedance measured as a function of water molecules adsorbed to the porous dielectric (usually metal oxides like Al_2O_3 or SiO_2) of a capacitor (Carr-Brion, 1986; Funke et al., 2003; McAndrew and Boucheron, 1992; McAndrew, 1997; Wiederhold, 1997).
Quartz crystal microbalance (QCM)	±10%	Measures the resonance frequency of an oscillating quarts crystal (piezoelectric) coated with a hygroscopic polymer. The frequency changes with mass as water molecules adsorb on the quartz crystal (Blakemore et al., 1986; Carr-Brion, 1986; Funke et al., 2003; McAndrew and Boucheron, 1992; McAndrew, 1997; Wiederhold, 1997).
Electrolytic cell	±10%	Measures current generated from electrolytic decomposition of water adsorbed in strongly hygroscopic P_2O_5 (Keidel, 1959).
CaC_2-GC	±10%	Conversion of water molecules to ethyne with CaC_2, followed by gas chromatographic (GC) separation and detection with e.g. a thermal conductivity or a flame ionisation detector (Knight and Weiss, 1962; Monroe, 1998).
Fibre-optic sensor	±2 °C	Measures a shift in reflection spectrum dependent on the amount of adsorbed water in a hygroscopic Fabry-Perot filter. "Fibre-optic" in the sense that light is emitted and reflected via fibre-optic cables (Willsch et al., 2005).
Karl Fischer titration	±10%	The Karl Fischer reaction: $ROH + SO_2 + R'N \rightarrow (R'NH)SO_3R$ $(R'NH)SO_3R + 2R'N + I_2 + \mathbf{H_2O} \rightarrow (R'NH)SO_4R + 2(R'NH)I$ ROH = alcohol, R'N = basic nitrogen compound For coulometric titration the amount of water is calculated by measuring the current needed for the electrochemical generation of iodine (I_2) from iodide (I^-) (Bruttel and Regina, 2006; ISO, 1993a,b).
Chilled mirror	±0.1 °C	Measures the temperature at which water molecules condense from the gas to form dew or frost on a mirror surface (Wiederhold, 1997, 2000).

are usually regarded as direct or absolute methods as they utilise a direct relationship between the measured quantity and the amount of moisture. Hence they often are preferred as reference methods.

1.3. Interpretation of moisture measurements

The amount of moisture in a natural gas can either be expressed as concentration (e.g. μmol/mol or mg/Sm^3 at some defined standard temperature and pressure) or as dew or frost point in degrees Celsius. The dew point is the highest temperature, at a specified pressure, where water can condense from the gas. The frost point is the highest temperature, at a specified pressure, where ice can precipitate from the gas (Løkken et al., 2008). In the temperature region between 0 °C and −20 °C it is difficult to predict whether the moisture will condense as dew or precipitate as ice. It is necessary to distinguish between the dew point and the frost point, as these could deviate with several degrees for the same moisture concentration. Accurate formulas for conversion between dew or frost point at atmospheric pressure and concentration (via saturation vapour pressure) are published by Sonntag (Sonntag, 1990, 1994). The following formula converts frost point to saturation vapour pressure:

For the given temperature range

$$173.15\ \mathrm{K} \le T_K \le 273.16\ \mathrm{K} \quad (-100\ ^\circ\mathrm{C} \le T_C \le 0.01\ ^\circ\mathrm{C})$$

$$\ln e_i(T_K) = -6024.5282T_K^{-1} + 24.7219 + 1.0613868 \times 10^{-2}T_K - 1.3198825 \times 10^{-5}T_K^2 - 0.49382577\ln T_K, \quad (1)$$

$e_i(T_K)$ is the saturation vapour pressure with respect to ice in hPa (hectopascal), T_K is frost point temperature in K.

Saturation vapour pressure can be converted to frost point by formula (2), which is derived from equation (1):

$$T_K = 12.1197y + 5.25112 \times 10^{-1}y^2 + 1.92206 \times 10^{-2}y^3 + 3.84403 \times 10^{-4}y^4 + 273.15 \quad (2)$$

In the conversion formula (2)

$$y = \ln(e_i(T_K)/6.11153) \quad (3)$$

For conversions between saturation vapour pressure and concentration the following formula can be used:

$$c_w = \frac{e_i(T_K) \times 10^6}{1013.26}, \quad (4)$$

c_w is concentration in μmol/mol. At elevated pressures the formulas of Sonntag are not applicable because of increasing non ideal behaviour of the gas.

Conversion between moisture concentration and dew point at elevated pressure has traditionally been performed by use of the correlation charts from McKetta and Wehe (1958) or by the formulas of Bukacek (1955). The methods are based on empirical data produced between the years of 1927 and 1955. The conversions always relate the moisture concentration to condensed water (dew), despite the thermodynamic most stable phase in the lower temperature regions being gas hydrates or ice (dependent of the pressure and temperature). These methods have gained widespread use when it comes to calculations of the moisture concentration or the dew point of unprocessed natural gas, and they have been important for design of dehydration processes.

The hygrometers returning dew or frost points as their primary unit of measurement are usually calibrated at ambient pressure using a high precision chilled mirror as the reference. The calibration process will start at the lowest moisture concentration, typically cooling the mirror to well below −40 °C, to make sure the temperature reading relates to ice. When ice is formed on the mirror surface, the condensed water phase will remain as ice until the mirror temperature increases to 0 °C again. As a consequence these hygrometers will return frost points for negative temperatures and dew points for positive temperatures. Converting frost points or dew points to concentration at atmospheric pressure is easy using Sonntag's formulas ((1)–(3)). Conversion utilising the chart of McKetta and Wehe or the formulas of Bukacek, should only be performed on dew points (≥0 °C). The errors involved using these methods directly on frost points (<0 °C) will increase as the temperature decrease.

Thermodynamic modelling is often a preferred alternative for calculating equilibrium water content of natural gas. In contrast to charts and simple formulas thermodynamic models usually have the possibilities of covering a broad range of compositions, pressure and temperature ranges. The equations of state (EoS) traditionally

used in the oil and natural gas industry, like the SRK- and PR-EoS, have shown to have severe limitations for description of aqueous systems and polar substances in general (Folas et al., 2007a,b; Løkken et al., 2008). More than 10 years ago, the European gas research group (GERG) proposed a modified PR-EoS, tailor-made for the modelling of water in gas with a primary working range of 5 bar to 100 bar and −5 °C to 15 °C (Althaus, 1999; Oellrich and Althaus, 2001). The model has been published in the form of an ISO standard (ISO, 2004). The CPA-EoS (Cubic Plus Association) is another thermodynamic model proven to accurately calculate equilibrium concentration of water as well as other polar substances in hydrocarbon systems (Folas et al., 2007a,b). This comprehensive model covers higher pressure and temperature ranges compared to the "GERG-Water-EoS", in addition to being able to model all phases (liquid, ice and hydrate) both stable and metastable ones (e.g. supercooled dew).

1.4. Moisture generator

Several methods for the generation of moisture in gases are described in the literature, such as the two-pressure, two-flow or two-temperature generator (Funke et al., 2003; Sonntag, 1994; Wiederhold, 1997). A lot of effort can be made in the aim of producing a stream of gas with a very accurate moisture concentration. Such equipment is often found at national measurement institutes, like NPL (National Physical Laboratory, United Kingdom) and NIST (National Institute of Standards and Technology, USA). In this work a simpler moisture generator was constructed, well suited for comparison of hygrometers rather than calibrating them accurately. Having applications for moisture in natural gas in mind, the main focus was to produce a gas with a sufficient long term, drift-free and controllable concentration of moisture.

2. Experimental set up

2.1. Test rig

A test rig for generation of moisture in gases was constructed as shown in Fig. 1. Table 2 summarises the pieces of equipment used. The test rig was able to generate a stream of nitrogen with drift-free concentrations of moisture for more than 40 days.

The nitrogen gas (>99.999% purity) was fed to the test rig at about 4 bar through a pressure regulator (V-1). The gas flow was split in two lines: one line for generation of saturated gas (T-2) and one for generation of dry gas for dilution (T-3). The gas was fed to the two lines via needle valves (V-2 and V-3).

In the first line (T-2) the gas was bubbled through water at room temperature (about 25 °C) for saturation inside two stainless steel cylinders in series for saturation (E-1 and E-2). The saturators were modified filter housings with a volume of 30 ml, each filled with 20 ml water (ion exchanged). A piece of 6 mm outer diameter stainless steel tubing (316L stainless steel) was welded to the inlet ports to guide the gas near the bottom of the cylinders. The saturated gas was further directed through three cylinders in series kept at a lower temperature (10 °C). The temperature was controlled with a cooling bath (E-6). These cylinders were empty and worked as condensers; the test gas leaving the last cylinder with a fixed concentration of water vapour according to the actual temperature and pressure. To facilitate an efficient cooling of the gas a submerged coil of approximately 1 meter long tubing (C-1) connected the first and second condenser.

The saturated test gas was diluted with nitrogen from the second line (T-3), dried through two molecular sieves in series (E-7 and E-8). The resulting total flow rate of approximately 6 Nl/min was sufficient to feed all the hygrometers in the test. The molecular

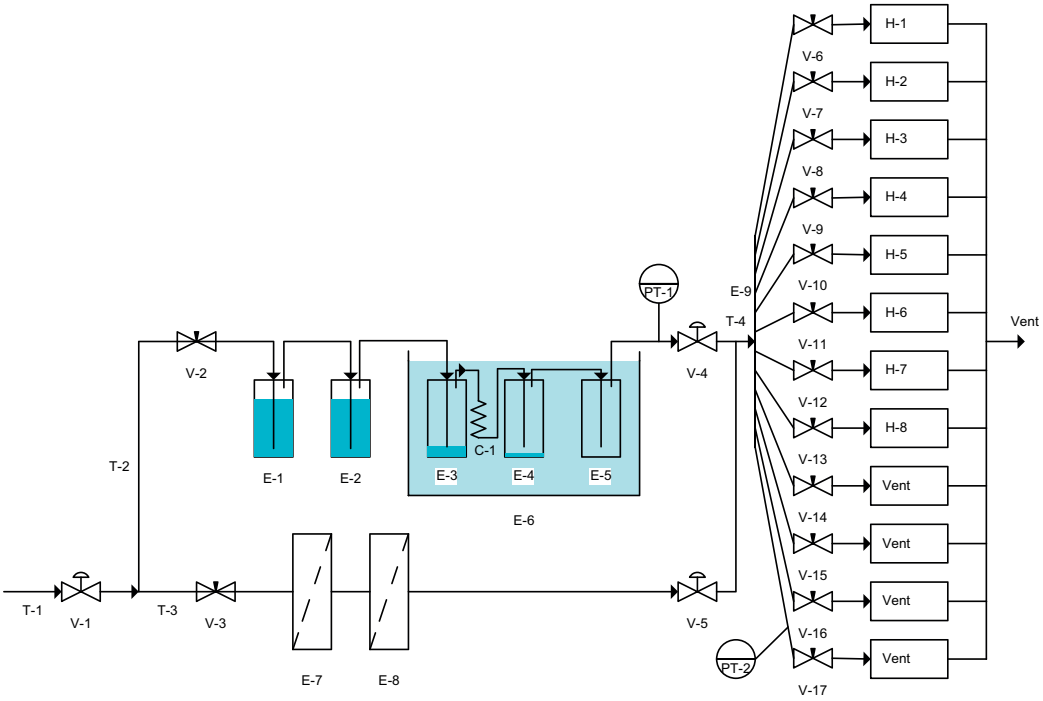

Fig. 1. Schematic representation of the moisture generator. Equipment description is found in Table 2.

Table 2
Equipment description, the codes refers to Fig. 1.

Code	Description	Model	Manufacturer
V-1	Single stage pressure regulator	SI15	SMT S.A.S., France
V-2 and V-3	Needle valves	3812F4Y	Hoke, USA
V-4	Flow controller	PC 8942	Brooks Instrument, USA
V-5	Flow controller	FMC-2000	FlowMatrix Inc., USA
V-6 to V17	Fine metering valve	SS-2MG	Swagelok, USA
E-1 and E-2	Modified filter housings, saturators	Model 122	Headline Filters, UK
E-3 to E-5	Modified filter housings, condensers	Model 122	Headline Filters, UK
E-6	Cooling bath	FP-45	Julabo Labortechnik GmbH, Germany
E-7 and E-8	Molecular sieves		Ametek, USA
E-9	Gas manifold	Z12M2	Vici AG International, Switzerland
PT-1	Pressure transmitter	PA-55X	Keller AG, Switzerland
PT-2	Pressure transducer	Model SA	Honeywell, USA
H-1	Capacitor A		
H-2	Capacitor B		
H-3	QCM		
H-4	CaC_2-GC		
H-4.1	Gas Chromatograph	CP4900 Micro-GC	Varian Inc., USA
H-4.2	GC separation column	CP-PoraPlot Q, 10 m long, 0.25 mm i.d.	Varian Inc., USA
H-5	Fibre-optic		
H-6	Karl Fischer	Model 831	Metrohm AG, Switzerland
H-6.1	Gas meter	TG 1 Mod. 5-8	Ritter, Germany
H-7	Chilled mirror	S4000 Integrale	Michell Instruments ltd., UK
H-8	Electrolytic		
C-1	1 m coil made of 1/8 × 0.035 inch, 316L stainless steel tubing	Sandvik 3R60	AB Sandvik Materials Technology, Sweden
T-1 to T-3	1/8 × 0.035 inch, 316L stainless steel tubing	Sandvik 3R60	AB Sandvik Materials Technology, Sweden
T-4	Treated 1/8 × 0.035 inch 316L stainless steel tubing	Siltek™	Restek Corporation, USA

sieves were specified to remove moisture to less than 50 nmol/mol. All connecting tubing was made of stainless steel (T-1 to T-4). The tubing between V-4 and V-5 and the hygrometers (H-1 to H-8) was electro polished and surface deactivated (T-4), to minimise surface adsorption. The test gas was split in 12 separate streams in a compact gas manifold (E-9). The hygrometers (H-1 to H-8) were connected to the gas manifold via equal lengths of tubing (1.2 meter) and fine metering valves (V-6 toV-17). Sufficient lengths of 1/8 inch stainless steel tubing were connected to the outlet ports of the hygrometers to prevent back-diffusion of moisture. Further downstream, the outlet streams were gathered in a gas manifold and guided to ventilation in 1/4 inch Teflon tubing.

2.2. Hygrometers

Eight hygrometers have been investigated in the experiments:

- two capacitor sensors of different brands
- one QCM
- one CaC_2-GC
- one fibre-optic sensor
- one electrolytic cell
- one Karl Fischer titrator
- one chilled mirror.

The hygrometers were equipped with control units for communication with the probes/sensors and transfer of data to a computer for storage. Data points were stored every 5 min. The concentration of ethyne (CaC_2-GC) was determined with a micro gas chromatograph (H-4.1) equipped with a separation column (H-4.2) and a micro thermal conductivity detector. The gas chromatograph was controlled by chromatography software (CP Maitre Elite) on the computer, which also stored the processed data collected approximately every 10 min.

Two direct methods were utilised for reference measurements, not being of interest with respect of continuous online measurements. These were a chilled mirror hygrometer (H-7) and a Karl Fischer titrator (H-6). The volume of the titrated gas was measured by a drum-type gas meter (H-6.1). The chilled mirror hygrometer was set up to perform continuous measurements, with storage of data every 5 min. The Karl Fischer titrations were performed manually during the experiments, but not continuously.

2.3. Operation of moisture generator

The mixing ratio of the two gas streams (moist and dry gas) was controlled by two manually operated flow controllers. The saturated gas was controlled between 30 and 300 Nml/min with a flow controller (V-4), while the dry gas was adjusted to about 7 Nl/min with another flow controller (V-5). The temperature in the cooling bath was set to 10 °C (±0.01 °C) and the pressure in the condensers was controlled at approximately 4 bar and monitored with a pressure transmitter (PT-1). By changing the settings on the two flow controllers, different concentrations of moisture could be produced and changed quickly between 1 and 200 μmol/mol. The pressure upstream the metering valves was about 2 bar, monitored by a pressure transducer (PT-2). The QCM had internal mass flow controllers which needed a sample pressure slightly elevated from atmospheric pressure. The other hygrometers were fed with test gas at ambient pressure. The flow rates to the different hygrometers were controlled in agreement with the recommendations made by the manufacturers. Excess test gas was distributed to vent through treated 1/8 inch stainless steel tubing (T-2) connected to the spare ports on the compact gas manifold. Fine metering valves were used to control the flow rates also on these gas streams.

2.4. Conversion between frost point and concentration

Some of the hygrometers returned dew or frost points typically in degrees Celsius, while others returned concentration typically in parts per million (molar or volume). To be able to compare data from all the hygrometers conversions between the different units were done. In this work the formulas of Sonntag (1990, 1994) were used for these conversions (Eqs. (1) and (2)).

2.5. Calibration of instruments

The hygrometers were calibrated by the manufacturer before they were made available for testing. No recalibration was done before or during the experiments. No special treatment was done prior to usage of the sensors. They were all stored in their original cover which contained a small bag of silica gel.

The probe (sintered metal filter, capacitor sensor and electronics unit) of the capacitor hygrometer from one of the manufacturers was exchanged several times during the experiments. Two of the exchanges were caused by readings which were apparently too low, while the third exchange was caused by technical problems with the probe.

The micro gas chromatograph (CaC_2-GC) was calibrated with respect to ethyne before the experiments. The calibration was checked during and after the experiment. Three calibration gas mixtures were used with ethyne concentrations in nitrogen at 11 μmol/mol (10% relative uncertainty), 53,4 μmol/mol (5% relative uncertainty), and 204 μmol/mol (5% relative uncertainty) respectively. The calibration gas mixtures, which were certified with international traceability, were purchased from Yara (Yara International ASA, Norway).

The chilled mirror hygrometer was recalibrated prior to the experiments at Michell Instruments (UKAS accredited calibration laboratory).

3. Results

3.1. Overall results

The moisture generator was set up to produce a stream of nitrogen with moisture levels according to Table 3. The moisture levels in the test gas were controlled by turning the manual flow regulator (V-4) regulating the moist gas flow. This changed the dilution of the moist gas at the same time obtaining minimal change of the total gas flow to the hygrometers. The temperature of the moist gas was not altered, and the pressure profiles of the gas streams were altered only to a minor extent. This way the time for generating new stable levels of moisture in the test gas was minimised.

Data from the hygrometers was collected during a total of 39 days, as described in the experimental section. The data from the experiments is presented in Fig. 2, where the readings from the hygrometers are expressed in the unit of concentration (μmol/mol). Fig. 3 shows the same data expressed as frost points (°C).

Data from Capacitor B is excluded during the first 15 days of experiments in Figs. 2 and 3 because of technical problems with the probe. A new probe was installed on day 15. The chilled mirror device was unable to cool the mirror much below −50 °C. This explains why data from the chilled mirror is excluded from Figs. 2 and 3 for the low levels of moisture. From day 32 to 35 the gas chromatograph analysing the ethyne concentration in the gas from the calcium carbide column was out of operation. Hence data from CaC_2-GC is missing in Figs. 2 and 3 during this period of time.

Table 3
Generation of moisture levels during the experiments.

Day	Moisture concentration level (μmol/mol)	Frost point level (°C)
1–16	50	−48
16–23	20	−55
23–35	120	−40
35–36	20	−55
36–39	50	−48

Figs. 2 and 3 show that QCM, CaC_2-GC and Fibre-optic return readings close to the readings from the reference methods (Chilled mirror and Karl Fischer) at all levels of moisture. Electrolytic and Capacitor A return considerable lower readings compared to the readings from the reference methods at all moisture levels. Capacitor B generally shows an evident downward drift during the experiments, starting at higher readings compared to the reference methods. During the experiments Capacitor B reads both higher and lower compared to the reference methods, and even agrees well with the reference methods around day 28 and from day 36 to 39. The tendency to drift downward can also be observed for Capacitor A, though to a considerably lower extent. The first 6 days of experiments and at the highest level of moisture, between day 24 and 35, a downward drift is observed for Electrolytic. Also a drift upwards is observed for Electrolytic, between 12 and 24 hours after the step change in moisture level from (20–120) μmol/mol. Another general observation from Figs. 2 and 3 is that the difference between the readings from the capacitor hygrometers and the reference methods changes when the moisture level is changed.

3.2. Response time

During the experiments the moisture concentration was changed four times (on day 16, 23, 35 and 36). The changes were done as step changes, in the sense that the moisture levels were expected to change faster than the response times of the hygrometers. Data collected during these step changes was examined to compare the response times for the hygrometers as represented in Fig. 4. To provide better readability of this figure all the readings, except for the reference techniques (Karl Fischer and Chilled mirror), are corrected to give the same starting point. The correction involves an absolute offset of the raw data, keeping the internal calibration of each moisture monitor unchanged. As the chilled mirror device was unable to cool the mirror much below −50 °C, data from the chilled mirror is excluded in Fig. 4A and C. In Fig. 4C data from CaC_2-GC is missing the first few hours of the experiment because of the micro gas chromatograph being out of operation. Karl Fischer titrations were not performed during the experiment referred to in Fig. 4D.

It can be observed in Fig. 4 that QCM shows the overall most rapid response to the step changes and readings from this hygrometer correspond well to the total step changes as defined by the reference methods. CaC_2-GC and Fibre-optic show a relative slower response to the step changes compared to the other hygrometers, but readings still correspond well to the total step changes as defined by the reference methods. Capacitor A, Capacitor B and Electrolytic respond generally slower to the step changes compared to QCM but quicker compared to CaC_2-GC and Fibre-optic. Capacitor A and Electrolytic read a smaller step change than the total step change as defined by the reference methods. Electrolytic shows the most severe deviation. Capacitor B corresponds well to the total step change as defined by the reference methods for the two first step changes (Fig. 4A and C) but deviates more from the reference methods for the two last step changes (Fig. 4C and D). The curve shapes for all the hygrometers are similar, except for CaC_2-GC in Fig. 4D.

The time constant (unit of time) indicates the time required for a system to change from one state to another, contained in the relation (Weik, 1996): $A_t = A_0 e^{-t/a}$, where A_t is the value of the state at time t, A_0 is the value of the state at time $t = 0$, e is the base of the natural logarithm, a is the time constant and t is the time that has elapsed from the start of the change. This is a concept often referred to when describing the response time of sensors responding asymptotically to a step change in the variable being measured. When $t = a$, the measured value corresponds to

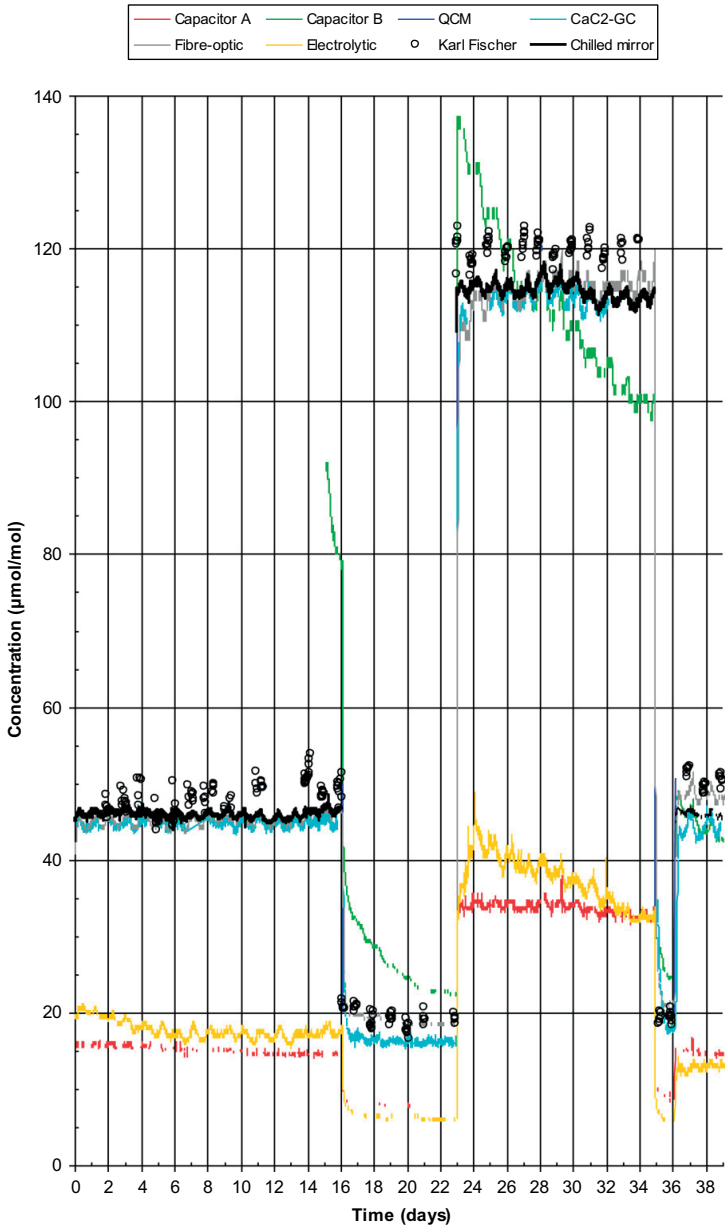

Fig. 2. Readings from the moisture monitors during 39 days of experiments, moisture content expressed as concentration (µmol/mol). Chilled mirror data is missing for low levels and CaC_2-GC data is missing for day 32 to 35 (explained in the text section 3.1). A new capacitor sensor of brand B replaced a malfunctioning one on day 15.

approximately 63% of the total change $(1-1/e)$. After the elapse of three times the time constant, corresponding to a 95% change $(1-1/e^3)$, the system can be considered to have changed its state. By calculating both 63% and 95% response times for the step changes, it is easier to compare the speed of response for the hygrometers in more detail, as expressed in Figs. 5 and 6, Tables 4 and 5. The unit (µmol/mol or °C) used for the calculation corresponds to the unit used in the original calibration of each hygrometer. The total change was calculated as the difference between measured moisture concentration or frost point just before the step change and 12 h after the step change. To obtain better resolution than the sampling frequency of 5 min (10 min for CaC_2-GC), the response times are obtained from values linearly interpolated between the actual data points. Response times for the

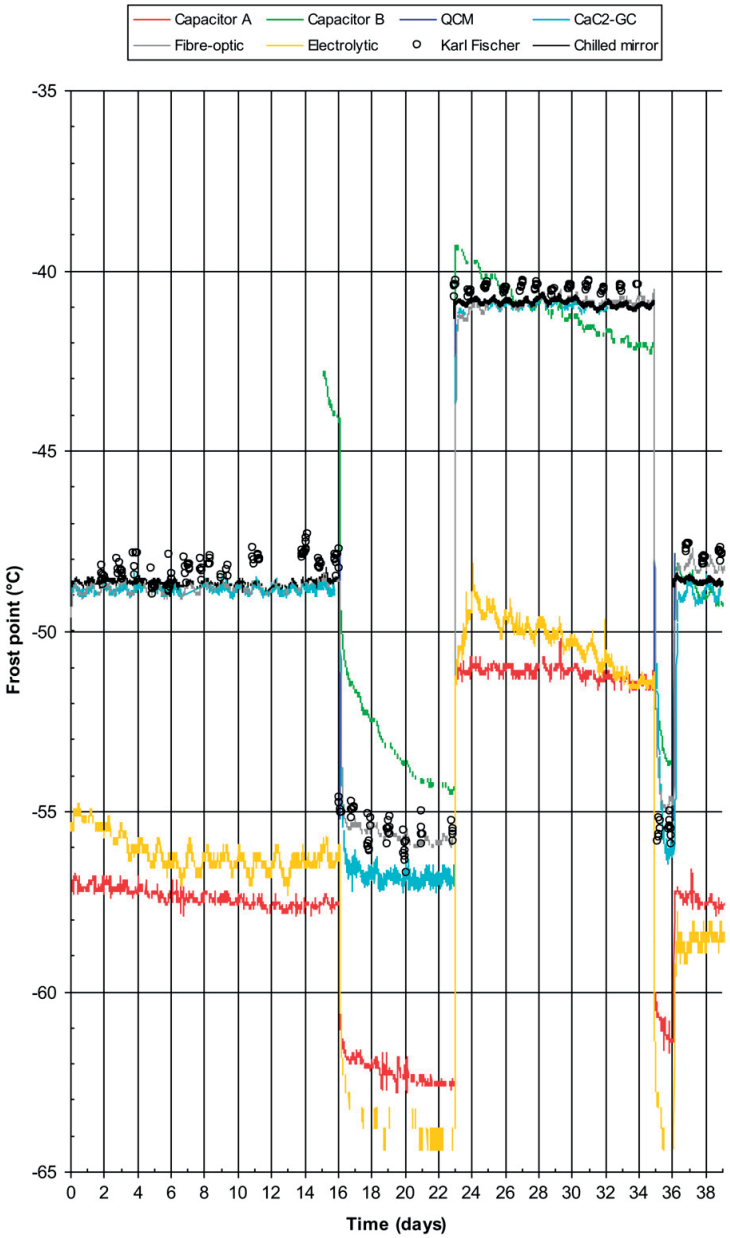

Fig. 3. Readings from the moisture monitors during 39 days of experiments, moisture content expressed as frost point (°C). Chilled mirror data is missing for low levels and CaC_2-GC data is missing for day 32 to 35 (explained in the text section 3.1). A new capacitor sensor of brand B replaced a malfunctioning one on day 15.

decrease in moisture concentration level from (50–20) μmol/mol and from (120–20) μmol/mol are represented in Fig. 5. Fig. 6 represents the response times for the corresponding increases in moisture concentration. The response times are reproduced in Tables 4 and 5.

QCM responds generally fastest of all the tested hygrometers, with the shortest response times both on increasing and decreasing moisture levels. This is true both for 63% and 95% response times, all being equal to or less than 6 min. For increasing moisture levels QCM and the capacitor hygrometers responded generally faster than CaC_2, Fibre-optic and Electrolytic. For decreasing moisture levels, when it comes to 63% response times, QCM, the capacitor hygrometers and Electrolytic responded faster (between 1 and 14 min) than CaC_2 and Fibre-optic (between 92 and 114 min).

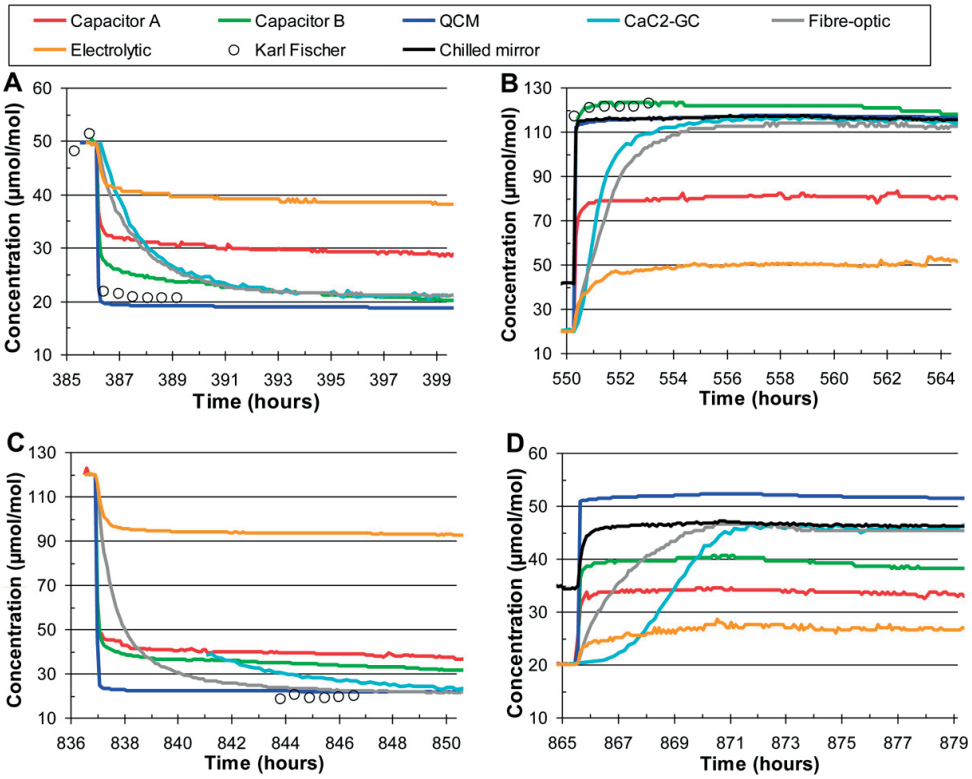

Fig. 4. Hygrometer readings after step changes of moisture levels. A: From (50 to 20) µmol/mol, B: (20 to 120) µmol/mol, C: (120 to 20) µmol/mol, D: (20 to 50) µmol/mol. Note varying scale. Different curves (not reference methods) are offset (see text section 3.2) to start at a common starting water concentration.

For the corresponding 95% response times only QCM maintained the shorter response times (6 min) while the capacitor hygrometers and Electrolytic performed at the same level as CaC_2-GC and Fibre-optic (between 163 and 455 min). Capacitor A, Capacitor B and Fibre-Optic responded faster to an increasing moisture level compared to a decreasing moisture level. This phenomenon is most pronounced for the 95% response times for the capacitor hygrometers.

3.3. Initial drifting of capacitor based sensors

Two additional probes with capacitor sensors of brand B were available during the testing period. This made it possible to collect start up data for a total of 4 individual capacitor sensors. Fig. 7 shows readings from Capacitor A and one of the capacitor sensors of brand B, the sensors being installed simultaneously on the test rig. According to the typical uncertainty of ±2 °C for capacitor

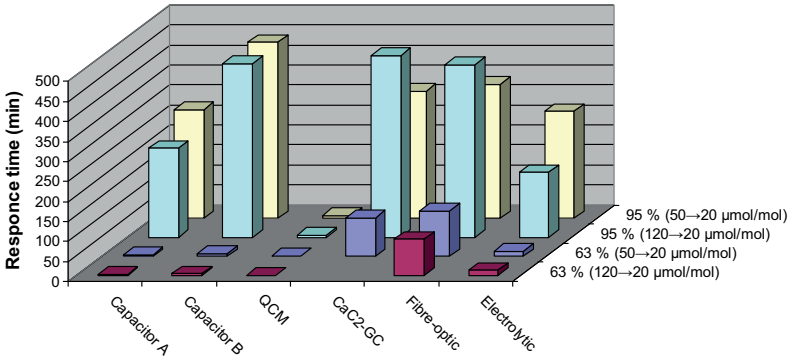

Fig. 5. Response times for decreasing moisture concentrations for changes of 63% and 95% of the step changes.

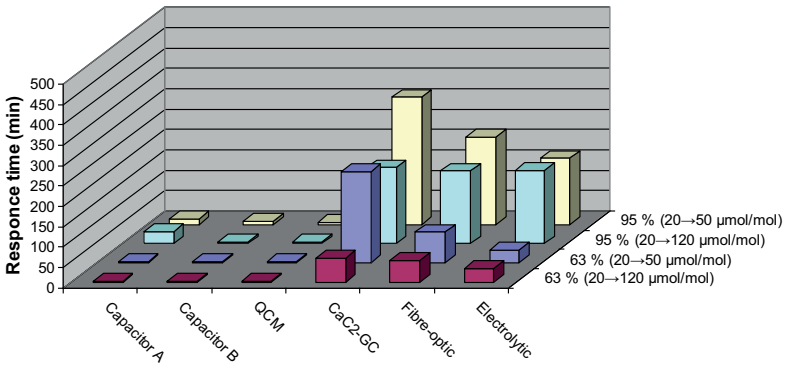

Fig. 6. Response times for increasing moisture concentrations for changes of 63% and 95% of the step changes.

hygrometers, these tolerance limits are marked on the figure. The sensors were calibrated by the manufacturer, and were used for the first time since the time of calibration. Linear trend lines were fitted to the data collected between hour 66 and 164 to demonstrate the initial drifting of these capacitor based hygrometers. The slopes of the linear trend lines were taken as the drift factor. Similar data for the two other sensors of brand B is added in Table 6, these being tested at different levels of moisture. The drift factor varied between −0.36 °C per day to −0.63 °C per day for the four capacitor sensors tested.

4. Discussion of results

4.1. Long term stability

The downward drift of capacitor sensors is described in several publications (Cremonesi, 1986; Hasegava, 1980; Mehrhoff, 1985; Mermoud et al., 1989). Some authors suggest that the drift is associated to a gradually changing pore structure of the capacitor dielectric (Carr-Brion, 1986; McAndrew and Boucheron, 1992; Nahar, 2000; Wiederhold, 1997). A gradual formation of stable chemisorbed hydroxyl ions on the metal oxide surfaces in the dielectric is also proposed as a cause of drift (Fenner and Zdankiewicz, 2001; Traversa, 1995). Drift factors for Capacitor A were calculated before the first step change of moisture level and after each step change during the experiments, as shown in Fig. 8. The drift factors were calculated as the slopes of linear trend lines fitted to data for a 12 hours period after each step change. A drift factor of −0.36 °C/day was calculated for Capacitor A, after the initial installation of this hygrometer (Chapter 3.3, Fig. 7 and Table 6). A drift factor of −0.04 °C/day during the first 16 days of the experiments, as shown in Fig. 8, implies that the tendency to drift decreases with time for this capacitor. A similar decreasing drift can be observed by a visual inspection of the readings from Capacitor B in Figs. 2 and 3. This agrees well with the findings of Mehrhoff (1985) for capacitors based on aluminium oxide. Fig. 8 also shows that the drift factor for Capacitor A increases when the moisture level is decreased and vice versa.

The observed drift for the electrolytic hygrometer, in contrast to the capacitor hygrometers, was discontinuous and appeared both upwards and downwards. This irregular behaviour is not easily explained by the shortcomings for electrolytic hygrometers described in the literature (Funke et al., 2003) (contamination, wash out of phosphorus pentoxide and shorting).

4.2. Accuracy

The hygrometers compared in this study all have their defined measurement uncertainty, often stated as accuracies by the manufacturers. The uncertainties differ for the various hygrometers and ranges from ±10% (concentration) to ±2 °C (frost point). In the tested concentration range of (20–120) µmol/mol an uncertainty of ±2 °C corresponds to ±20% up to ±30% in concentration (dependent on concentration level). Hence the compared hygrometers could be expected to perform differently regarding accuracy. The stated uncertainty of the chilled mirror is 0.1 °C. The uncertainty of the Karl Fischer technique is estimated to be no better than ±10%, mainly caused by variable leak rates of moisture from surroundings into the titration vessel and uncertainty in the determination of titrated gas volumes by the gas meter. The conversion between concentration and frost point will also contribute to some uncertainty but this is low compared to the uncertainties for the hygrometers. Taking the different uncertainties into account QCM, CaC_2-GC and Fibre-optic show good agreement in their readings and correspond well with the readings from the reference methods, while Capacitor A and Electrolytic clearly do not (Figs. 2 and 3).

Table 4
Response times for decreasing moisture concentrations represented as response times for a change of 63% and 95% of the step changes.

	63% response times (min)		95% response times (min)	
Hygrometer	50 → 20 µmol/mol	120 → 20 µmol/mol	50 → 20 µmol/mol	120 → 20 µmol/mol
Capacitor A	4	3	271	223
Capacitor B	7	5	440	435
QCM	1	1	6	6
CaC_2-GC	97		317	455
Fibre-optic	114	92	335	431
Electrolytic	14	14	267	163

Table 5
Response times for increasing moisture concentrations represented as response times for a change of 63% and 95% of the step changes.

	63% response times (min)		95% response times (min)	
Hygrometer	20 → 50 μmol/mol	20 → 120 μmol/mol	20 → 50 μmol/mol	20 → 120 μmol/mol
Capacitor A	3	3	14	30
Capacitor B	4	2	8	5
QCM	4	2	6	4
CaC2-GC	225	59	312	187
Fibre-optic	76	53	215	178
Electrolytic	32	34	162	179

Capacitor A was exposed to nitrogen with moisture concentrations between 25 μmol/mol and 80 μmol/mol for 35 days prior to the experiments referred to in Figs. 2 and 3. During this time the readings from Capacitor A drifted downwards, explaining the rather large discrepancy when compared to the readings of the reference methods. When the electrolytic hygrometer was first installed, prior to the experiments, it read at the expected moisture level for the first few hours. During the first two days, for reasons unknown, the readings declined and stabilised at a level around 45% of the concentration read by the reference methods. A contaminated electrolytic cell will prevent the moisture from complete absorption in the phosphorus pentoxide and can possibly explain the low readings observed (Feldman, 1990), but this was not further investigated. Taking the ±2 °C uncertainty as a basis, the readings from Capacitor B agree with the readings from the reference methods, except for the first three days after installation.

One strategy for improving the accuracy of hygrometers would be to periodically perform offset adjustments, based on some sort of reliable reference measurements. This is demonstrated in Fig. 8, where the original readings of Capacitor A are corrected by adding 8.5 °C (represented in the figure as "Capacitor A +8.5 °C") to match the readings of the reference methods on day 1. An adjustment like this involves only one reference concentration and it is assumed that the shape of the original calibration curve is still valid. Taking an uncertainty band of ±2 °C for the adjusted readings, these are with a few exceptions in agreement with the readings from the reference methods during the 39 days of experiments (taking also the uncertainties of the reference methods into account). To reduce the level of uncertainty for the capacitor hygrometers, frequent reference measurements and offset adjustments have to be performed. Mermoud et al. (1989) reported the need for weekly offset adjustments to keep the uncertainty of two tested aluminium oxide capacitor sensors within ±10% (concentration), moisture concentrations ranging from 0.2 to 20 μmol/mol. The same frequency would keep the readings from "Capacitor A +8.5 °C" well within ±10% as long as the moisture level is kept unchanged. As soon as the moisture level decreases, the readings from the capacitor hygrometers change their divergence to the readings from the reference methods and the uncertainty band has to be expanded. As can be observed in Fig. 8, the divergence is dependent on the size and direction of the step change. This history dependent response, often referred to as hysteresis (Hasegava, 1980), of the two capacitor hygrometers in this test will restrict their achievable accuracy.

4.3. Response time

All the tested hygrometers, except the QCM, rely on equilibrium conditions for moisture to obtain stable readings. The QCM bases the measurements on fixed time periods (30 seconds) for migration of moisture to and from the sensor. This is believed to be the main reason why the QCM respond faster on step changes in moisture concentration compared to the other hygrometers (Blakemore et al., 1986). For the capacitor, the CaC_2-GC and the fibre-optic hygrometers, porous structures with given adsorption, desorption and diffusion kinetics are involved. Hence it is expected that the speed of response depends on parameters like chemical composition, thickness and pore size distribution of the porous structure. Also the operational temperature will presumably play an

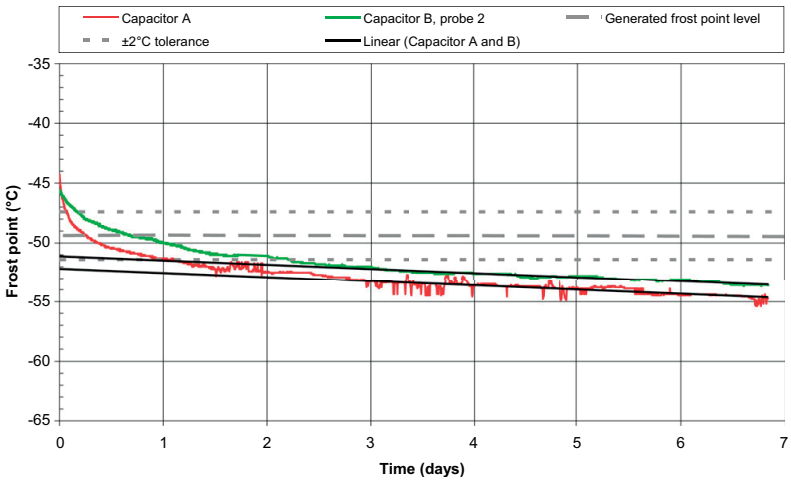

Fig. 7. Demonstration of initial drift of capacitor sensors from two different brands. Linear trend lines were fitted to the data between hour 66 and 164.

Table 6
Calculated drift of capacitor sensors from 66 h to 164 h after start of experiment.

	Frost point level (moisture concentration level)	Drift factor
Capacitor A	−49 °C (44 μmol/mol)	−0.36 °C/day
Capacitor B, probe 1	−35 °C (222 μmol/mol)	−0.42 °C/day
Capacitor B, probe 2	−49 °C (44 μmol/mol)	−0.36 °C/day
Capacitor B, probe 3	−56 °C (18 μmol/mol)	−0.63 °C/day

important role. With this in mind one would expect to find different performances among hygrometers, even if they are based on the same technology.

Several of the hygrometers demonstrated longer response times for decreasing moisture levels compared to increasing ones, as observed in Figs. 5 and 6. This can be addressed to activation energies for desorption being generally higher than activation energies for adsorption (Qu et al., 1999; Wang et al., 2011). Water molecules will either be chemisorbed (first molecule layer) or physisorbed (outer multiple molecule layers) to metal oxide surfaces (Fenner and Zdankiewicz, 2001; Traversa, 1995; Wang et al., 2011). Capillary condensation of water is also possible if the pores are small enough (Traversa, 1995). Different adsorption mechanisms involve different desorption activation energies. The higher desorption activation energy of chemisorbed water molecules will contribute increasingly to the combined activating energy during a desorption process, as the ratio between chemisorbed and physisorbed water will increase (Wang et al., 2011). Consequently sensors with long 95% response times for decreasing moisture levels could still have short 63% response times (e.g. capacitor hygrometers, Fig. 5). Although not observed in this work, electrolytic hygrometers are also described to have slower response on decreasing moisture levels, explained by relatively slow rates of diffusion within the electrolytic film (phosphorus pentoxide) (Keidel, 1959).

During operation of the CaC_2-GC hygrometer, particulate calcium hydroxide will be produced, accumulating in the front end of the reactor. The produced calcium hydroxide appears as fines, the particles being considerably smaller than the calcium carbide. Moisture will adsorb to calcium hydroxide as well as to calcium carbide and the concentration of both substances changes during operation. Only water adsorbed to calcium carbide will undergo reaction to ethyne (Lindblom et al., 1992). Adding the reaction kinetics to the combined adsorption kinetics the result is a rather complex equilibrium regime which affects the speed of response for this hygrometer. As can be observed in Figs. 5 and 6, Tables 4 and 5 the CaC_2-GC hygrometer did not follow the general trend of shorter response times for increasing moisture levels, as illustrated by the relatively long response time for the last step change ((20–120) μmol/mol). This is probably due to the continuously increasing zone of calcium hydroxide in the front end of the reactor, decreasing the speed of response as a function of operation time. The divergent curve shape observed for CaC_2-GC after the last step change (Fig. 4D) is believed to come from the same reason.

4.4. Moisture monitoring of high pressure natural gas

Moisture monitoring at high sample pressures has traditionally been a widespread practice in the natural gas industry. To maintain the sample integrity measurements are performed at sample line pressure or at some intermediate pressure as given by a dew point or frost point sales or transport specification. Hygrometers for high pressure measurements are typically calibrated at ambient pressure to provide traceability to national or international standards. High pressure measurements will break this traceability chain and increase the uncertainty of the measurements. Quality control is often performed by use of portable hygrometers operating at ambient pressure. This practice usually generates the need for conversions of frost points (sub-zero temperatures) at one pressure to a corresponding frost point at another pressure, eventually combined with conversion of units (e.g. between °C and μmol/mol). The conversions can be subjected to large uncertainties and errors, as available conversion tools are generally unsuited for calculations at elevated pressures involving frost points. At ambient pressure the conversions between different units can be performed with reliable conversion methods (e.g. formulas of Sonntag (1990, 1994), and the measurements can be related to certified standards (e.g. reference gas standards or permeation tubes). Hence, presumed that the sampling system is adequate, moisture monitoring at

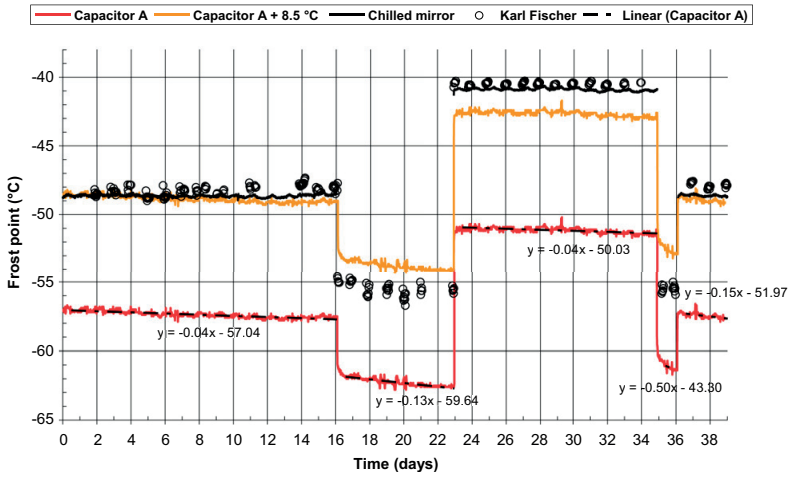

Fig. 8. Original readings of Capacitor A and offset adjusted version (+8.5 °C) of the original readings. For determination of drift factors linear trend lines and their equations are shown for the original Capacitor A readings.

ambient pressure will make the quality control easier and generally improve the measurement uncertainty.

Many natural gas applications involve traces of polar compounds in the gas sample, other than water. Alcohols, glycols, alcohol amines are examples of such compounds which are frequently used in the processing of natural gas. Even if several of these trace compounds have low volatility, they will exert some minimum vapour pressure, dependent on pressure and temperature. The presence of a polar trace compound will complicate the traditional water dew point or frost point concept. Condensed phases (dew or ice) will not necessarily be pure water anymore, but rather mixtures of water and the trace compound (Løkken et al., 2008). Hence this condensed phase will exhibit different characteristics regarding gas hydrate formation and corrosion compared to pure condensed water. A thermodynamic model being able to deal with hydrocarbons, water and other polar substances (e.g. CPA-EoS (Folas et al., 2007a,b)) is necessary to model such complex systems.

The choice of hygrometer has to be determined by requirements of the application with regards to accuracy and speed of response. E.g. process regulation based on moisture monitoring will typically require faster response times than monitoring for corrosion control. Low margins to gas hydrate formation conditions require more accuracy and shorter response time than if the margins are higher. A strategy for quality control can be crucial for successful measurements, as demonstrated by the performances of the hygrometers tested in this work. In contrast to laboratory conditions a real natural gas application will have to cope with several additional challenges as high pressure sample, traces of various chemicals, semivolatile hydrocarbons and even liquid droplets and particles. This adds complexity to the applications and an adequate sampling system becomes vital to success. The interval between reference measurements is dependent of both the chosen hygrometer and the needed accuracy, spanning from a few days to several weeks. Automated systems for calibration checks and adjustments are more frequently included in hygrometers designed for process online measurements. These hygrometers are typically more expensive, but they will not have the same need for external quality control which will have to involve more man hours and additional equipment (e.g. portable hygrometer and calibration gas).

5. Conclusions

The results from this work demonstrated that various hygrometers perform very differently with respect to accuracy, stability and response time. The capacitor hygrometers and the electrolytic cell hygrometer tested in this work showed a tendency to drift, which reduced their accuracy. The QCM, fibre-optic and CaC_2-GC hygrometer showed good accuracy and long term stability. The QCM hygrometer had the overall shortest response times. The type of hygrometer and the strategy for quality control has to be chosen carefully to fit the requirements of a specific natural gas application.

Acknowledgements

The author gratefully acknowledges Statoil ASA and Gassco for financial support of this work. The assistance from and discussions with colleagues at the R&D Centre of Statoil is highly appreciated. Thanks to colleagues in the laboratory for help during the planning, construction and adaption of the test rig. Thanks to Dr. Arne Olav Fredheim, Statoil R&D Centre, and Dr. Rudolf Schmid, NorwegianUniversity of Science and Technology (NTNU), for patient supervision and to Trond Kirkerød for many fruitful discussions on the topic of moisture measurements.

Nomenclature

Abbreviations

CaC_2-GC	hygrometer based on a calcium carbide reactor and gas chromatographic analysis
CPA-EoS	Cubic-Plus-Association equation of state
EoS	equation of state
GERG	European Gas Research Group
ISO	International Organization for Standardization
NIST	National Institute of Standards and Technology
NPL	National Physical Laboratory
PR-EoS	Peng–Robinson equation of state
SRK-EoS	Soave-Redlich-Kwong equation of state
UKAS	United Kingdom Accreditation Service
QCM	quartz crystal microbalance

List of symbols

a	time constant
A_0	value of a state at time $t = 0$
A_t	value of a state at time t
c_w	concentration (μmol/mol)
$e_i(T)$	saturation pressure (hectopascal)
e	natural logarithm
t	time elapsed from start of a change
T_C	temperature (°C)
T_K	temperature (K)

References

Althaus, K., 1999. Messung und Berechnung von Wassergehalten kohlenwasserstoffhaltiger Gasgemische. Fortschritt-Berichte VDI, Reihe 3, nr. 590. VDI Verlag GmbH, Düsseldorf.

Blakemore, C.B., Steichen, J.C., Dallas, G., Van Rossum, G.J., 1986. Continuous trace moisture analysis. In: Rossum, G.J.V. (Ed.), Gas Quality. Elsevier Science Publishers B.V., Groningen, pp. 327–335.

Bruttel, P.A., Regina, S., 2006. Water Determination by Karl Fischer Titration. Monograph 8.026.5003. Metrohm Ltd., Herisau.

Bukacek, R.F., 1955. Equilibrium moisture content of natural gases. Research Bulletin 8. Institute of Gas Technology, Chicago.

Carr-Brion, K., 1986. Moisture Sensors in Process Control. Elsevier Applied Science Publishers, London and New York.

Cremonesi, P.L., 1986. Practical experiences with on-line water dew point determination in natural gas transmission pipelines. In: Rossum, G.J.V. (Ed.), Gas Quality. Elsevier Science Publishers B.V., Groningen, pp. 301–310.

Feldman, R.R., 1990. Devices for moisture measurement in natural gas. 65th International School of Hydrocarbon Measurement, Oklahoma City, pp. 414–415.

Fenner, R., Zdankiewicz, E., 2001. Micromachined water vapor sensors: a review of sensing technologies. IEEE Sens. J. 1 (4), 309–317.

Folas, G.K., et al., 2007a. High-pressure vapor–liquid equilibria of systems containing ethylene glycol, water and methane – experimental measurements and modeling. Fluid Phase Equilib. 251 (1), 52–58.

Folas, G.K., Froyna, E.W., Lovland, J., Kontogeorgis, G.M., Solbraa, E., 2007b. Data and prediction of water content of high pressure nitrogen, methane and natural gas. Fluid Phase Equilib. 252 (1–2), 162–174.

Funke, H.H., Grissom, B.L., McGrew, C.E., Raynor, M.W., 2003. Techniques for the measurement of trace moisture in high-purity electronic specialty gases. Rev. Sci. Instrum. 74 (9), 3909–3933.

Hasegava, S., 1980. Performance characteristics of a thin-film aluminium oxide humidity sensor. In: IEEE (Ed.), 30th Electronic Components Conference. IEEE, p. 386.

ISO, 1993a. ISO 10101-1:1993: Natural Gas – Determination of Water by the Karl Fischer Method – Part 1: Introduction. ISO, Genève.

ISO, 1993b. ISO 10101-3:1993: Natural Gas – Determination of Water by the Karl Fischer Method – Part 3: Coulometric Procedure. ISO, Genève.

ISO, 2004. ISO 18453:2004 Natural Gas – Correlation between Water Content and Water Dew Point. ISO, Genève.

Jamieson, A.W., Sikkenga, H.J., 1986. On-line water dewpoint measurement in natural gas. In: Rossum, G.J.v. (Ed.), Gas Quality. Elsevier Science Publishers B.V., Groningen, pp. 289–299.

Keidel, F.A., 1959. Determination of water by direct amperometric measurement. Anal. Chem. 31 (12), 2043–2048.

Knight, H.S., Weiss, F.T., 1962. Determination of traces of water in hydrocarbons – a calcium carbide-gas liquid chromatography method. Anal. Chem. 34 (7), 749–751.

Lindblom, M., Andersson, L.A., Bjerle, I., 1992. Water determination in pyrolysis gases using calcium carbide. Chem. Eng. Technol. 15, 99–102.

Løkken, T.V., Bersås, A., Christensen, K.O., Nygaard, C.F., Solbraa, E., 2008. Water Content of High Pressure Natural Gas: Data, Prediction and Experience from Field, International Gas Research Conference. Curran Associates Inc., Paris.
McAndrew, J.J., Boucheron, D., 1992. Moisture analysis in process gas streams. Solid State Technol. 35 (2), 52–60.
McAndrew, J.J.F., 1997. Humidity measurement in gases for semiconductor processing. In: Hogan, J.D. (Ed.), Speciality Gas Analysis: A Practical Guidebook. Wiley-VCH, New York, pp. 21–42.
McKetta, J.J., Wehe, A.H., 1958. Use this chart for water content of natural gases. Petrol. Ref. 37 (8), 153–154.
Mehrhoff, T.K., 1985. Comparison of continuous moisture monitors in the range 1 to 15 ppm. Rev. Sci. Instrum. 56 (10), 1930–1933.
Mermoud, F., MBrandt, M.D., Weinstein, B.L., 1989. Recalibration of capacitive-type moisture sensors. Solid State Technol. 32 (5), 59–61.
Monroe, S., 1998. Trace moisture in ammonia: gas chromatography using calcium carbide. J. IEST 41 (1), 21–25.
Mychajliw, B.J., 2002. Determination of water vapor and hydrocarbon dew point in gas. 77th International School of Hydrocarbon Measurement, Oklahoma City, pp. 507–510.
Nahar, R.K., 2000. Study of the performance degradation of thin film aluminum oxide sensor at high humidity. Sens. Actuators B 63 (1–2), 49–54.
Oellrich, L.R., Althaus, K., 2001. Relationship between Water Content and Water Dew Point Keeping in Consideration the Gas Composition in the Field of Natural Gas. GERG Technical Monograph TM14, Fortschritt-Berichte VDI, Reihe 3, nr. 679. VDI Verlag GmbH, Düsseldorf.
Qu, W., Haeusler, A., Meyer, J.-U., Wlodarski, W., 1999. Thick-film gas and humidity sensing array based on semiconducting metal oxides. In: IEEE (Ed.), Conference on Optoelectronic and Microelectronis Materials and Devices. IEEE, Perth, WA, Australia.
Sonntag, D., 1990. Important new values of the physical constants of 1986, vapor pressure formulations based on the ITS-90, and psychrometer formulae. Z. Meteorol. 40 (5), 340–344.
Sonntag, D., 1994. Advancements in the field of hygrometry. Meteorol. Z. 3 (2), 51–66.
Traversa, E., 1995. Ceramic sensors for humidity detection: the state-of-the-art and future developments. Sens. Actuators B 23, 135–156.
Wang, H., Yao, J., Shadman, F., 2011. Characterization of the surface properties of nanoparticles using moisture adsorption dynamic profiling. Chem. Eng. Sci. 66, 2545–2553.
Weik, M.H., 1996. Communications Standard Dictionary. Chapman & Hall, New York.
Wiederhold, P.R., 1997. Water Vapor Measurement. Marcel Dekker Inc., New York.
Wiederhold, P.R., 2000. The principles of chilled mirror hygrometry. Sensors 17 (7), 46–51.
Willsch, R., Ecke, W., Schwotzer, G., 2005. Spectrally encoded optical fibre sensor systems and their application in process control, environmental and structural monitoring. In: Jaroszewicz, L.R., Culshaw, B., Mignani, A.G. (Eds.), Congress on Optics and Optoelectronics. SPIE, Warsaw.

Paper II

Journal of Natural Gas Science and Engineering 7 (2012) 7–15

Contents lists available at SciVerse ScienceDirect

Journal of Natural Gas Science and Engineering

journal homepage: www.elsevier.com/locate/jngse

Water vapour monitoring in natural gas in the presence of methanol

T.V. Løkken

Statoil ASA, Research and Development, Arkitekt Ebbels Veg 10, N-7005 Trondheim, Norway

ARTICLE INFO

Article history:
Received 23 February 2012
Received in revised form
23 March 2012
Accepted 26 March 2012
Available online 21 April 2012

Keywords:
Water dew point
Capacitor sensor
Quartz crystal microbalance
Electrolytic cell
Fibre-optic sensor
Calcium carbide

ABSTRACT

Hygrometers for monitoring of water vapour (moisture) in natural gases have been investigated with respect to influence from methanol co-exposure, during a total of 34 days of experiments. The tested hygrometers are based on capacitor sensor, quartz crystal microbalance (QCM), electrolytic cell, fibre-optic sensor and conversion of water to ethyne with calcium carbide (CaC_2-GC), respectively. In the latter technique ethyne was quantified by a gas chromatograph (GC). While monitoring moisture at the level of 45 μmol/mol, the hygrometers were exposed to approximately (10, 170 and 750) μmol/mol gaseous methanol. The experiments were performed in the laboratory, using nitrogen as the matrix gas. Exposure to approximately 10 μmol/mol methanol demonstrated no clear effect on the tested hygrometers. At the higher levels of 170 μmol/mol and 750 μmol/mol methanol, the readings from several hygrometers were affected. Taken into account the specified uncertainty of the hygrometers, only the electrolytic cell and one of the two tested capacitor sensors (Capacitor B) were significantly affected during the test period. They demonstrated severe misreading as a result of methanol exposure. The readings from the fibre-optic sensor drifted slowly upwards during exposure to the higher methanol levels. The drift speed increased with increasing methanol concentration. However, despite the drift, the readings from the fibre-optic sensor stayed within its specified uncertainty (±2 °C) during the test period. The QCM made a minor shift to higher readings when exposed to 750 μmol/mol methanol. Similar shifts were noticed for the two different brands of capacitor sensors tested. Both capacitor sensors also demonstrated a permanent downward drift during the experiments, one of them increasing the drift speed upon increased methanol concentration. The CaC_2-GC did not show any clear influence from methanol. The results imply that methanol exposure should be taken into consideration when choosing equipment for moisture monitoring and when determining a quality control strategy for the monitoring.

1. Introduction

1.1. Background

Accurate determination of water vapour, often referred to as moisture, in natural gases is crucial for maintaining a stable and safe processing and transport of natural gas. Underestimated moisture concentration in the natural gas can lead to condensation of liquid water in process equipment or pipelines. When combined with compounds such as hydrogen sulphide and carbon dioxide condensed water will increase the corrosion potential (Mychajliw, 2002). Accurate moisture monitoring is also important to avoid the formation of gas hydrates (Jamieson and Sikkenga, 1986). Gas hydrates can plug pipelines or process units, resulting in loss of production or obstructed transportation of natural gas. Methanol is a popular hydrate inhibitor in addition to being used for dehydration, removal of hydrogen sulphide and carbon dioxide and for recovery of heavy hydrocarbons (Esteban et al., 2000; Kohl and Nielsen, 1997). The higher vapour pressure of methanol, compared to many other chemicals used in the processing of natural gas, can lead to significant concentrations of methanol in the natural gas. In the case of continuous use of methanol the natural gas will always contain some methanol, the concentration being dependent of the process conditions and the concentration of methanol in the injected aqueous phase. More widespread is the intermittent use of methanol, e.g. as a hydrate inhibitor during process start-up or shutdown (Bahadori and Vuthaluru, 2010). In this case the concentration of methanol will vary, from no detectable methanol at all to high concentrations (several thousand μmol/mol).

The aim of this work is to investigate how devices for monitoring of moisture in gases, referred to as hygrometers, are influenced by the presence of gaseous methanol.

E-mail address: tvl@statoil.com.

1875-5100/$ – see front matter © 2012 Published by Elsevier B.V.
doi:10.1016/j.jngse.2012.03.005

1.2. Measuring techniques

Throughout the years numerous methods for moisture measurements in gases have been developed and established. Most of them are thoroughly described in published literature (Blakemore et al., 1986; Bruttel and Regina, 2006; Carr-Brion, 1986; Funke et al., 2003; ISO, 1993a,b; Keidel, 1959; Knight and Weiss, 1962; McAndrew and Boucheron, 1992; McAndrew, 1997; Monroe, 1998; Wiederhold, 1997a, 2000; Willsch et al., 2005). Hygrometers based on capacitor sensor, quartz crystal microbalance (QCM), electrolytic cell, fibre-optic sensor, CaC_2-GC, chilled mirror and Karl Fischer titration have been investigated in this work. The basic principles for these methods are briefly summarised in Table 1. Karl Fischer titration and chilled mirror hygrometry are usually regarded as direct or absolute methods as they utilise a direct relationship between the measured quantity and the amount of moisture. Hence they often are preferred as reference methods.

1.3. Interpretation of moisture measurements

The amount of moisture in a natural gas can either be expressed as concentration (e.g. μmol/mol or mg/Sm^3 at some defined standard temperature and pressure) or as dew or frost point in degrees Celsius. The dew point is the highest temperature, at a specified pressure, where water can condense from the gas. The frost point is the highest temperature, at a specified pressure, where ice can precipitate from the gas (Løkken et al., 2008). In the temperature region between 0 °C and −20 °C it is difficult to predict whether the moisture will condense as dew or precipitate as ice. It is necessary to distinguish between the dew point and the frost point, as these could deviate with several degrees for the same moisture concentration. Well recognised and accurate formulas for conversion between dew or frost point at atmospheric pressure and concentration (via saturation vapour pressure) are published by Sonntag (1990, 1994). The following formula converts frost point to saturation vapour pressure:

For the given temperature range

$$173.15\ \mathrm{K} \le T_\mathrm{K} \le 273.16\ \mathrm{K} (-100\ ^\circ\mathrm{C} \le T_\mathrm{C} \le 0.01\ ^\circ\mathrm{C})$$

$$\ln e_i(T_\mathrm{K}) = -6024.5282 T_\mathrm{K}^{-1} + 24.7219 + 1.0613868 \times 10^{-2} T_\mathrm{K} - 1.3198825 \times 10^{-5} T_\mathrm{K}^2 - 0.49382577 \ln T_\mathrm{K}, \quad (1)$$

$e_i(T_\mathrm{K})$ is the saturation vapour pressure with respect to ice in hPa (hectopascal), T_K is frost point temperature in K.

Saturation vapour pressure can be converted to frost point by formula (2), which is derived from Eq. (1):

$$T_\mathrm{K} = 12.1197 y + 5.25112 \times 10^{-1} y^2 + 1.92206 \times 10^{-2} y^3 + 3.84403 \times 10^{-4} y^4 + 273.15 \quad (2)$$

In the conversion formula (2)

$$y = \ln(e_i(T_\mathrm{K})/6.11153) \quad (3)$$

For conversions between saturation vapour pressure and concentration the following formula can be used:

$$c_\mathrm{w} = \frac{e_i(T_\mathrm{K}) \times 10^6}{1013.26}, \quad (4)$$

c_w is concentration in μmol/mol. At elevated pressures the formulas of Sonntag are not applicable because of increasing non ideal behaviour of the gas.

1.4. Moisture generator

Several methods for the generation of moisture in gases are described in the literature, such as the two-pressure, two-flow or two-temperature generator (Funke et al., 2003; Hasegava and Little, 1977; Sonntag, 1994; Wiederhold, 1997a). Much effort is

Table 1
Summary of methods for moisture measurements in gases.

Method	Typical uncertainty	Working principle
Capacitor sensor	(1–3) °C	Capacitance or impedance measured as a function of water molecules adsorbed to the porous dielectric (usually metal oxides like Al_2O_3 or SiO_2) of a capacitor. (Carr-Brion, 1986; Funke et al., 2003; McAndrew and Boucheron, 1992; McAndrew, 1997; Wiederhold, 1997a)
Quartz crystal microbalance (QCM)	±10%	Measures the resonance frequency of an oscillating quartz crystal (piezoelectric) coated with a hygroscopic polymer. The frequency changes with mass as water molecules adsorb on the quartz crystal. (Blakemore et al., 1986; Carr-Brion, 1986; Funke et al., 2003; McAndrew and Boucheron, 1992; McAndrew, 1997; Wiederhold, 1997a)
Electrolytic cell	±10%	Measures current generated from electrolytic decomposition of water adsorbed in strongly hygroscopic P_2O_5. (Keidel, 1959)
CaC_2-GC	±10%	Water and calcium carbide (CaC_2) reacts to form ethyne: $2H_2O + CaC_2 \rightarrow \mathbf{C_2H_2} + Ca(OH)_2$. Quantification of ethyne by gas chromatographic (GC) separation and detection e.g. with a thermal conductivity or a flame ionisation detector. (Knight and Weiss, 1962; Monroe, 1998)
Fibre-optic sensor	±2 °C	Measures a shift in reflection spectrum dependent on the amount of adsorbed water in a hygroscopic Fabry-Perot filter. "Fibre-optic" in the sense that light is emitted and reflected via fibre-optic cables. (Rittersma, 2002; Willsch et al., 2005)
Karl Fischer titration	±10%	The Karl Fischer reaction: $ROH + SO_2 + R'N \rightarrow (R'NH)SO_3R$ $(R'NH)SO_3R + 2R'N + I_2 + \mathbf{H_2O} \rightarrow (R'NH)SO_4R + 2(R'NH)I$ ROH = alcohol, R′N = basic nitrogen compound For coulometric titration the amount of water is calculated by measuring the current needed for the electrochemical generation of iodine (I_2) from iodide (I^-). (Bruttel and Regina, 2006; ISO, 1993a; ISO, 1993b)
Chilled mirror	±0.2 °C	Measures the temperature at which water molecules condense from the gas to form dew or frost on a reflective surface (mirror). The dew or frost is detected on the surface optically by an electro-optic detector. (Wiederhold, 1997a, 2000)

required to produce a stream of gas with a very accurate moisture concentration. Equipment for this purpose is typically found at national measurement institutes, like NPL (National Physical Laboratory, United Kingdom) and NIST (National Institute of Standards and Technology, USA). For this work a much simpler moisture generator was constructed, with the option to introduce an additional volatile chemical. The equipment is well suited for comparison of hygrometers rather than calibrating them accurately. Having applications for moisture in natural gas in mind, the main focus was to produce a gas with sufficient long term, drift-free and controllable concentrations of both moisture and a volatile chemical.

2. Experimental set up

2.1. Test rig

A test rig for generation of mixtures of moisture and methanol in gases was established as shown in Fig. 1. Table 2 summarises pieces of equipment used in the test rig. It was able to generate a stream of nitrogen gas with drift-free concentrations of moisture and methanol. The nitrogen gas (>99.999% purity) was fed to the test rig at about 4 bar through a pressure regulator (V-1). The gas flow was split in three lines: one line for generation of dry gas for dilution (T-2) and two lines for generation of gas saturated with moisture and methanol respectively (T-3 and T-4). The gas was fed to the three lines via needle valves (V-2 to V-4).

In the first line (T-2) two molecular sieve traps in series (E-1 and E-2) dried the nitrogen gas. The traps were specified to remove moisture to less than 50 nmol/mol. In the second line (T-3) nitrogen gas was bubbled for saturation through water at room temperature (about 25 °C) inside two stainless steel cylinders (saturators) in series (E-3 and E-4). The saturators were modified filter housings with a volume of 30 ml, each filled with 20 ml water (ion exchanged). A piece of 6 mm outer diameter stainless steel tubing (316L stainless steel) was welded to the inlet ports to introduce the gas into the liquid near the bottom of the cylinders. The saturated gas was further directed through three cylinders in series (E-5 to E-7) kept at a lower temperature (10 °C). This temperature was controlled with a cooling bath (E-8). These empty cylinders acted as condensers; the test gas leaving the last cylinder was at a constant moisture concentration, determined by the actual temperature and pressure in the condensers. To facilitate an efficient cooling of the gas, a submerged coil of tubing (C-1), approximately 1 meter long, connected the first and second condenser. The third line (T-4) was identical to the second line (T-3), with separate saturators (E-9 and E-10), condensers (E-11 to E-13), coil (C-2) and cooling bath (E-14). The saturators in this line were filled with methanol instead of water. The flow rates of the three gas streams (T-2, T-3 and T-4) were controlled by separate manual flow controllers (V-5, V-6 and V-7) and combined in an union cross to produce the final test gas stream (T-5), containing both moisture and methanol. The total flow rate of the test gas was approximately 6 Nl/min and was sufficient to feed all hygrometers. The test gas stream was directed to a compact gas manifold (E-15) for further distribution to the hygrometers (H-1 to H-8) and ventilation lines. The hygrometers were connected to the gas manifold via equal lengths (1.2 meter) of tubing and fine metering valves (V-8 toV-14). Sufficient lengths of 1/8 inch stainless steel tubing were connected to the outlet ports of the hygrometers to prevent back-diffusion of moisture from the atmosphere. Further downstream, the outlet streams were gathered in a gas manifold and guided to ventilation in 1/4 inch Teflon tubing. All connecting tubing (T-1 to T-4) was made of stainless steel. The tubing (T-5) between V-5, V-6 and V-7 and the

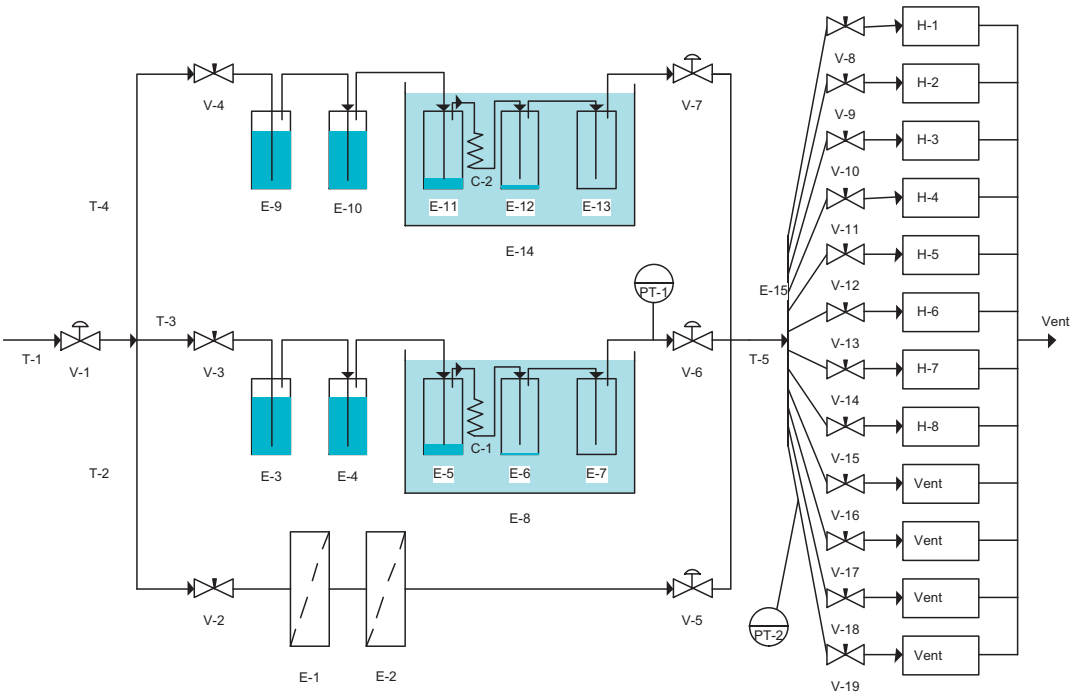

Fig. 1. Schematic representation of the test rig. Equipment description is found in Table 2.

Table 2
Equipment description, the codes refers to Fig. 1.

Code	Description	Model	Manufacturer
V-1	Single stage pressure regulator	SI15	SMT S.A.S., France
V-2 to V-4	Needle valves	3812F4Y	Hoke, USA
V-5	Flow controller	PC 8942	Brooks Instrument, USA
V-6 and V-7	Flow controller	FMC-2000	FlowMatrix Inc., USA
V-8 to V19	Fine metering valve	SS-2MG	Swagelok, USA
E-1 and E-2	Molecular sieves		Ametek, USA
E-3, E-4, E-9 and E-10	Modified filter housings, saturators	Model 122	Headline Filters, UK
E-5 to E-7 and E-11 to E-13	Modified filter housings, condensers	Model 122	Headline Filters, UK
E-8 and E-14	Cooling bath	FP-45	Julabo Labortechnik GmbH, Germany
E-15	Gas manifold	Z12M2	Vici AG International, Switzerland
PT-1	Pressure transmitter	PA-55X	Keller AG, Switzerland
PT-2	Pressure transducer	Model SA	Honeywell, USA
H-1	Capacitor A		
H-2	Capacitor B		
H-3	QCM		
H-4	CaC_2-GC		
H-4.1	Reactor with grinded calcium carbide	Particles with diameter from 0.3 mm to 1 mm	Merck KGaA, Germany
H-4.2	Gas Chromatograph	CP4900 Micro-GC	Varian Inc., USA
H-4.3	GC separation column	CP-PoraPlot Q, 10 m long, 0.25 mm i.d.	Varian Inc., USA
H-5	Fibre-optic		
H-6	Karl Fischer	Model 831	Metrohm AG, Switzerland
H-6.1	Gas meter	TG 1 Mod. 5-8	Ritter, Germany
H-7	Chilled mirror	S4000 Integrale	Michell Instruments ltd., UK
H-8	Electrolytic		
C-1	1 m coil made of 1/8 × 0.035 inch, 316L stainless steel tubing	Sandvik 3R60	AB Sandvik Materials Technology, Sweden
T-1 to T-4	1/8 × 0.035 inch, 316L stainless steel tubing	Sandvik 3R60	AB Sandvik Materials Technology, Sweden
T-5	Treated 1/8 × 0.035 inch 316L stainless steel tubing	Siltek™	Restek Corporation, USA

hygrometers (H-1 to H-8) was electro polished and surface deactivated, to minimise surface adsorption.

2.2. Hygrometers

Hygrometers based on capacitor sensor (two different brands), quartz crystal microbalance (QCM), CaC_2-GC, fibre-optic sensor, electrolytic cell, Karl Fischer titration and chilled mirror (continuously operated) have been investigated in the experiments.

The hygrometers were equipped with control units for communication with the probes or sensors and transfer of data to a computer for storage. Data points were stored every 5 min. The CaC_2-GC hygrometer consisted of a calcium carbide reactor (H-4.1) for conversion of moisture to ethyne and a micro gas chromatograph (H-4.2) for quantification of the ethyne. The micro gas chromatograph was equipped with a separation column (H-4.3) and a micro thermal conductivity detector and was controlled by chromatography software (CP Maitre Elite) on the computer. The processed data from CP Maitre Elite was collected approximately every 10 min.

Two direct methods were used for reference measurements, being of minor interest with respect to continuous online process monitoring. These were a chilled mirror hygrometer (H-7) and a Karl Fischer titrator (H-6). The volume of the titrated gas was measured by a drum-type gas meter (H-6.1). The chilled mirror hygrometer was set to perform continuous measurements, with storage of data every 5 min. The Karl Fischer titrations were performed manually on weekdays (between 3 and 9 parallels each day) during the experiments.

2.3. Operation of test rig

The mixing ratio of the three gas streams (T-2, T-3 and T-4) was controlled by three manually operated flow controllers (V-5, V-6 and V-7). The two gas streams saturated with moisture and methanol respectively were controlled between 10 and 300 Nml/min with flow controllers (V-6 and V-7), while the dry dilution gas was adjusted to a final combined flow of about 6 Nl/min with another flow controller (V-5). The temperature in the cooling bath for line 2 (moisture) was set to 10 °C (±0.01 °C) and the pressure in the condensers was controlled at approximately 4 bar and monitored with a pressure transmitter (PT-1). The temperature in the cooling bath for line 3 (methanol) was initially set to −10 °C (±0.01 °C). By adjusting the three flow controllers, or changing the temperature in the cooling baths, different concentrations of moisture and methanol could be produced and changed quickly. The pressure upstream the metering valves (V-8 to V-19) was about 2 bar, monitored by a pressure transducer (PT-2). The QCM had internal mass flow controllers which needed a sample pressure slightly elevated from atmospheric pressure. The other hygrometers were fed with test gas at ambient pressure. The flow rates to the different hygrometers were controlled in agreement with the recommendations made by the manufacturers. Excess test gas was distributed to vent through 1/8 inch stainless steel tubing connected to the spare ports on the compact gas manifold (E-15). Fine metering valves (V-15 to V19) were used to control the flow rates also on these gas streams.

2.4. Conversion between frost point and concentration

Some of the hygrometers returned dew or frost points (capacitor sensors, fibre-optic sensor and chilled mirror), typically in degrees Celsius, while others returned concentration (QCM, CaC_2-GC, electrolytic cell and Karl Fischer titration) in parts per million (molar or volume). To be able to compare data from all the hygrometers conversions between the different units were necessary. In this work the formulas of Sonntag (1990, 1994) were used for these conversions (Eqs. (1)–(4)).

2.5. Quantification of methanol

The concentration of methanol was monitored using the same gas chromatographic equipment as for ethyne (chapter 2.2). The gas chromatographic method provided sufficient separation between ethyne and methanol on the separation column (H-4.2), for quantification of both species simultaneously. Thus, methanol was injected to the gas chromatograph via the calcium carbide reactor as long as the CaC_2-GC hygrometer was monitoring moisture. Methanol was injected directly to the gas chromatograph only when the calcium carbide reactor was bypassed.

2.6. Calibration of instruments

The chilled mirror hygrometer was recalibrated prior to the experiments at Michell Instruments (UKAS accredited calibration laboratory). The other hygrometers were calibrated by the manufacturers before they were made available for testing. No special treatment was done prior to usage of the sensors. No recalibration was performed before or during the experiments.

The micro gas chromatograph (CaC_2-GC) was calibrated with respect to ethyne and methanol before the experiments. Three calibration gas mixtures were used with ethyne concentrations in nitrogen of 11 μmol/mol (10% relative uncertainty), 53.4 μmol/mol (5% relative uncertainty), and 204 μmol/mol (5% relative uncertainty) respectively. Two calibration gas mixtures were used with methanol concentrations in nitrogen at 10.7 μmol/mol and 101 μmol/mol (10% relative uncertainty). The calibration gas mixtures, which were certified with international traceability, were purchased from Yara (Yara International ASA, Norway).

3. Results

3.1. Moisture and methanol concentrations during the experiments

The test rig was initially set to produce a stream of nitrogen with a moisture concentration level of 45 μmol/mol and a methanol (gaseous) concentration of approximately 10 μmol/mol (low level). After 6 days the flow rate of the gas stream supplying the test gas with methanol was increased, to produce a methanol concentration level at 170 μmol/mol (medium level). The methanol concentration was held at this level for 7 days. On day 13 the temperature in the cooling bath for the methanol condensation (chapter 2.1) was increased from −10 °C to 15 °C. This produced a methanol concentration level of 750 μmol/mol (high level). On day 14 the methanol concentration started to decrease. From day 23 the methanol concentration was too low to be quantified.

3.2. General explanation of result presentation

Figs. 2 and 3 show the moisture readings from the tested hygrometers during the methanol exposure (methanol concentration on secondary y-axis). The hygrometers originally returning frost point readings, being the capacitor sensors, fibre-optic sensor and the chilled mirror, are grouped together in Fig. 2. The Karl Fischer readings are originally expressed as concentration (μmol/mol), but converted to frost point in Fig. 2 by use of the formulas of Sonntag (Eqs. (2)–(4), chapter 1.3). The QCM, CaC_2-GC and the electrolytic cell returned readings as concentration (μmol/mol) and these are grouped together with Karl Fischer and chilled mirror readings in Fig. 3. The chilled mirror readings are originally expressed as frost points but are converted to concentration in μmol/mol in Fig. 3 by use of the formulas of Sonntag (Eq. (1), chapter 1.3). Data from the chilled mirror is left out during exposure to the medium and high concentration level of methanol in Figs. 2 and 3. At these methanol concentrations stable frost point readings from the chilled mirror were difficult to obtain. When the methanol concentration was increased on day 6 and day 13 the calcium carbide reactor was bypassed for some hours, to get direct injection of the test gas to the gas chromatograph. The same operation was performed on day 21. During these periods of direct injections, readings from CaC_2-GC are missing, as can be registered in Fig. 3. On day 5 a short power break disturbed the experiments, which can be seen in Figs. 2 and 3.

The readings from all hygrometers follow a diurnal rhythm which is synchronous with the ambient temperature variation during the day and night.

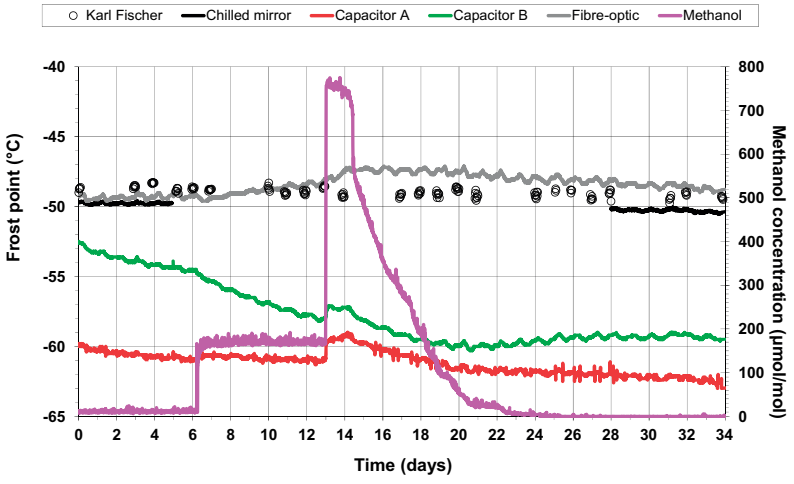

Fig. 2. Frost point readings from Capacitor A, Capacitor B and Fibre-optic, at a moisture concentration level of 45 μmol/mol during variable methanol exposure, together with readings from the reference hygrometers (Karl Fischer and Chilled mirror). The methanol concentration is plotted against the secondary *y*-axis. The chilled mirror readings are plotted only at the lowest methanol exposures due to interferences at the higher methanol concentrations.

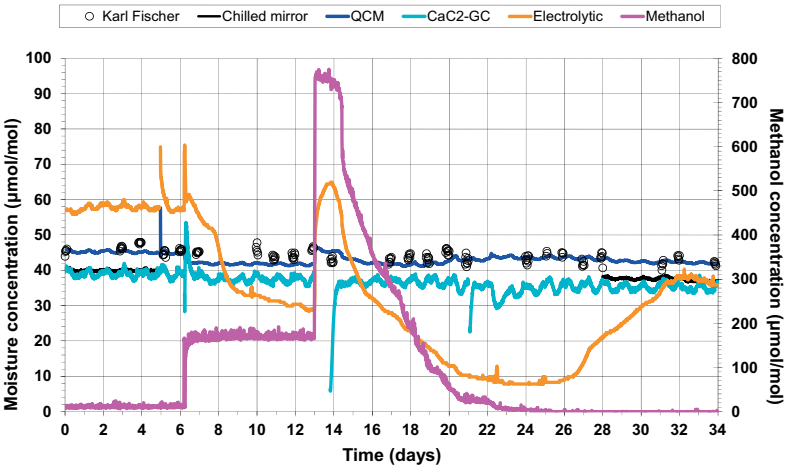

Fig. 3. Moisture concentration readings from QCM, CaC2-GC and Electrolytic, at a moisture concentration level of 45 µmol/mol during variable methanol exposure, together with readings from the reference hygrometers (Karl Fischer and Chilled mirror). The methanol concentration is plotted against the secondary *y*-axis. The chilled mirror readings are plotted only at the lowest methanol exposures due to interferences at the higher methanol concentrations.

3.3. Low level of methanol

At the 10 µmol/mol concentration level of methanol the reference hygrometers (Karl Fischer and Chilled mirror) read between −48 °C and −49.5 °C, corresponding to between 39 µmol/mol and 49 µmol/mol. The readings had no observable drift. The average of the Chilled mirror readings were 6 µmol/mol lower than the Karl Fischer readings during these first 6 days of experiments. The readings from Fibre-optic and CaC_2-GC corresponded well with the chilled mirror. The readings from QCM corresponded well with the Karl Fischer readings. The readings from Electrolytic were at a higher level (between 56 µmol/mol and 60 µmol/mol) compared to the reference hygrometers. At the starting point of the experiments the two capacitor sensors returned frost points more than 10 °C (Capacitor A) and 3 °C (Capacitor B) lower than the frost point readings of the chilled mirror. Unlike the other hygrometers, the Capacitor A and Capacitor B demonstrated a downward drift of their readings, increasing the deviation from the reference hygrometers.

3.4. Medium level of methanol

When the methanol concentration increased to 170 µmol/mol on day 6, the moisture readings from QCM and CaC_2-GC shifted to a slightly lower level, stabilizing at this new level. The size of the shift was approximately 2 µmol/mol. No such change was recognised for the Karl Fischer readings. The readings from Fibre-optic started to drift upwards, while the readings from Electrolytic started to drift downwards. The readings from Capacitor A showed a minor shift upwards after the elevation of the methanol concentration, but the downward drift seemed to remain unchanged. In the case of Capacitor B, no shift was observed but a marked increase in the drift speed was noticed.

3.5. High level of methanol

On day 13 the methanol concentration was increased to a level of 750 µmol/mol. The readings from QCM, Electrolytic, Capacitor A and Capacitor B made upwards shifts when the methanol concentration increased. The magnitudes of the shifts were approximately 5 µmol/mol for QCM, 35 µmol/mol for Electrolytic, 2 °C for Capacitor A and 1 °C for Capacitor B. The readings from CaC_2-GC were low during the first hours of operation after ending the bypass period for the calcium carbide rector. Later the CaC_2-GC readings stabilized at its former level. The readings from Fibre-optic did not make a distinct shift, but the upward drift observed at medium methanol level increased slightly in speed. The reference measurements (Karl Fischer) were not noticeably affected by the increased methanol concentration.

3.6. Decreasing methanol concentration from 750 µmol/mol to zero

The methanol concentration began to decrease after day 14, reaching a level of less than 10 µmol/mol after day 22. From day 25 the methanol concentration was generally too low to be measured, the lowest limit of detection (3 times the noise level) being approximately 4 µmol/mol. The Karl Fischer readings remained stable also during this phase of the experiments. The QCM readings decreased during the decreasing methanol concentration and returned to the level read between day 6 and 13 (medium level of methanol). After day 18 the QCM readings drifted slightly upwards for some days, but still corresponded well with the Karl Fischer readings.

The CaC_2-GC readings were stable between day 14 and day 20, during which the methanol concentration decreased by approximately 700 µmol/mol. Between day 20 and 26 the CaC_2-GC readings decreased almost 5 µmol/mol and then increased again, towards its former level. The readings from Electrolytic continued to decrease during the methanol decline and reached a minimum around day 24 before increasing during the last week of the experiments. The direction of the drift for Fibre-optic changed from upwards to downwards when the methanol concentration started to decrease. This downward drift was permanent during the remainder of the experiments. The readings from the Capacitor B continued to drift downwards while the methanol concentration was decreasing. The drift speed was similar to the one observed during exposure to methanol at the 170 µmol/mol concentration level. During this phase of the experiments Capacitor A drifted in a similar way as Capacitor B. After day 20 the readings from Capacitor A returned to a lower drift speed while the readings from Capacitor B drifted upwards from day 20.

4. Discussion

4.1. Reference hygrometers

The Karl Fischer technique is not expected to be interfered by methanol (Bruttel and Regina, 2006; ISO, 1993a; Lurvey, 1977). Correct subtraction of response from background moisture, diffusing into the titration cell through various connections, is one of the major challenges when using Karl Fischer for determination of trace amounts of moisture in gas (Dong et al., 2005). Accurate measurement of the titrated gas volume is another challenge. These are determining factors for the accuracy and precision obtainable for moisture measurements using the Karl Fischer technique. For the Karl Fischer equipment used in this work the uncertainty is estimated to be no better than ±10% (with respect to concentration).

The chilled mirror technique is based on the condensation of dew or precipitation of ice on a metallic mirror surface when the mirror is chilled down to the dew point temperature or the frost point temperature of the gas. The accuracy of the chilled mirror used in this work is stated to be ±0.1°C. As with many stated accuracies also this is expected to increase during long term use of the hygrometer (Wiederhold, 1997a,b). Hence, a more realistic achievable uncertainty for a chilled mirror, when used in an application like in this work, will be between ±0.2 °C and ±0.5 °C. The dew or frost point temperatures are generally expected to change with the presence of methanol in the gas (Cremonesi, 1986; ISO, 1981), as the condensed or precipitated layer on the mirror surface will be a mixture of methanol and water rather than water only. For a moisture concentration of 45 μmol/mol thermodynamic simulation with the CPA model (Folas et al., 2005a,b) indicates that a methanol concentration of 10 μmol/mol or 170 μmol/mol will change the frost point less than 0.1 °C. At the methanol concentration of 750 μmol/mol, a frost point increase of approximately 3.5 °C is indicated. This means that the moisture readings from a chilled mirror are expected to be practically unaffected in the presence of both 10 μmol/mol and 170 μmol/mol methanol, from a thermodynamic point of view. The reason why the chilled mirror was unable to return stable readings at the methanol level of 170 μmol/mol or higher was not investigated. The literature suggests accumulation of particulate or volatile contaminants on the mirror surface, disturbing the optical detection of the dew or frost layer, as the major source of error for chilled mirrors (Fenner and Zdankiewicz, 2001; Funke et al., 2003; Wiederhold, 2000). For the low methanol concentrations, the frost point measurements appeared to be unaffected by the methanol, in the sense that the instrument was able to establish stable measurements at the expected moisture level. The chilled mirror readings were on average 6 μmol/mol lower than the Karl Fischer readings during exposure to 10 μmol/mol methanol. Taken into account an uncertainty band of at least ±10% for the Karl Fischer technique and ±0.2 °C for the chilled mirror, the readings from these two techniques are hardly significantly different.

4.2. Changing the methanol concentration

The first increase of the methanol concentration (day 6) was achieved by increasing the flow of the methanol saturated nitrogen. This resulted in a corresponding slight decrease in moisture concentration due to dilution. Based on flow calculations and saturation pressures of water and methanol (calculated using the CPA model), the decrease in moisture concentration was estimated to be approximately 1.6 μmol/mol. Hence the observed shift in the readings from QCM and CaC_2-GC (Fig. 3) is believed to be a response due to the decreased moisture concentration rather than being a response due to the increased methanol concentration. Though not very distinct, the decrease in moisture concentration can be observed for the Karl Fischer readings also (Fig. 3). The Karl Fischer measurements have relative poor precision (within 3% relative standard deviation) compared to the other hygrometers, which makes it rather difficult to pick up small changes of moisture concentration. A *t*-test performed for the moisture readings from Karl Fischer collected before and after day 6 demonstrated a significant decrease of 2.3 μmol/mol for the readings collected after day 6. The second increase of the methanol concentration was achieved by increasing the condensation temperature for the methanol line in the test rig, from −10 °C to 15 °C. Hence, the moisture level is not expected to decrease due to dilution for this increase of methanol concentration. The decreasing methanol concentration between day 14 and 23 was a result of the significant methanol consumption during saturation, decreasing the liquid level in the saturators beneath a critical level for effective saturation. Finally, no methanol was left in the saturators, and as a consequence no methanol was measurable in the test gas during the last 9 days of the experiments.

4.3. Capacitor sensors

The capacitor sensors are well known for their tendency to drift downwards (Hasegava, 1980; Løkken, 2012; Mehrhoff, 1985; Mermoud et al., 1989). The capacitor sensors tested in this work had already drifted for some time, during operation in previous tests (Løkken, 2012). This explains their low readings compared to the reference measurements. The drift rates observed for Capacitor A and Capacitor B during the first 6 days of the experiments (Fig. 3) are consistent with observations in the previous tests, which were performed without methanol exposure. The general problem with drifting capacitor sensors demands for careful quality control and frequent calibrations to improve the accuracy of these hygrometers. The results in this work indicate that methanol exposure increases the measurement uncertainty for capacitor sensors, through increased drift speed or shifts in the moisture readings, or both. The dielectric constants of methanol and water are 33 and 80 respectively (Mohsen-Nia et al., 2010). This means that methanol can be expected to contribute to the response (capacitance or impedance) of a capacitor sensor, though to a lesser extent than water. The kinetic diameters of methanol and water are 0.26 nm and 0.40 nm respectively (ten Elshof et al., 2003). Hence the accessibility for methanol to the dielectrics of the capacitor sensor is dependent of pore sizes of the various structures of the sensor. Different manufacturers design their capacitor sensors differently with regards to pore sizes, which will determine their response to methanol.

4.4. Electrolytic cell

The electrolytic cell demonstrated the most severe response to methanol exposure, compared to the other hygrometers in this test. Methanol is expected to interfere with the moisture measurement, as methanol will readily combine with phosphorous pentoxide (P_2O_5) and produce water (Wiederhold, 1997a). The results from this work suggest that the influence from methanol is concentration dependent, decreasing moisture readings at medium concentration, but increasing moisture readings at higher concentration.

4.5. Fibre-optic sensor

As with the capacitor sensors, also the pore sizes of the fibre-optic sensor will determine the potential for methanol to interfere with its moisture detection. The manufacturer claims that the

pore diameters of the sensor are lower than 0.40 nm, which seems to be insufficient to totally prevent the methanol from adsorption to the sensor structure. The moisture readings during methanol exposure at the two highest methanol concentrations did not stabilize during the time of exposure. Even if the total upwards drift was restricted to 1.4 °C, a prolonged period with methanol exposure would probably soon have made the readings from the fibre-optic sensor exceed its uncertainty band of ±2 °C. No drift was noticeably at the low level of 10 μmol/mol methanol, which indicates that the fibre-optic sensor can handle low levels of methanol. This hygrometer needs a lot of time to recover after methanol exposure, as demonstrated by the slow downward drift during the last 16 days of the experiments (Fig. 2), with little or no methanol in the test gas.

4.6. QCM and CaC_2-GC

In this work the CaC_2-GC and the QCM demonstrated no or only minor response to methanol. Even if the upwards shift of the QCM was marked when exposed to 750 μmol/mol methanol (Fig. 3), the size of the shift was within the uncertainty band of the hygrometer (±10%). The instability of the QCM readings during the decreasing methanol concentration was within the same acceptable range. If, and eventually to which extent, even higher concentrations of methanol will increase the shifts is not clarified, and should be tested in the future. The QCM relies on a selective adsorption of moisture on a hygroscopic layer attached to the quartz crystal. Hence any significant co-adsorption of other polar compounds on this hygroscopic layer will contribute to the response of the QCM. The readings from the CaC_2-GC had a local minimum on day 22. Detailed inspection of the data implies that this originates from a small pressure spike in the system, temporarily interrupting the equilibrium situation in the calcium carbide reactor.

4.7. Quality control of hygrometers

The general importance of adequate quality control of hygrometers is pointed out by several authors (Løkken, 2012; Mermoud et al., 1989). In applications with potential for methanol exposure, e.g. certain natural gas applications, the choice of hygrometer and the strategy for quality control should be given special attention.

5. Conclusions

The results from this work clearly demonstrate that for some hygrometers methanol exposure has the potential of interfering with moisture monitoring. During monitoring of moisture at the level of 45 μmol/mol, exposure to approximately 10 μmol/mol methanol had no significant effect for the tested hygrometers. At the higher levels of 170 μmol/mol and 750 μmol/mol methanol, the moisture readings from several hygrometers were affected. Taken into account the uncertainty specifications of the hygrometers, only the electrolytic cell and one of the two tested capacitor sensors (Capacitor B) were significantly affected. They, however, demonstrated severe misreading as a result of methanol exposure. The readings from the fibre-optic sensor drifted slowly upwards during exposure to the higher methanol levels. The drift speed increased with increasing methanol concentration. Despite this drifting, the readings from the fibre-optic sensor stayed within its specified uncertainty (±2 °C) during the test period. The QCM made a minor shift to higher moisture readings when exposed to 750 μmol/mol methanol. Similar shifts were noticed for the two different brands of capacitor sensors tested. Both capacitor sensors also demonstrated a permanent downward drift during the experiments, one of them increasing the drift speed upon increased methanol concentration. The CaC_2-GC did not show any clear influence from methanol. The results imply that methanol exposure should be taken into consideration when choosing equipment for moisture monitoring and when determining a quality control strategy for the monitoring.

Acknowledgements

The author gratefully acknowledges Statoil ASA and Gassco for financial support of this work. The assistance from and discussions with colleagues at the R&D Centre of Statoil is highly appreciated. Thanks to colleagues in the laboratory for help during the planning, construction and adaption of the test rig. Thanks to Dr. Arne Olav Fredheim, Statoil R&D Centre, and Dr. Rudolf Schmid, Norwegian University of Science and Technology (NTNU), for patient supervision and to Trond Kirkerød for many fruitful discussions on the topic of moisture measurements.

Nomenclature

Abbreviations

CaC_2-GC	hygrometer based on a calcium carbide reactor and gas chromatographic analysis
CPA	Cubic-Plus-Association, an equation of state
NIST	National Institute of Standards and Technology
NPL	National Physical Laboratory
UKAS	United Kingdom Accreditation Service
QCM	quartz crystal microbalance

List of symbols

c_w	concentration (μmol/mol)
$e_i(T_K)$	saturation pressure (hectopascal)
T_C	temperature (°C)
T_K	temperature (K)

References

Bahadori, A., Vuthaluru, H.B., 2010. Prediction of methanol loss in vapor phase during gas hydrate inhibition using Arrhenius-type functions. J. Loss Prevent. Proc. 23 (3), 379–384.
Blakemore, C.B., Steichen, J.C., Dallas, G., Van Rossum, G.J., 1986. Continuous trace moisture analysis. In: Rossum, G.J.v. (Ed.), Gas Quality. Elsevier Science Publishers B.V., Groningen, pp. 327–335.
Bruttel, P.A., Regina, S., 2006. Water Determination by Karl Fischer Titration. Monograph 8.026.5003. Metrohm Ltd, Herisau.
Carr-Brion, K., 1986. Moisture Sensors in Process Control. Elsevier Applied Science publishers, London and New York.
Cremonesi, P.L., 1986. Practical experiences with on-line water dew point determination in natural gas transmission pipelines. In: Rossum, G.J.V. (Ed.), Gas Quality. Elsevier Science Publishers B.V., Groningen, pp. 301–310.
Dong, H., Bi, P., Cao, J., Zhao, S., 2005. Determination of trace water in gas samples by an improved Karl Fischer Coulometer. Analytical Sciences 21 (4), 421–423.
Esteban, A., Hernandez, V., Lunsford, K., 2000. Exploit the benefits of methanol. In: 79th Annual GPA Convention. Gas Processors Association, Atlanta, GA, USA.
Fenner, R., Zdankiewicz, E., 2001. Micromachined water vapor sensors: a review of sensing technologies. IEEE Sens. J. 1 (4), 309–317.
Folas, G.K., Derawi, S.O., Michelsen, M.L., Stenby, E.H., Kontogeorgis, G.M., 2005a. Recent applications of the cubic-plus-association (CPA) equation of state to industrially important systems. Fluid Phase Equilib. 228–229, 121–126.
Folas, G.K., Gabrielsen, J., Michelsen, M.L., Stenby, E.H., Kontogeorgis, G.M., 2005b. Application of the Cubic-Plus-Association (CPA) equation of state to cross-associating systems. Indust. Eng. Chem. Res. 44 (10), 3823–3833.
Funke, H.H., Grissom, B.L., McGrew, C.E., Raynor, M.W., 2003. Techniques for the measurement of trace moisture in high-purity electronic specialty gases. Rev. Sci. Instrum. 74 (9), 3909–3933.
Hasegava, S., Little, J.W., 1977. The NBS two-pressure humidity generator, mark 2. J. Res. Nat. Bur. Stand. Sect. A. Phys. Chem. 81A (1), 81–88.
Hasegava, S., 1980. Performance characteristics of a thin-film aluminium oxide humidity sensor. In: IEEE (Ed.), 30th Electronic Components Conference. IEEE, p. 386.
ISO, 1981. ISO 6327:1981: Gas Analysis – Determination of the Water Dew Point of Natural Gas – Cooled Surface Condensation Hygrometers. ISO, Genève.

ISO, 1993a. ISO 10101-1:1993: Natural Gas – Determination of Water by the Karl Fischer Method – Part 1: Introduction. ISO, Genève.
ISO, 1993b. ISO 10101-3:1993: Natural Gas – Determination of Water by the Karl Fischer Method – Part 3: Coulometric Procedure. ISO, Genève.
Jamieson, A.W., Sikkenga, H.J., 1986. On-line water dewpoint measurement in natural gas. In: Rossum, G.J.v. (Ed.), Gas Quality. Elsevier Science Publishers B.V., Groningen, pp. 289–299.
Keidel, F.A., 1959. Determination of water by direct amperometric measurement. Anal. Chem. 31 (12), 2043–2048.
Knight, H.S., Weiss, F.T., 1962. Determination of traces of water in hydrocarbons – a calcium carbide-gas liquid chromatography method. Anal. Chem. 34 (7), 749–751.
Kohl, A., Nielsen, R., 1997. Gas Purification. Gulf Publishing Company.
Lurvey, D.T., 1977. Determination of Water Vapor Content of Natural Gas, Am. Gas Assoc. Transm. Conf., St. Louis, pp. 191.
Løkken, T.V., Bersås, A., Christensen, K.O., Nygaard, C.F., Solbraa, E., 2008. Water Content of High Pressure Natural Gas: Data, Prediction and Experience from Field, International Gas Research Conference. Curran Associates Inc., Paris.
Løkken,, T.V., 2012. Comparison of hygrometers for monitoring of water vapour in natural gas. JNGSE 6, 24–36.
McAndrew, J.J., Boucheron, D., 1992. Moisture analysis in process gas streams. Solid State Technol. 35 (2), 52–60.
McAndrew, J.J.F., 1997. Humidity measurement in gases for semiconductor processing. In: Hogan, J.D. (Ed.), Speciality Gas Analysis: A Practical Guidebook. Wiley-VCH, New York, pp. 21–42.
Mehrhoff, T.K., 1985. Comparison of continuous moisture monitors in the range 1 to 15 ppm. Rev. Sci. Instrum. 56 (10), 1930–1933.
Mermoud, F., MBrandt, M.D., Weinstein, B.L., 1989. Recalibration of capacitive-type moisture sensors. Solid State Technol. 32 (5), 59–61.
Mohsen-Nia, M., Amiri, H., Jazi, B., 2010. Dielectric constants of water, methanol, ethanol, butanol and acetone: measurement and computational study. J. Solution Chem. 39 (5), 701–708.
Monroe, S., 1998. Trace moisture in ammonia: gas chromatography using calcium carbide. J. IEST 41 (1), 21–25.
Mychajliw, B.J., 2002. Determination of Water Vapor and Hydrocarbon Dew Point in Gas, 77th International School of Hydrocarbon Measurement, Oklahoma City, pp. 507–510.
Rittersma, Z.M., 2002. Recent achievements in miniaturised humidity sensors–a review of transduction techniques. Sensors and Actuators A: Physical 96 (2–3), 196.
Sonntag, D., 1990. Important new values of the physical constants of 1986, vapor pressure formulations based on the ITS-90, and psychrometer formulae. Z. Meteorol. 40 (5), 340–344.
Sonntag, D., 1994. Advancements in the field of hygrometry. Meteorol. Z. 3 (2), 51–66.
ten Elshof, J.E., Abadal, C.R., Sekulić, J., Chowdhury, S.R., Blank, D.H.A., 2003. Transport mechanisms of water and organic solvents through microporous silica in the pervaporation of binary liquids. Microporous Mesoporous Mater. 65 (2–3), 197–208.
Wiederhold, P.R., 1997a. Water Vapor Measurement. Marcel Dekker Inc., New York.
Wiederhold, P.R., 1997b. True accuracy of humidity measurement. Sensors 14 (9), 14–22.
Wiederhold, P.R., 2000. The principles of chilled mirror hygrometry. Sensors 17 (7), 46–51.
Willsch, R., Ecke, W., Schwotzer, G., 2005. Spectrally encoded optical fibre sensor systems and their application in process control, environmental and structural monitoring. In: Jaroszewicz, L.R., Culshaw, B., Mignani, A.G. (Eds.), Congress on Optics and Optoelectronics. SPIE, Warsaw.

Paper III

Journal of Natural Gas Science and Engineering 12 (2013) 13–21

Contents lists available at SciVerse ScienceDirect

Journal of Natural Gas Science and Engineering

journal homepage: www.elsevier.com/locate/jngse

Water vapour measurements in natural gas in the presence of ethylene glycol

T.V. Løkken*

Statoil ASA, Research and Development, Arkitekt Ebbels veg 10, N-7005 Trondheim, Norway

ARTICLE INFO

Article history:
Received 5 June 2012
Received in revised form
18 November 2012
Accepted 13 January 2013
Available online 27 February 2013

Keywords:
Water dew point
Frost point
Capacitor sensor
Quartz crystal microbalance
Fibre-optic sensor
Calcium carbide

ABSTRACT

An investigation of hygrometers for monitoring of water vapour (moisture) in natural gas has been performed, with respect to response on ethylene glycol co-exposure. The tested hygrometers are based on: 1. capacitor sensor, 2. quartz crystal microbalance (QCM), 3. fibre-optic sensor and 4. conversion of water to ethyne, quantified by a gas chromatograph (CaC_2-GC). The moisture concentration level in the test gas was 50 μmol/mol during the experiments, corresponding to a frost point of approximately −48 °C (atmospheric pressure). The experiments were performed in the laboratory, using nitrogen as matrix gas. The QCM hygrometer responded with a downward drift of the frost point readings in the presence of traces of ethylene glycol (0.25 μmol/mol and 0.66 μmol/mol, respectively). The drift increased initially when the ethylene glycol concentration increased, and the frost point readings from the QCM hygrometer decreased close to 5 °C during a total of 20 days of ethylene glycol exposure. The QCM hygrometer seemed to recover slowly from the ethylene glycol exposure, indicated by a decreasing upward drift as soon as the ethylene glycol exposure ended. Both tested capacitor hygrometers responded significantly to ethylene glycol exposure. The responses were not uniform, though, with one performing considerably better than the other one. The experiments also demonstrated the insufficiency of chilled mirror techniques for interpreting water frost points or water dew points, with subsequent moisture concentration calculation, in the presence of ethylene glycol, even at trace amounts. This made the chilled mirror technique totally unsuitable for reference measurements after the introduction of ethylene glycol to the test gas. The fibre-optic sensor hygrometer and the CaC_2-GC hygrometer showed minor response for ethylene glycol. In general the results from this work demonstrate the need for careful evaluation of individual moisture monitoring applications, before choosing a hygrometer. A well-considered strategy for quality control of the moisture monitoring, regardless of the chosen hygrometer, is of utmost importance to establish a moisture monitoring system with high accuracy.

1. Introduction

1.1. Background

Water vapour, often referred to as moisture, has to be monitored with high accuracy to maintain safe and regular processing and transport of natural gas. Condensation of water may occur if the water vapour concentration is underestimated. When combined with hydrogen sulphide and carbon dioxide condensed water will increase the corrosion potential (Mychajliw, 2002). The formation of gas hydrates is another possible consequence of inaccurate water vapour monitoring (Jamieson and Sikkenga, 1986). Gas hydrates can plug pipelines or process units, resulting in loss of production or obstructed transportation of natural gas. Ethylene glycol is a preferred hydrate inhibitor in many multiphase systems, where the inhibitor is regenerated and recirculated. Ethylene glycol is also occasionally used for dehydration of natural gas. Despite having a relative low vapour pressure, some of the ethylene glycol will be lost to the gas phase. The resulting concentration in natural gas will be dependent on process conditions, but often gaseous ethylene glycol at concentrations less than 1 μmol/mol are obtained. Moisture monitors, herein called hygrometers, used in these systems will be exposed to this ethylene glycol. Like water, ethylene glycol is a relatively polar molecule and adsorbs easily to surfaces. These similarities make ethylene glycol suspicious when it comes to interference with moisture monitoring. A literature study did not reveal any specific information, either theoretical or experimental, describing the influence from ethylene glycol on the measurement of moisture.

* Tel.: +47 95273028.
E-mail address: tvl@statoil.com.

1875-5100/$ – see front matter © 2013 Elsevier B.V. All rights reserved.
http://dx.doi.org/10.1016/j.jngse.2013.01.002

In this work several different hygrometers were investigated with respect to response to ethylene glycol, for concentration levels at 0.25 μmol/mol and 0.66 μmol/mol respectively, when monitoring moisture at a concentration level of 50 μmol/mol.

1.2. Measuring techniques

Throughout the years numerous methods for moisture measurements in gases have been developed and established. Most of them are thoroughly described in published literature (Blakemore et al., 1986; Bruttel and Regina, 2006; Carr-Brion, 1986; Funke et al., 2003; ISO, 1993a, 1993b; Keidel, 1959; Knight and Weiss, 1962; McAndrew and Boucheron, 1992; McAndrew, 1997; Monroe, 1998; Rittersma, 2002; Wiederhold, 1997, 2000; Willsch et al., 2005). Hygrometers based on capacitor sensor, quartz crystal microbalance (QCM), fibre-optic sensor, CaC_2-GC, chilled mirror and Karl Fischer titration have been investigated in this work. The basic principles for these methods are briefly summarised in Table 1. Karl Fischer titration and chilled mirror hygrometry are usually regarded as direct or absolute methods as they utilise a direct relationship between the measured quantity and the amount of moisture. Hence they often are preferred as reference methods.

1.3. Interpretation of moisture measurements

The amount of moisture in a natural gas can either be expressed as concentration (e.g. μmol/mol or mg/Sm^3 at some defined standard temperature and pressure) or as dew or frost point in degrees Celsius. The dew point is the highest temperature, at a specified pressure, where water can condense from the gas. The frost point is the highest temperature, at a specified pressure, where ice can precipitate from the gas (Løkken et al., 2008). In the temperature region between 0 °C and −20 °C it is difficult to predict whether the moisture will condense as dew or precipitate as ice. It is necessary to distinguish between the dew point and the frost point, as these could deviate with several degrees for the same moisture concentration. Well recognised and accurate formulae for conversion between dew or frost point at atmospheric pressure and concentration (via saturation vapour pressure) are published by Sonntag (Sonntag, 1990, 1994). The following formula converts frost point to saturation vapour pressure:

For the given temperature range

$$173.15\ \mathrm{K} \le T_\mathrm{K} \le 273.16\ \mathrm{K} \quad (-100^\circ\mathrm{C} \le T_\mathrm{C} \le 0.01\ ^\circ\mathrm{C})$$

$$\ln e_i(T_\mathrm{K}) = -6024.5282T_\mathrm{K}^{-1} + 24.7219 + 1.0613868 \times 10^{-2}T_\mathrm{K} - 1.3198825 \times 10^{-5}T_\mathrm{K}^2 - 0.49382577 \ln T_\mathrm{K}, \quad (1)$$

$e_i(T_\mathrm{K})$ is the saturation vapour pressure with respect to ice in hPa (hectopascal), T_K is frost point temperature in K.

Saturation vapour pressure can be converted to frost point by formula (2), which is derived from Equation (1):

$$T_\mathrm{K} = 12.1197y + 5.25112 \times 10^{-1}y^2 + 1.92206 \times 10^{-2}y^3 + 3.84403 \times 10^{-4}y^4 + 273.15 \quad (2)$$

In the conversion formula (2)

$$y = \ln(e_i(T_\mathrm{K})/6.11153) \quad (3)$$

For conversions between saturation vapour pressure and concentration the following formula can be used:

$$c_\mathrm{w} = \frac{e_i(T_\mathrm{K}) \times 10^6}{1013.26}, \quad (4)$$

c_w is concentration in μmol/mol. At elevated pressures the formulae of Sonntag are not applicable because of increasing non-ideal behaviour of the gas.

1.4. Moisture generator

Several methods for the generation of moisture in gases are described in the literature, such as the two-pressure, two-flow or two-temperature generator (Funke et al., 2003; Hasegava and Little, 1977; Sonntag, 1994; Wiederhold, 1997). A lot of effort can be made in the aim of producing a stream of gas with a very accurate moisture concentration. Such equipment is often found at national measurement institutes, like NPL (National Physical Laboratory, United Kingdom) and NIST (National Institute of Standards and Technology, USA). In this work a much simpler moisture generator was established, with the option to mix in a volatile

Table 1
Summary of methods for moisture measurements in gases.

Method	Typical uncertainty	Working principle
Capacitor sensor	(1–3) °C	Capacitance or impedance measured as a function of water molecules adsorbed to the porous dielectric (usually metal oxides like Al_2O_3 or SiO_2) of a capacitor (Carr-Brion, 1986; Funke et al., 2003; McAndrew and Boucheron, 1992; McAndrew, 1997; Wiederhold, 1997).
Quartz crystal microbalance (QCM)	±10%	Measures the resonance frequency of an oscillating quartz crystal (piezoelectric) coated with a hygroscopic polymer. The frequency changes with mass as water molecules adsorb on the quartz crystal (Blakemore et al., 1986; Carr-Brion, 1986; Funke et al., 2003; McAndrew and Boucheron, 1992; McAndrew, 1997; Wiederhold, 1997).
CaC_2-GC	±10%	Water and calcium carbide (CaC_2) reacts to form ethyne: $2H_2O + CaC_2 \rightarrow \mathbf{C_2H_2} + Ca(OH)_2$. Quantification of ethyne by gas chromatographic (GC) separation and detection e.g. with a thermal conductivity or a flame ionisation detector (Knight and Weiss, 1962; Monroe, 1998).
Fibre-optic sensor	±2 °C	Measures a shift in reflection spectrum dependent on the amount of adsorbed water in a hygroscopic Fabry–Perot filter. "Fibre-optic" in the sense that light is emitted and reflected via fibre-optic cables (Rittersma, 2002; Willsch et al., 2005).
Karl Fischer titration	±10%	The Karl Fischer reaction: $ROH + SO_2 + R'N \rightarrow (R'NH)SO_3R$ $(R'NH)SO_3R + 2R'N + I_2 + \mathbf{H_2O} \rightarrow (R'NH)SO_4R + 2(R'NH)I$ ROH = alcohol, R′N = basic nitrogen compound For coulometric titration the amount of water is calculated by measuring the current needed for the electrochemical generation of iodine (I_2) from iodide (I^-) (Bruttel and Regina, 2006; ISO, 1993a, 1993b).
Chilled mirror	±0.2 °C	Measures the temperature at which water molecules condense from the gas to form dew or frost on a reflective surface (mirror). The dew or frost is detected on the surface optically by an electro-optic detector (Wiederhold, 1997, 2000).

chemical. The equipment is well suited for comparison of hygrometers rather than calibrating them accurately. Having applications for moisture in natural gas in mind, the main focus was to produce a gas with sufficient long term, drift-free and controllable concentrations of both moisture and a volatile chemical.

2. Experimental set up

2.1. Test rig

A test rig for generation of mixtures of moisture and ethylene glycol in gases was established as shown in Fig. 1. Table 2 summarises the pieces of equipment used. The test rig was able to generate a stream of nitrogen gas with drift-free concentrations of moisture and ethylene glycol. The nitrogen gas (>99.999% purity) was fed to the test rig at about 4 bar through a pressure regulator (V-1). The gas flow was split in three lines: one line for generation of dry gas for dilution (T-2) and two lines for generation of gas saturated with moisture and ethylene glycol respectively (T-3 and T-4). The gas was fed to the three lines via needle valves (V-2 to V-4).

In the first line (T-2) nitrogen gas was dried through two molecular sieve traps in series (E-1 and E-2). The molecular sieves were specified to remove moisture to less than 50 nmol/mol. In the second line (T-3) nitrogen gas was bubbled through ion exchanged water at room temperature (about 25 °C) for saturation inside two stainless steel cylinders (saturators) in series (E-3 and E-4). The saturators were modified filter housings with a volume of 30 mL, each filled with 20 mL water. A piece of 6 mm outer diameter stainless steel tubing (316 L stainless steel) was welded to the inlet ports to guide the gas near the bottom of the cylinders. The saturated gas was further directed through three cylinders in series (E-5 to E-7) kept at a lower temperature (10 °C). The temperature was controlled with a cooling bath (E-8). These cylinders were empty and acted as condensers; the test gas leaving the last cylinder with a fixed concentration of water vapour according to the actual temperature and pressure. To facilitate an efficient cooling of the gas a submerged coil of approximately 1 m long tubing (C-1) connected the first and second condenser. The third line (T-4) was identical to the second line (T-3), with separate saturators (E-9 and E-10), condensers (E-11 to E-13), coil (C-2) and cooling bath (E-14). The saturators in this line were filled with ethylene glycol (purity > 99.5%) instead of water. The flow rate of the three gas streams (T-2, T-3 and T-4) were controlled by manual flow controllers (V-5, V-6 and V-7) and mixed across a union cross to produce the final test gas stream (T-5) containing both moisture and ethylene glycol. The total flow rate of the test gas was approximately 6 dm^3/min (ambient conditions) and was sufficient to feed all hygrometers. The test gas stream was directed to a compact gas manifold (E-15) for further distribution to the hygrometers (H-1 to H-7) and ventilation lines. The hygrometers were connected to the gas manifold via equal lengths (1.2 m) of tubing and fine metering valves (V-8 toV-14). Sufficient lengths of 1/8 inch stainless steel tubing were connected to the outlet ports of the hygrometers to prevent back-diffusion of moisture from the atmosphere. Further downstream, the outlet streams were gathered in a gas manifold and guided to ventilation in 1/4 inch Teflon tubing. All connecting tubing (T-1 to T-4) was made of stainless steel. The tubing (T-5) between V-5, V-5 and V-6 and the hygrometers (H-1 to H-8) was electro polished and surface deactivated, to minimise surface adsorption.

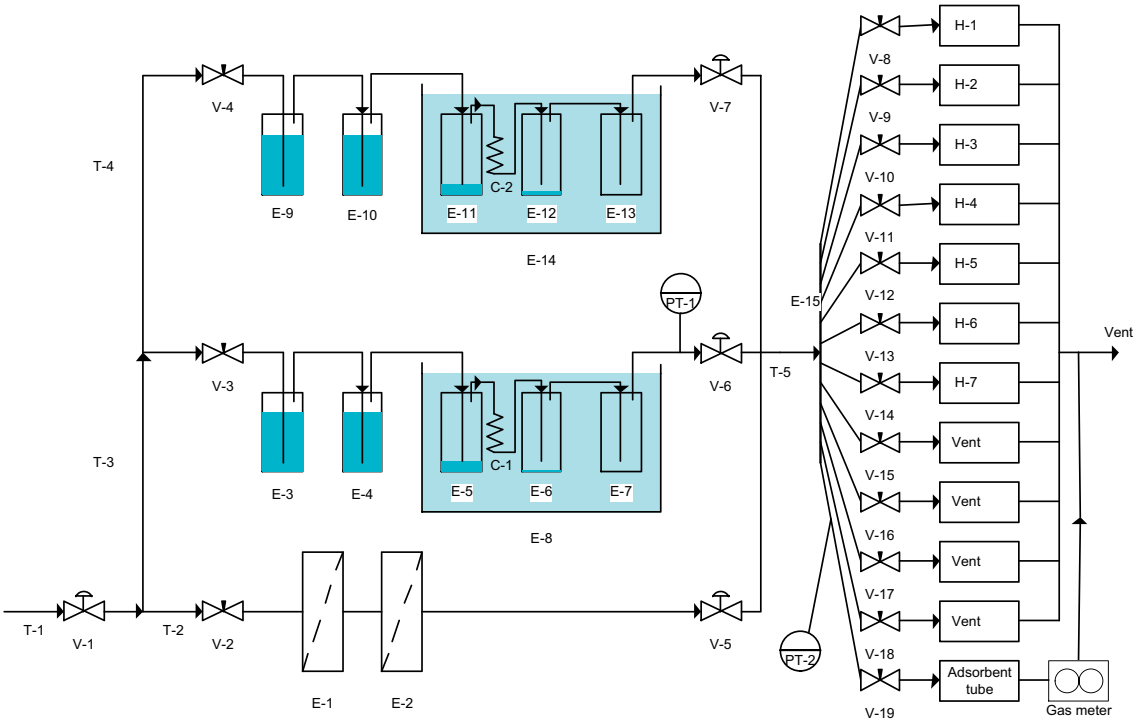

Fig. 1. Schematic representation of the test rig. Equipment description is found in Table 2. Adsorbent tube and gas meter description is found in Table 3.

Table 2
Equipment description, the codes refer to Fig. 1.

Code	Description	Model	Manufacturer
V-1	Single stage pressure regulator	SI15	SMT S.A.S., France
V-2 to V-4	Needle valves	3812F4Y	Hoke, USA
V-5	Flow controller	PC 8942	Brooks Instrument, USA
V-6 and V-7	Flow controller	FMC-2000	FlowMatrix Inc., USA
V-8 to V19	Fine metering valve	SS-2MG	Swagelok, USA
E-1 and E-2	Molecular sieves		Ametek, USA
E-3, E-4, E-9 and E-10	Modified filter housings, saturators	Model 122	Headline Filters, UK
E-5 to E-7 and E-11 to E-13	Modified filter housings, condensers	Model 122	Headline Filters, UK
E-8 and E-14	Cooling bath	FP-45	Julabo Labortechnik GmbH, Germany
E-15	Gas manifold	Z12M2	Vici AG International, Switzerland
PT-1	Pressure transmitter	PA-55X	Keller AG, Switzerland
PT-2	Pressure transducer	Model SA	Honeywell, USA
H-1	Capacitor A		
H-2	Capacitor B		
H-3	QCM		
H-4	CaC_2-GC		
H-4.1	Reactor with grinded calcium carbide	Particles with diameter from 0.3 mm to 1 mm	Merck KGaA, Germany
H-4.2	Gas Chromatograph	CP4900 Micro-GC	Varian Inc., USA
H-4.3	GC separation column	CP-PoraPlot Q, 10 m long, 0.25 mm i.d.	Varian Inc., USA
H-5	Fibre-optic		
H-6	Karl Fischer	Model 831	Metrohm AG, Switzerland
H-6.1	Gas meter	TG 1 Mod. 5–8	Ritter, Germany
H-7	Chilled mirror	S4000 Integrale	Michell Instruments ltd., UK
C-1	1 m coil made of 1/8 × 0.035 inch, 316 L stainless steel tubing	Sandvik 3R60	AB Sandvik Materials Technology, Sweden
T-1 to T-4	1/8 × 0.035 inch, 316 L stainless steel tubing	Sandvik 3R60	AB Sandvik Materials Technology, Sweden
T-5	Treated 1/8 × 0.035 inch 316 L stainless steel tubing	Siltek™	Restek Corporation, USA

2.2. Hygrometers

Seven hygrometers, based on capacitor sensor (two different brands), quartz crystal microbalance (QCM), CaC_2-GC, fibre-optic sensor, Karl Fischer titration and chilled mirror (continuously operated), have been investigated in the experiments.

The hygrometers were equipped with control units for communication with the probes or sensors and transfer of data to a computer for storage. Data points were stored every 5 min. The CaC_2-GC hygrometer consisted of a calcium carbide reactor (H-4.1) for conversion of moisture to ethyne and a micro gas chromatograph (H-4.2) for quantification of ethyne. The micro gas chromatograph was equipped with a separation column (H-4.3) and a micro thermal conductivity detector and was controlled by chromatography software (CP Maitre Elite) on the computer. The processed data from CP Maitre Elite was collected approximately every 10 min.

Two direct methods were utilised for reference measurements, not being of interest with respect of continuous online process monitoring. These were a chilled mirror hygrometer (H-7) and a Karl Fischer titrator (H-6). The volume of the titrated gas was measured by a drum-type gas meter (H-6.1). The chilled mirror hygrometer was set up to perform continuous measurements, with storage of data every 5 min. The Karl Fischer titrations (between 3 and 9 parallels) were performed manually on weekdays during the experiments.

2.3. Operation of moisture generator

The mixing ratio of the three gas streams (T-2, T-3 and T-4) was controlled by three manually operated flow controllers (V-5, V-6 and V-7). The two gas streams, saturated with moisture and ethylene glycol respectively, were controlled between 0 and 300 cm^3/min (ambient conditions) with flow controllers (V-6 and V-7), while the dry dilution gas was adjusted to about 6 dm^3/min (ambient conditions) with another flow controller (V-5). The temperature in the cooling bath for line 2 (moisture) was set to 10 °C (±0.01 °C) and the pressure in the condensers was controlled at approximately 4 bar and monitored with a pressure transmitter (PT-1). The temperature in the cooling bath for line 3 (ethylene glycol) was initially set to −10 °C (±0.01 °C). By changing the settings on the three flow controllers, and eventually changing the temperature in the cooling baths different concentrations of moisture and ethylene could be produced and changed quickly. The pressure upstream the metering valves (V-8 to V-19) was about 2 bar, monitored by a pressure transducer (PT-2). The QCM had internal mass flow controllers which needed a sample pressure slightly elevated from atmospheric pressure. The other hygrometers were fed with test gas at ambient pressure. The flow rates to the different hygrometers were controlled in agreement with the recommendations made by the manufacturers. Excess test gas was distributed to vent through 1/8 inch stainless steel tubing connected to the spare ports on the compact gas manifold (E-15). Fine metering valves (V-15 to V19) were used to control the flow rates also on these gas streams.

The gas upstream V6 and V7 was expected to be saturated with respect to water and ethylene glycol respectively. The gas temperature decrease due to Joule Thomson cooling, when reducing the pressure from 4 to 2 bar, was compensated with a temperature increase in the system from 10 °C (water) and-10 °C (ethylene glycol) to approximately 25 °C (room temperature) prior to pressure reduction. This temperature increase, combined with dilution with dry nitrogen, prevented condensation of water and ethylene glycol associated with the pressure reduction step.

2.4. Conversion between frost point and concentration

Some of the hygrometers returned dew or frost points (capacitor sensors, fibre-optic sensor and chilled mirror), typically in degrees Celsius, while others returned concentration (QCM, CaC_2-GC and

Karl Fischer titration) in parts per million (molar or volume). To be able to compare data from all the hygrometers conversions between the different units were necessary. In this work the formulae of Sonntag (Sonntag, 1990, 1994) were used for these conversions (Equations (1)–(4)).

2.5. Quantification of ethylene glycol

An analytical system based on thermal desorption, gas chromatographic separation and mass spectrometric detection (TD-GC/MS) was used for the quantification of ethylene glycol in nitrogen. Fig. 2 illustrates the analytical system, while details about the equipment are listed in Table 3. The ethylene glycol was collected, from a gas volume of 1500 mL from the test rig, on adsorbent tubes (Fig. 1). The gas volume was measured with a gas meter. The adsorbent tubes were then placed in a thermal desorber (TD) which transferred the analyte to an electrically cooled cold trap (first stage thermal desorption). The small inner diameter (2 mm) of the cold trap (packed with adsorbent) and its ability to be heated rapidly, provided an efficient transfer of analyte from the cold trap to a gas chromatograph (GC). The GC was equipped with a capillary column for separation of analytes and a mass spectrometer (MS) for qualitative and quantitative detection.

Solutions with known amounts (by weight) of ethylene glycol in methanol were prepared in volumetric flasks for calibration of the TD-GC/MS system. Known volumes of these standard solutions were injected directly on adsorption tubes with a syringe suited for injection of volumes between 0.1 and 5 μL. The adsorption tubes were purged with helium (purity 99.9999%) for 1 min (100 mL/min) after application of standard solution, to sweep off most of the methanol from the tubes. This way adsorption tubes, which worked as a series of calibration standards, were prepared containing 0.5, 1, 5 and 10 μg ethylene glycol respectively. A new calibration curve was constructed from an analysed series of standards just before the analysis of every new series of unknown samples from the test rig.

Control of the TD-GC/MS system, included data acquisition and data treatment, were performed with TurboMatrix TD software and TurboMass GC/MS software (Perkin Elmer, USA). Applied method parameters for the thermal desorber, gas chromatograph and mass spectrometer during TD-GC/MS analysis are summarised in Tables 4–6, respectively. Quantification of ethylene glycol was based on selected ion monitoring, using the molecular mass to charge ratio (m/z): 31.

2.6. Calibration of hygrometers

The chilled mirror hygrometer was recalibrated prior to the experiments at Michell Instruments (UKAS accredited calibration laboratory). The other hygrometers were calibrated by the manufacturers before they were made available for testing. No special treatment was done prior to usage of the sensors. No recalibration was done before or during the experiments.

Table 3
Equipment used for quantification of ethylene glycol.

Description	Model/Type	Manufacturer
Gas meter	TG 1 Mod. 5–8	Ritter, Germany
Thermal desorber	TurboMatrix ATD	Perkin Elmer, USA
Adsorbent tubes	Prepacked Tenax TA, product no. 25055	Supelco Analytical,
Cold trap	Prepacked Tenax TA, product no. M0413535	Perkin Elmer, USA
Gas chromatograph	AutoSystem XL	Perkin Elmer, USA
Capillary column	CP-Wax 52 CB, 30 m × 0.25 mm × 0.5 μm, product no. CP8746	Agilent Technologies, USA
Mass spectrometer	TurboMass	Perkin Elmer, USA
Chromatography software	TurboMass 4.0	Perkin Elmer, USA

The micro gas chromatograph (CaC_2-GC) was calibrated with respect to ethyne prior to the experiments. Three calibration gas mixtures were used with ethyne concentrations in nitrogen at 11 μmol/mol (10% relative uncertainty), 53,4 μmol/mol (5% relative uncertainty), and 204 μmol/mol (5% relative uncertainty) respectively. The calibration gas mixtures, which were certified with international traceability, were purchased from Yara (Yara International ASA, Norway).

3. Results

3.1. Moisture and ethylene glycol concentrations during the experiments

The test rig (Fig. 1) was initially set up to produce a stream of nitrogen gas with a moisture concentration level of 50 μmol/mol, corresponding to a frost point level of −48 °C (atmospheric pressure). On day 6, a small gas stream of nitrogen saturated with ethylene glycol was introduced to the original gas stream, producing a test gas with approximately 0.25 μmol/mol ethylene glycol. This introduction caused a minor decrease of the moisture concentration. The concentration of ethylene glycol (0.25 μmol/mol) and moisture were held constant for 14 days. On day 20, the condenser temperature for the ethylene glycol line was increased from 5 °C to 15 °C. This increased the ethylene glycol concentration to approximately 0.66 μmol/mol, while leaving the moisture concentration virtually unchanged. The latter composition of the test gas was maintained for 6 days, before the supply stream of gas saturated with ethylene glycol was closed. Measurements were made on the test gas which showed that the ethylene glycol concentration was less than the 25 nmol/mol from day 27. The ethylene

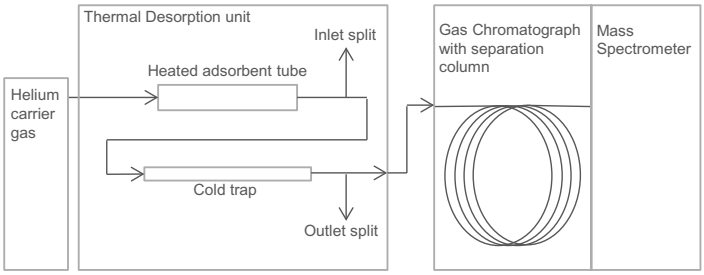

Fig. 2. Simplified illustration of a TD-GC/MS system.

Table 4
Thermal desorption method settings.

Parameter	Condition
Adsorbent tube desorption temperature	230 °C
Adsorbent tube desorption flow	110 mL/min
Adsorbent tube desorption time	2.5 min
Cold trap adsorption temperature	10 °C
Cold trap desorption temperature	230 °C
Cold trap heating temperature rate	5 °C/s
Cold trap desorption time	2.5 min
Heated valve temperature	190 °C
Transfer line temperature	230 °C
Inlet split ratio	10:1
Outlet split ratio	50:1
Total split ratio	500:1
Tube purge flow	110 mL/min
Tube purge temperature	50 °C

glycol analyses are summarised in Table 7. A test period of 33 days in total was divided into four experiments, as shown in Fig. 3, representing: the initial experiment with no ethylene glycol (Experiment 1), the experiment with 0.25 μmol/mol ethylene glycol (Experiment 2), the experiment with 0.66 μmol/mol ethylene glycol (Experiment 3) and the experiment with <25 nmol/mol ethylene glycol (Experiment 4), respectively.

3.2. General presentation of results

The frost point readings for all the hygrometers during the experiments are presented in Fig. 3. Chilled mirror, Fibre-optic and the capacitor sensor hygrometers returned frost points (°C) as their original unit of measurement. The other hygrometers originally returned moisture concentration (μmol/mol) as their original unit of measurement. The readings from these were converted to frost points with the help of the formulae of Sonntag (Sonntag, 1990, 1994). The readings from some of the hygrometers followed a distinct diurnal rhythm which was synchronous with the temperature variation during the day and night.

Data from the chilled mirror hygrometer are left out from day 6 of the experiments, as the readings from this hygrometer did not represent the water frost point after the introduction of ethylene glycol to the test gas. On day 15 (a Friday afternoon) a power break halted the collection of data from all hygrometers. As the test rig was left unattained during weekends, the collection of data was not restarted before day 18. On day 24 the gas chromatograph went out of operation, explaining the missing data for CaC_2-GC between day 24 and 26.

To enhance the interpretation of the test data, presented in Fig. 3, statistical treatment of the test data was performed. For the last three experiments, data were left out from the statistical calculations for the first 6 h after the change of conditions, to give some time for the system to equilibrate. In Table 8 the calculated means and standard deviations for the hygrometer frost point readings during the four experiments are presented. The number of measurements (n) for each mean is tabulated in Table 9. Two-tailed t-tests were performed to evaluate if the means changed significantly when the ethylene glycol concentration changed (Miller and Miller, 1988). Two-tailed f-tests were performed to assess if the t-tests should be based on equal or unequal variances. A significance level (α) of 0.01 was used. The results from the significance tests are summarised in Table 10.

Table 5
Gas chromatograph method settings.

Parameter	Condition
Initial oven temperature	45 °C for 1 min
Oven temperature rate	20 °C/min
Final oven temperature	230 °C for 6.75 min
Carrier gas	Helium (purity 99.9999%)
Carrier gas head pressure	7 psi

Table 6
Mass spectrometer method settings.

Parameter	Condition
Ionisation mode	EI positive
MS Electron Energy	70 eV
Emission Current	50 μA
Ion source temperature	175 °C
Acquisition method	Scan and selected ion monitoring
Scan range	m/z: 30–250
Selected ion monitoring	m/z: 31 and 62

3.3. Experiment 1

During the first 6 days of the experiments (Experiment 1), the means for the reference hygrometers were −47.8 °C (Chilled mirror) and −47.7 °C (Karl Fischer). A two-tailed t-test (unequal variances, $\alpha = 0.01$) implied that the two means were not significantly different. Closest to the reference hygrometers were the means for QCM and Fibre-optic, which differed less than 0.5 °C from reference hygrometers. The mean for CaC_2-GC was almost 1 °C lower than for the reference hygrometers. The means for the two capacitor hygrometers were approximately 14 °C (Capacitor A) and 9 °C (Capacitor B) lower compared to the reference hygrometers. None of the hygrometers demonstrated any tendency to drift during the first 6 days of the experiments.

3.4. Experiment 2

When ethylene glycol was introduced to the test gas, on day 6, Karl Fischer, Fibre-optic and CaC_2-GC made significant shifts to lower frost points. The sizes of the shifts were approximately 0.5 °C for all three hygrometers. Capacitor A made a shift to approximately 2 °C higher frost points, while a minor, but significant, shift to 0.01 °C lower frost points was found for Capacitor B. The frost point readings for QCM initially shifted to approximately 0.5 °C lower frost points and then started to drift downwards. The drift decreased with time. During the 14 days of ethylene glycol exposure (0.25 μmol/mol) the frost point readings from QCM decreased with approximately 3.5 °C.

3.5. Experiment 3

The elevation of the ethylene glycol concentration to 0.66 μmol/mol, on day 20, did not significantly change the frost point readings for Karl Fischer. Fibre-optic and CaC_2-GC made minor, but significant, changes to approximately 0.1 °C lower frost point means. Capacitor A made another shift to approximately 1.5 °C higher frost points, while Capacitor B also responded with

Table 7
Measurements of ethylene glycol (EG), concentration calculations are based on a gas volume of 1500 mL at ambient conditions.

	Day 6–20 ($n = 16$)	Day 21–26 ($n = 11$)
Average EG mass	0.94 μg	2.5 μg
Average EG concentration	0.25 μmol/mol	0.66 μmol/mol
Standard deviation	0.024 μmol/mol	0.047 μmol/mol

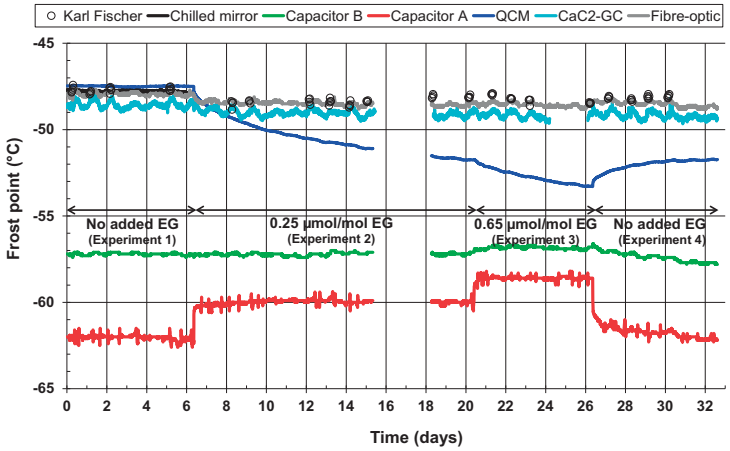

Fig. 3. Frost point readings of the tested hygrometers during co-exposure to ethylene glycol, at a moisture concentration level of 50 μmol/mol (corresponding to a frost point of approximately −48 °C).

a shift to less than 0.5 °C higher frost points. QCM initially responded with an increased downward drift when the ethylene glycol concentration was elevated. This drift decreased with time, in a similar manner to the drift observed for Experiment 2. The frost point readings from QCM drifted approximately 1.5 °C downwards during Experiment 3.

3.6. Experiment 4

When the ethylene glycol source was closed on day 26, the concentration fell to less than 0.025 μmol/mol within one day. A small change (0.05 °C) towards higher frost point readings were found for Fibre-optic, while no significant changes were found for Karl Fischer and CaC_2-GC. The frost point readings for QCM had a small upward shift and subsequently started to drift upwards. This upward drift continued throughout the rest of the experiment, though the drift did gradually decrease. Capacitor A initially made a shift downwards equivalent to about 2 °C, and then started to drift slowly downwards. Capacitor B also started to drift downwards similarly to Capacitor A, but did not make any distinct shift. At the end of the Experiment 4 the drift for both capacitor hygrometers was hardly noticeable.

4. Discussion

There was no significant difference between the averages of the readings from the two reference hygrometers (Karl Fischer and Chilled mirror) during the first 6 days of the experiments (two-tailed *t*-test, $P = 0.01$). Taken into account the expected uncertainties for the hygrometers (Table 1) only the two capacitor hygrometers deviate significantly from the reference hygrometers.

Capacitor based hygrometers are generally well known for their tendency to drift (Hasegava, 1980; Løkken, 2012a; Mehrhoff, 1985; Mermoud et al., 1989). During earlier testing (Løkken, 2012a), the two capacitor sensor hygrometers tested in the current work were allowed to drift to a level of frost points far below the expected frost point of the test gas. During prolonged time in operation, their drift slowed down, a characteristic which has been described in other publications (Løkken, 2012a; Mehrhoff, 1985). This characteristic is believed to explain why Capacitor A and Capacitor B showed no observable drift during the first 6 days of the experiments.

The first introduction of ethylene glycol to the test gas diluted the original moisture level. The expected frost point decrease was approximately 0.5 °C, based on flow calculations and vapour pressures of water and ethylene glycol. The vapour pressures were calculated using the "equation of state" based CPA model (Folas et al., 2007; Løkken et al., 2008). The expected frost point decrease corresponded well with the observed frost point shifts for Karl Fischer, Fibre-optic and CaC_2-GC on day 6. Even not easily observed from Fig. 3, the same frost point shift was also present for QCM. When the gas stream feeding the test gas with ethylene glycol was shut off on day 26, a frost point increase was expected, similar to the decrease at the first introduction of ethylene glycol. A small increase of the frost point mean was noticed only for Fibre-optic (0.05 °C increased frost point mean) and QCM (approximately 0.2 °C initially increased frost point readings). The hygroscopic ethylene glycol, which adsorbed to surfaces inside the test rig, including sensing parts of the hygrometers, is believed to slow

Table 8
Calculated means from frost point readings with standard deviations (*s*) for the four experiments. Find number of measurements (*n*) in Table 9.

Hygrometer	Experiment 1		Experiment 2		Experiment 3		Experiment 4	
	Mean (°C)	*s* (°C)	Mean (°C)	*s* (°C)	Mean (°C)	*s* (°C)	Mean (°C)	*s* (°C)
Karl Fischer	−47.70	0.152	−48.33	0.210	−48.24	0.217	−48.14	0.119
Chilled mirror	−47.79	0.051						
Capacitor A	−62.04	0.144	−59.98	0.133	−58.59	0.101	−61.77	0.290
Capacitor B	−57.20	0.065	−57.21	0.084	−56.85	0.085	−57.40	0.256
QCM	−47.49	0.020	−50.39	0.923	−52.75	0.387	−51.99	0.270
CaC_2-GC	−48.58	0.568	−49.04	0.182	−49.17	0.181	−49.23	0.946
Fibre-optic	−47.93	0.100	−48.47	0.117	−48.56	0.118	−48.51	0.157

Table 9
Number of measurements (n) for the four experiments.

Hygrometer	Experiment 1	Experiment 2	Experiment 3	Experiment 4
Karl Fischer	19	33	16	18
Chilled mirror	1825			
Cap A	1825	3118	1657	1736
Cap B	1825	3118	1657	1736
QCM	1825	3118	1657	1736
CaC2	847	1449	513	805
Fibre Optic	1825	3118	1657	1736

down the equilibrium processes for moisture. This probably resulted in longer response times for the test rig when it came to changes in frost point levels, as well as effects on the response times of the individual hygrometers.

The Karl Fischer technique is not expected to be affected by ethylene glycol exposure, based on information from the literature (Bruttel and Regina, 2006; Lurvey, 1977). Therefore the technique is preferred as a reference in these experiments.

As for other hygroscopic chemicals, the chilled mirror technique is expected to be sensitive to ethylene glycol. When both ethylene glycol and moisture are present in a gas, the temperatures at which condensation or precipitation occurs do not relate to the water concentration alone. The temperatures for phase changes will now relate to the concentration of both moisture and ethylene glycol. Hence the term "water dew point" or "water frost point" will not be meaningful with such gases (Jamieson and Sikkenga, 1986). In this work, while the moisture concentration was constant at 50 μmol/mol, the chilled mirror hygrometer returned readings at approximately −28 °C and −21 °C for 0.25 μmol/mol and 0.66 μmol/mol ethylene glycol, respectively (not shown in Fig. 3). Calculations with the CPA model showed that these temperature readings corresponded well with the condensation of an ethylene glycol rich liquid phase on the mirror surface.

It is interesting to note that two capacitor hygrometers, which are based on the same technology, respond quite differently on ethylene glycol exposure. The relatively small response from ethylene glycol on Capacitor B is well within its claimed uncertainty of ±2 °C. The situation for Capacitor A is more severe, with a total shift of approximately 3.5 °C. The dielectric constants of ethylene glycol and water are 41.4 and 80.1 respectively (Lide, 1996), which means that ethylene glycol is susceptible to contribute to the sensor signal if considerable amounts of ethylene glycol are adsorbed to the porous dielectrics of the sensor. The kinetic molecular sizes of ethylene glycol and water are 41 nm and 26 nm respectively (Sekulić et al., 2004; ten Elshof et al., 2003). Hence the pore sizes of the sensor structures can be decisive when it comes to amounts of adsorbed water molecules versus ethylene glycol molecules. The total of 3.5 °C upward shift corresponds to approximately 25 μmol/mol increase in moisture concentration. This rather severe response is therefore somewhat surprising, and not easily explained by the relatively low ethylene glycol concentration, which is about 100 times lower than the moisture concentration.

QCM demonstrated a distinct concentration dependent response on ethylene glycol. The QCM hygrometer is essentially a mass sensitive detector (Mecea, 2006). Hence, the downward drift of the QCM observed in this work, implies that the total mass of substance adsorbed to the hygroscopic surface of the sensor decreases during ethylene glycol exposure. As ethylene glycol is a relatively polar molecule, it was expected that this compound could adsorb to the hygroscopic layer of the sensor and eventually lead to increased frost point readings. This behaviour has been observed for a QCM hygrometer, at a similar frost point level, with methanol exposure at 750 μmol/mol concentration level (Løkken, 2012b). However, it seems as if the ethylene glycol gradually prevents moisture from adsorbing to the sensor, leading to a net mass decrease of the sensor. Further investigations are needed to fully understand the mechanism behind this behaviour.

The natural gas business utilises many chemicals, for various reasons, during transport and processing of natural gas. The concentration of the chemicals in the natural gas will typically vary from nmol/mol levels to mmol/mol levels, dependent on e.g. volatility of the chemical, process conditions and pattern of use. Many of these chemicals can have the potential to interfere with moisture measurements through various mechanisms. In this work ethylene glycol was investigated and found to interfere even at concentrations less than 1 μmol/mol, while in an earlier work (Løkken, 2012b) methanol was found to interfere at higher μmol/mol concentrations. Examples of other frequently used chemicals in the natural gas business, not included in these investigations, are triethylene glycol (TEG – state of the art dehydration chemical) and various amine based chemicals (for removal of CO_2 and H_2S). It is difficult to predict, based on the results obtained for ethylene glycol and methanol, if and how TEG and amines eventually will interfere with moisture measurements. It is apparent, though, that it is necessary to have some strategy for quality control, which will make it possible to reveal significant effects from chemicals on the moisture measurements.

Table 10
Results from two-tailed t-tests, $\alpha = 0.01$ (data from Tables 8 and 9). Adopted null hypotheses are that calculated means from frost point readings are not different, when comparing adjacent experiments (Experiment 1 and 2, Experiment 2 and 3, Experiment 3 and 4). "Not different" in table means not significant different calculated means (retained null hypothesis). "Different" in table means significant different calculated means (rejected null hypothesis).

Hygrometer	Experiment 1 and 2	Experiment 2 and 3	Experiment 3 and 4
Karl Fischer	Different	Not different	Not different
Cap A	Different	Different	Different
Cap B	Different	Different	Different
QCM	Different	Different	Different
CaC2	Different	Different	Not different
Fibre Optic	Different	Different	Different

5. Conclusions

An investigation of several hygrometers, with respect to response on ethylene glycol exposure, has been performed. The moisture concentration level of the test gas was 50 μmol/mol during the experiments, corresponding to a frost point of approximately −48 °C.

The QCM hygrometer responded with a downward drift of the frost point readings, in the presence of traces of ethylene glycol (0.25 μmol/mol and 0.66 μmol/mol, respectively). The drift increased initially when the ethylene glycol concentration increased, and the frost point readings from the QCM hygrometer decreased close to 5 °C during a total of 20 days of ethylene glycol exposure. The QCM hygrometer seemed to recover slowly from the ethylene glycol exposure, indicated by a decreasing upward drift as soon as the ethylene glycol exposure ended.

Both tested capacitor hygrometers responded significantly to ethylene glycol exposure. The responses were not uniform, though, with one performing considerably better than the other one.

The experiments also demonstrated the insufficiency of chilled mirror techniques for interpreting water frost points or water dew points, with subsequent moisture concentration calculation, in the presence of ethylene glycol, even at trace amounts. This made the chilled mirror technique totally unsuitable for reference measurements after the introduction of ethylene glycol to the test gas.

The fibre-optic sensor hygrometer and the CaC_2-GC hygrometer showed minor response for ethylene glycol.

In general the results from this work demonstrate the need for careful evaluation of individual moisture monitoring applications, before choosing a hygrometer. This evaluation should be made with special attention to the presence of polar chemicals. A well-considered strategy for quality control of the moisture monitoring, regardless of the chosen hygrometer, is of utmost importance, to establish a moisture monitoring system with high accuracy.

Acknowledgements

The author gratefully acknowledges Statoil ASA and Gassco for financial support of this work. The assistance from and discussions with colleagues at the R&D Centre of Statoil is highly appreciated. Thanks to colleagues in the laboratory for help during the planning, construction and adaptation of the test rig. Thanks to Dr. Arne Olav Fredheim, Statoil R&D Centre, and Dr. Rudolf Schmid, Norwegian University of Science and Technology (NTNU), for patient supervision and to Trond Kirkerød for many fruitful discussions on the topic of moisture measurements.

Nomenclature

Abbreviations

CaC_2-GC	hygrometer based on a calcium carbide reactor and gas chromatographic analysis
CPA	Cubic-Plus-Association, an equation of state
TD-GC/MS	thermal desorption combined with gas chromatographic separation and mass spectrometric detection
m/z	molecular mass to charge ratio of an ion, a term used in mass spectrometry
NIST	National Institute of Standards and Technology
NPL	National Physical Laboratory
UKAS	United Kingdom Accreditation Service
QCM	quartz crystal microbalance

List of symbols

α	significance level
c_w	concentration (μmol/mol)
$e_i(T_K)$	saturation pressure (hectopascal)
n	number of measurements
T_C	temperature (°C)
T_K	temperature (K)

References

Blakemore, C.B., Steichen, J.C., Dallas, G., Van Rossum, G.J., 1986. Continuous trace moisture analysis. In: Rossum, G.J.v. (Ed.), Gas Quality. Elsevier Science Publishers B.V., Groningen, pp. 327–335.

Bruttel, P.A., Regina, S., 2006. Water Determination by Karl Fischer Titration. Monograph 8.026.5003. Metrohm Ltd., Herisau.

Carr-Brion, K., 1986. Moisture Sensors in Process Control. Elsevier Applied Science Publishers, London and New York.

Folas, G.K., et al., 2007. High-pressure vapor–liquid equilibria of systems containing ethylene glycol, water and methane: experimental measurements and modeling. Fluid Phase Equilibria 251 (1), 52–58.

Funke, H.H., Grissom, B.L., McGrew, C.E., Raynor, M.W., 2003. Techniques for the measurement of trace moisture in high-purity electronic specialty gases. Rev. Sci. Instrum. 74 (9), 3909–3933.

Hasegava, S., Little, J.W., 1977. The NBS two-pressure humidity generator, mark 2. J. Res. Nat. Bur. Stand. Sect. A. Phys. Chem. 81A (1), 81–88.

Hasegava, S., 1980. Performance characteristics of a thin-film aluminium oxide humidity sensor. In: IEEE (Ed.), 30th Electronic Components Conference. IEEE, p. 386.

ISO, 1993a. ISO 10101-1:1993: Natural Gas – Determination of Water by the Karl Fischer Method – Part 1: Introduction. ISO, Genève.

ISO, 1993b. ISO 10101-3:1993: Natural Gas – Determination of Water by the Karl Fischer Method – Part 3: Coulometric Procedure. ISO, Genève.

Jamieson, A.W., Sikkenga, H.J., 1986. On-line water dewpoint measurement in natural gas. In: Rossum, G.J.v. (Ed.), Gas Quality. Elsevier Science Publishers B.V., Groningen, pp. 289–299.

Keidel, F.A., 1959. Determination of water by direct amperometric measurement. Anal. Chem. 31 (12), 2043–2048.

Knight, H.S., Weiss, F.T., 1962. Determination of traces of water in hydrocarbons – a calcium carbide-gas liquid chromatography method. Anal. Chem. 34 (7), 749–751.

Lide, D.R., 1996. CRC Handbook of Chemistry and Physics, 84th ed. CRC Press.

Løkken, T.V., Bersås, A., Christensen, K.O., Nygaard, C.F., Solbraa, E., 2008. Water content of high pressure natural gas: data, prediction and experience from field. In: International Gas Research Conference. Curran Associates Inc., Paris.

Løkken, T.V., 2012a. Comparison of hygrometers for monitoring of water vapour in natural gas. J. Nat. Gas Sci. Eng. 6 (0), 24–36.

Løkken, T.V., 2012b. Water vapour monitoring in natural gas in the presence of methanol. J. Nat. Gas Sci. Eng. 7 (0), 7–15.

Lurvey, D.T., 1977. Determination of water vapor content of natural gas. In: Am. Gas Assoc. Transm. Conf., St. Louis, p. 191.

McAndrew, J.J., Boucheron, D., 1992. Moisture analysis in process gas streams. Solid State Technol. 35 (2), 52–60.

McAndrew, J.J.F., 1997. Humidity measurement in gases for semiconductor processing. In: Hogan, J.D. (Ed.), Speciality Gas Analysis: a Practical Guidebook. Wiley-VCH, New York, pp. 21–42.

Mecea, V.M., 2006. Is quartz crystal microbalance really a mass sensor? Sens. Actuators A: Phys. 128 (2), 270–277.

Mehrhoff, T.K., 1985. Comparison of continuous moisture monitors in the range 1 to 15 ppm. Rev. Sci. Instrum. 56 (10), 1930–1933.

Mermoud, F., MBrandt, M.D., Weinstein, B.L., 1989. Recalibration of capacitive-type moisture sensors. Solid State Technol. 32 (5), 59–61.

Miller, J.C., Miller, J.N., 1988. Statistics for Analytical Chemistry. In: Ellis Horwood Series in Analytical Chemistry. Ellis Horwood Limited, Chichester.

Monroe, S., 1998. Trace moisture in ammonia: gas chromatography using calcium carbide. J. IEST. 41 (1), 21–25.

Mychajliw, B.J., 2002. Determination of water vapor and hydrocarbon dew point in gas. In: 77th International School of Hydrocarbon Measurement, Oklahoma City, pp. 507–510.

Rittersma, Z.M., 2002. Recent achievements in miniaturised humidity sensors–a review of transduction techniques. Sens. Actuators A: Phys. 96 (2–3), 196.

Sekulić, J., ten Elshof, J.E., Blank, D.H.A., 2004. Selective pervaporation of water through a nonselective microporous titania membrane by a dynamically induced molecular sieving mechanism. Langmuir 21 (2), 508–510.

Sonntag, D., 1990. Important new values of the physical constants of 1986, vapor pressure formulations based on the ITS-90, and psychrometer formulae. Meteorol. Z. 40 (5), 340–344.

Sonntag, D., 1994. Advancements in the field of hygrometry. Meteorol. Z. 3 (2), 51–66.

ten Elshof, J.E., Abadal, C.R., Sekulić, J., Chowdhury, S.R., Blank, D.H.A., 2003. Transport mechanisms of water and organic solvents through microporous silica in the pervaporation of binary liquids. Microporous Mesoporous Mater. 65 (2–3), 197–208.

Wiederhold, P.R., 1997. Water Vapor Measurement. Marcel Dekker Inc., New York.

Wiederhold, P.R., 2000. The principles of chilled mirror hygrometry. Sensors 17 (7), 46–51.

Willsch, R., Ecke, W., Schwotzer, G., 2005. Spectrally encoded optical fibre sensor systems and their application in process control, environmental and structural monitoring. In: Jaroszewicz, L.R., Culshaw, B., Mignani, A.G. (Eds.), Congress on Optics and Optoelectronics. SPIE, Warsaw.

Paper IV

Water content of high pressure natural gas: Data, prediction and experience from field

Main author
Torbjørn Vegard Løkken
StatoilHydro Research Centre
N-7005 Trondheim
Norway
tvl@statoilhydro.com

Co-authors
Anita Bersås
Kjersti Omdahl Christensen
Cecilie Fjeld Nygaard
Even Solbraa
All from StatoilHydro

1 ABSTRACT

Knowledge related to precipitation and transport of water, ice, hydrate or an aqueous phase in pipelines and process equipment are of great importance to the natural gas industry. Such phase behaviour can e.g. lead to blockages or corrosion of equipment, and need to be kept under control from well to the end consumer. This work covers four of the most important topics related to water dew point control in natural gas.

- Methods for water dew point control (dehydration and analysis) and general phase behaviour of natural gas with water and other trace components (e.g. glycols)
- Operational challenges related to water and trace components in natural gas seen from a gas producers point of view
- New experimental data for water content in natural gas in stable equilibrium with liquid water, ice and natural gas hydrate
- Evaluation of existing methods and presentation of an accurate thermodynamic model for calculation of equilibrium water vapour concentration and dew point of natural gas

The equilibrium water content in methane and a natural gas has been measured in the temperature range -20 to 20ºC and pressures up to 150 bar. The experimental data is presented as the water content in equilibrium with the most stable phase (water, ice or hydrate) at the experimental temperature and pressure.

A review of published methods (graphical-, empirical- and thermodynamic models) for the calculation of equilibrium water content in natural gas is presented. The model suggested and used in this work is based on the Cubic Plus Association Equation of State (CPA-EoS) combined with thermodynamic models for the ice and gas hydrate phase. This model is shown to give excellent result, both for the calculation of equilibrium water content of natural gas, water dew point-, natural gas hydrate- and ice precipitation temperature as well as the aqueous dew points. The model is compared to the ISO 18453 developed for water dew point calculation of natural gas, and shown to be superior when it comes to extrapolation of pressure, temperature and gas composition. An accurate chart for graphical reading of water content of a sweet natural gas is presented. The method and data presented in this paper can be used in design of water removal processes.

This paper present phase behaviour of natural gas with focus on saturation points and phase behaviour for water and selected trace components. The phase behaviour will be related to the various water removal processes used for dew point control of natural gas. The paper describes why various water related saturation points have to be considered in design and operation of gas production and transport systems. Experience related to the precipitation of water, hydrate, ice or an aqueous phase in process equipment and pipelines are presented. This work presents and discusses experiences from selected gas processing plants in operation where precipitation of water, ice- or hydrate has created operational disturbances. The experience from these situations is compared to the results from the experimental and modelling work.

CONTENTS

2 INTRODUCTION

Natural gas always contains water in varying amounts dependent on upstream conditions. This water is naturally present in the gas, originating from the reservoir. Alternative sources can be water saturation in various gas processing operations (e.g. acid gas removal). Water in natural gas can create problems during transportation and processing, of which the most severe is the formation of gas hydrates or ice which may block pipelines, process equipment and instruments. Corrosion of materials in contact with natural gas and condensed water is also a common problem in the oil and gas industry.

Natural gas reservoir temperature and pressure conditions are typically in the range 100 to 1000 bar and from 50 to 200ºC. Pipeline operating conditions are usually at pressures up to 250 bar and in the temperature range −20 to 50°C. Temperatures during LNG processing can typically be as low as -180ºC. Accurate measurements and calculations of the maximum water vapour concentration in natural gas at all these conditions are of great importance to the natural gas industry.

Accurate experimental data and methods for calculating the water vapour concentration in natural gas in equilibrium with condensed water, an aqueous phase, ice or hydrate are necessary in various situations. Such knowledge is the basis for the requirements of a drying process, or as a tool for trouble shooting in real process plants. This paper will present new data and modelling of the equilibrium concentration of water vapour in high pressure natural gas, and relate it to experience from disturbances observed in some of our gas processing plants. The water vapour concentration and dew point specifications of pipeline gas and LNG will be evaluated and the need for accuracy of equipment for online water content analysis will be discussed.

2.1 Dehydration of natural gas

Three of the most common methods for dehydration of natural gas are physical absorption using glycols, adsorption on solids (e.g. molecular sieve/silica gel) and condensation by a combination of cooling and chemical injection (ethylene glycol/methanol). Triethylene glycol (TEG) dehydration is the most frequent method used to meet pipeline sales specifications. Adsorption processes are used to obtain very low water vapour concentration (0.1 ppm or less) required in low temperature processing such as deep NGL extraction and LNG plants. Some relatively new processes for dehydration involve applying isentropic cooling and separation using high centrifugal forces in supersonic gas flow [1]. To estimate the limits of such techniques it is important to have models that can calculate water vapour concentration in equilibrium with hydrate, ice and water in natural gas at operational temperature and pressure.

A distinct difference between the chemical based (e.g. glycol absorption) and the non-chemical based (e.g. adsorption) dehydration techniques is that the chemical based techniques will saturate the gas with chemicals at operational conditions. Both techniques can in principle remove almost all the water from the gas, but the phase behaviour of the natural gas leaving the processes will be different. Even though chemicals used for absorption in general will have low vapour pressure and relatively small amounts will condense per cubic meter gas, the effect of condensation has to be considered in design of pipelines and process equipment. In the following list, we have given some definitions of water related dew points that will be used throughout this paper.

Definitions:
Water dew point temperature – The highest temperature, at a specified pressure, where water spontaneously can condense from the natural gas

Aqueous dew point temperature – The highest temperature, at a specified pressure, where a solution of water and trace chemicals (e.g. monoethylene- and triethylene glycol) can spontaneously condense from the natural gas
Frost point temperature – The highest temperature, at a specified pressure, where ice can spontaneously precipitate from natural gas
Hydrate point temperature – The highest temperature, at a specified pressure, where natural gas hydrate can spontaneously form in a gas mixture
Maximum water precipitation temperature - The highest temperature, at a specified pressure, where water can spontaneously precipitate in any form (liquid water, aqueous solution, ice or hydrate) in a gas mixture
Glycol freezing point – The highest temperature, at specified pressure, where solid glycol can spontaneously precipitate

2.1.1 Phase behaviour of dehydrated natural gas

Adsorption of water on solid surfaces such as molecular sieves and silica gel are commonly used to remove water in natural gas to very low levels. Such solid adsorbent based processes can also be designed to remove traces of chemicals such as TEG and MEG from the natural gas. In the treated natural gas the content of chemicals will normally be too low to influence the precipitation of water. For such a case water will precipitate directly as liquid water (with insignificant traces of chemicals), ice or natural gas hydrate. Dependent on temperature, pressure and water vapour concentration, the maximum water precipitation temperature will correspond either to the water dew point, the frost point or the hydrate point. In a conservative design the specification of water vapour concentration should be based on this maximum precipitation temperature, and not the traditional water dew point temperature. Accurate conversion between water vapour concentration and precipitation temperature is therefore crucial.

In Figure 1 the typical phase behaviour of a natural gas is illustrated, where water has been removed in an adsorption process. The water content in the gas is 40 ppm(mole) and does not have any traces of chemicals. For this gas the hydrate saturation line appears at higher temperatures than the equivalent lines for ice and sub cooled water. In a cooling process though, ice and liquid water (sub cooled) can be formed before hydrates because of the relative slow kinetics of hydrate formation. It is often discussed if hydrates can form directly from the gas phase. Even though the process is expected to be kinetically slow, direct hydrate formation can occur from a thermodynamic point of view. In this work we have not looked into proving if this can happen, but in design we would generally use the highest temperature where water, ice or hydrate can precipitate, i.e. the maximum water precipitation temperature.

As we can see from Figure 1, natural gas hydrate will generally be the first thermodynamically stable phase that can precipitate in the whole pressure range. If the water content in the gas is higher, we can have pressure regions where water or ice can precipitate at higher temperature than gas hydrate.

Sufficient dehydration is commonly achieved by contacting the natural gas with a triethylene glycol (TEG) solution at high pressure and relatively low temperature (typically 50-100 bar and 20-40°C). The treated natural gas from a TEG contactor will be at its aqueous dew point downstream the glycol absorber; hence it is saturated with TEG and water. It is a good approximation that the treated gas is in thermodynamic equilibrium with the lean TEG. A typical lean TEG composition is 99wt% TEG and 1wt% water. If the treated gas temperature decreases, a solution of water and TEG will start to condense from the natural gas. At absorber operating pressure, the first droplet that is formed will have the same composition as the lean TEG. The aqueous dew point at glycol absorber operation pressure is therefore equal to the temperature of the gas leaving the absorber. TEG will work as a hydrate inhibitor in the condensed phase.

Because water has a much higher vapour pressure than TEG, water will dilute the TEG in the condensed phase when the temperature is reduced below the aqueous dew point. If the temperature is further reduced below the aqueous dew point, the TEG in the aqueous phase will be diluted with water, and the aqueous phase approaches its hydrate, frost or TEG freezing point.

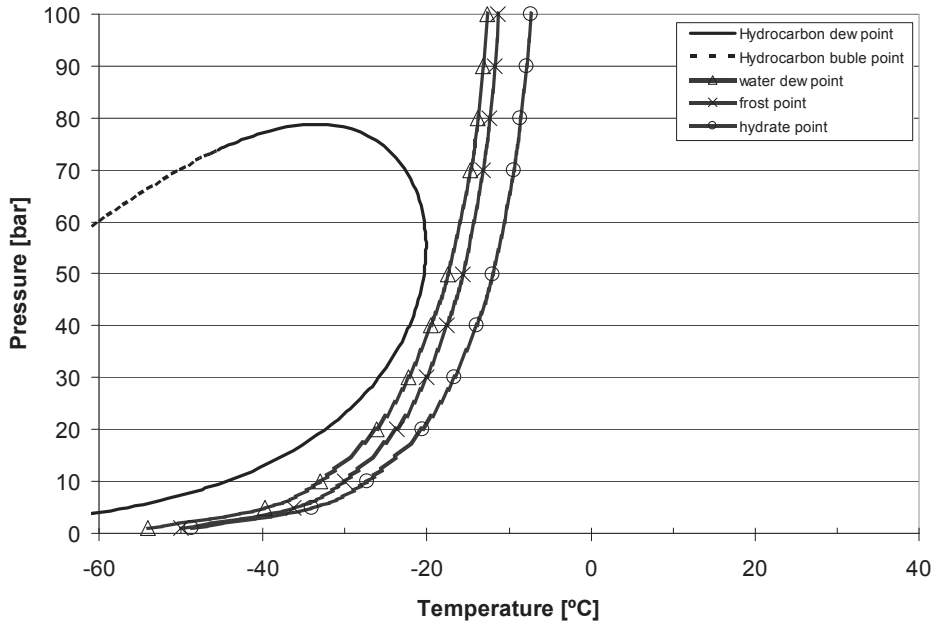

Figure 1: Phase behaviour of natural gas with traces of water (40 ppm(mole)), NG composition (mole): 85 % C1, 10 % C2, 4 % C3, 0.5 % nC4, 0.5 % iC4

In Figure 2 the phase behaviour of a gas with 85mol% methane and hydrocarbons up to nC4 with traces of water (40 ppm) and TEG (0.5 ppm) is illustrated. The thermodynamic model developed in this work and described in the coming chapters has been used to generate the saturation lines in the figure. In making the figure, absorber operating conditions of 80 bar and 30ºC have been assumed. As can be seen, the aqueous dew point line crosses this operational condition at 80 bar and 30ºC. It is important to note that entrainment of TEG (droplets or aerosol) is neglected in making this figure. The calculated frost point and hydrate point is influenced by the inhibiting effect of TEG in the aqueous film. TEG freezes at about -6 ºC at pressures up to 80 bar (the freezing point of pure TEG is -6ºC at atmospheric conditions). At higher pressure the TEG freezing point is reduced due to water dilution of the aqueous TEG phase. The various calculated saturation lines after dehydration with TEG are shown in Figure 2. The aqueous dew point line will generally show a different curvature than traditional water dew point lines (Figure 1). The reason for the curvature of the aqueous dew point line is that the solubility of vapour TEG in the gas phase increases with increased pressure (for pressures higher than about 20 bar). The equilibrium water vapour concentration in natural gas generally decreases when the pressure increases. As seen from Figure 1, condensation of water can be avoided by reducing the pressure at constant temperature. This is not necessarily the case for the aqueous dew point. Depending on the operating point, decreased pressure might lead to condensation of an aqueous phase.

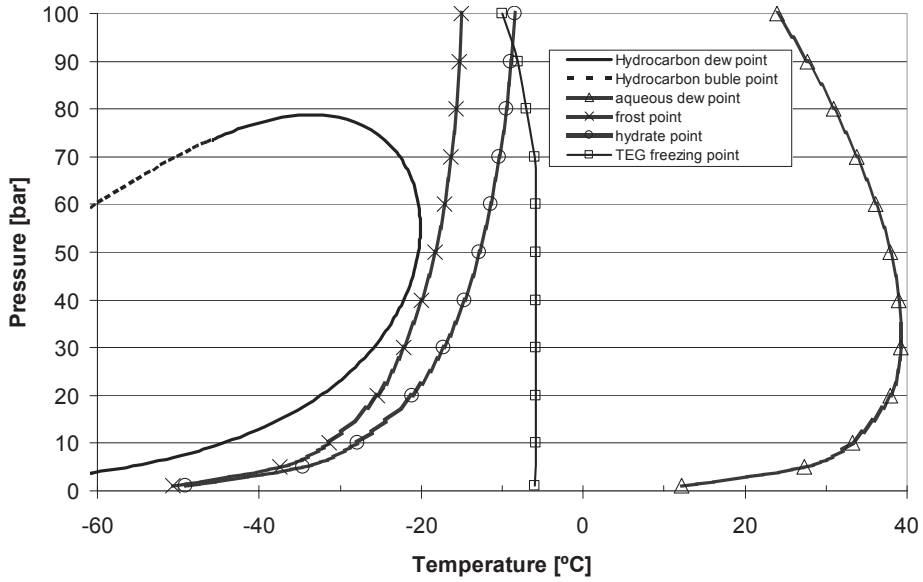

Figure 2: Phase behaviour of natural gas with traces of water (40 ppm(mole)) and TEG (0.5 ppm(mole)), NG composition (mole): 85 % C1, 10 % C2, 4 % C3, 0.5 % nC4, 0.5 % iC4

Dependent on upstream conditions, aqueous, water, ice, hydrate and solid TEG precipitation can be of importance in design and daily operations. Even though the water dew point temperature specification used in natural transport and sales agreement (typically -8ºC at 70 bar) can be under control, caution must always be taken to evaluate the effect of precipitation of all possible condensed and solid phases.

2.2 Analysis of water in natural gas

Even though analyses of trace amounts of water vapour in different gases have been performed for more than 50 years, this still is one of the most demanding trace gas analyses. One reason for this is the high polarity of water, making it extremely adsorptive. Consequently surfaces regarded as dry is usually coated with a thin film of moisture [2]. Also the fact that water is omnipresent makes trace analysis a challenge, with the potential for background signals from the surroundings. High pressure natural gas often with traces of production chemicals and condensable hydrocarbons add another level of analytical challenge.

Many different techniques exist for quantitative determination of low levels of water vapour in gases. Descriptions of these techniques and their advantages and disadvantages are documented by several authors [3], [4], [5]. The most common water vapour measuring devices used in the oil and natural gas industry are capacitor sensors (aluminium oxide or silicium oxide based), piezoelectric sensors or chilled mirror apparatus. Capacitor based water dew point determination is still by far the most used technique in StatoilHydro when it comes to online analysers.

The amount of water vapour in natural gas has traditionally been referred to as a dew point or frost point temperature. Moreover the term dew point is often used as a general term, without distinguishing between dew point and frost point. When using the chilled mirror technique this

dew point or frost point is directly read from the instrument as the mirror temperature when the first trace of condensed water or ice is observed. Capacitor based water dew point sensors do not directly measure the water dew point or frost point, they are generally calibrated against chilled mirror devices at atmospheric pressures. As a consequence these sensors are set up to return a dew point (>0°C) or frost point (<0°C) when used Table 1: Typical specification for water in natural gas productsby the oil and gas industry. Piezoelectric devices on the other hand are generally calibrated against known water vapour concentration (usually ppm-mole). Hence the water vapour concentration returned from piezoelectric devices has to be converted to a dew point or frost point temperature to be compared to dew point specifications or measurements from capacitor based sensors, or vice versa.

In recent years StatoilHydro has tested several of the available techniques [8]. In Figure 3 results from tests of various techniques for water vapour determination are presented. The tests were performed by analysing the water vapour concentration in nitrogen in identical streams generated and humidified in laboratory facilities. As can be seen, the readings from different techniques can show relatively large individual deviation, even for such a simple system. Some techniques also show a tendency to drift with time. This illustrates that accurate water vapour determination is nontrivial and much care have to be put into the analysis system to obtain stable and reliable results.

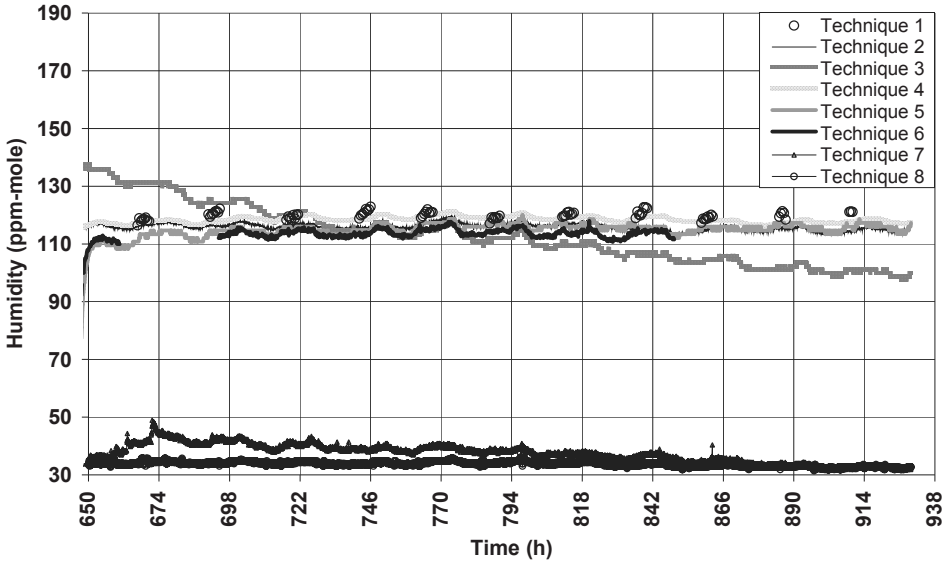

Figure 3: Water vapour determination in nitrogen by various techniques

In Figure 4 the results from a similar laboratory experiment are shown. In this case small concentrations of gaseous ethylene glycol (MEG) are added to the humidified nitrogen during the experiment. The results clearly demonstrate that small amounts of certain production chemicals can affect the humidity determination and that the effect is dependent on the chosen humidity technology.

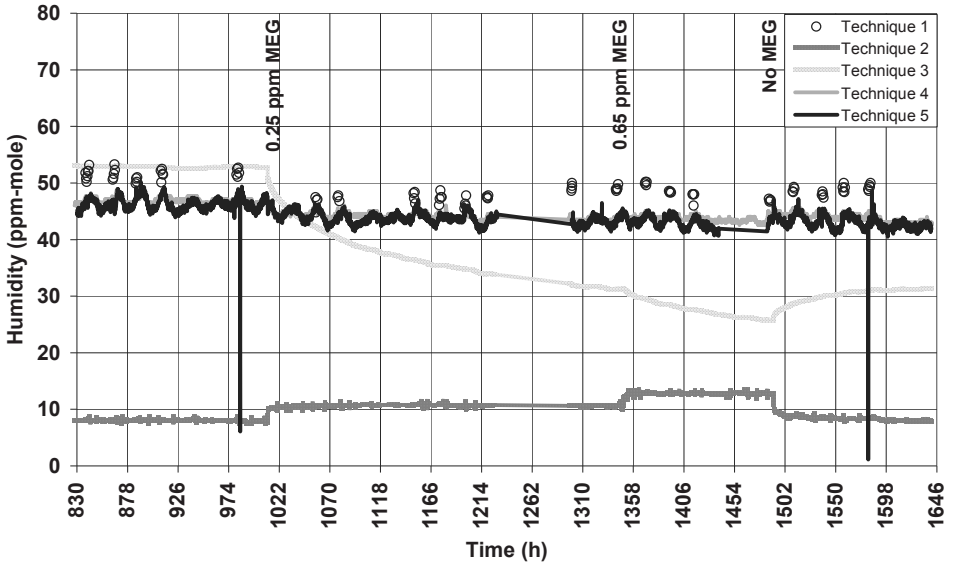

Figure 4: Water vapour determination in nitrogen by various techniques, with low concentrations of gaseous ethylene glycol added

When considering techniques for water analysis in natural gas it is important to carefully evaluate the applicability of the techniques with various important considerations in mind; accuracy, speed of response, tendency to drift, influence of traces of production chemicals, sampling system, need for maintenance and calibration. Inadequate water vapour analysis systems can lead to situations where hydrate formation can occur, even if the online analyser indicates acceptable water vapour levels.

3 EXPERIENCE FROM OPERATION RELATED TO WATER PRECIPITATION AND DEW POINT CONTROL

Control of water in natural gas is of high importance in natural gas production. The natural gas is generally saturated with water at reservoir conditions. The temperatures in the gas reservoirs can be very high, and temperatures up to about 1000°C are experienced in the Norwegian Sea in high pressure and high temperature (HPHT) reservoirs. Under such conditions the water vapour concentration of natural gas can be >1 mole% in the reservoir and it need to be reduced to typically 1-50 ppm(mole) to fulfil processing or transport specification. Water condensation, ice and hydrate formation are of the most common problems observed in natural gas production systems. Important control mechanisms for preventing blockages due to water in gas are: Inhibition of the well stream using antifreeze chemicals (e.g. MEG) and dehydration of the gas by absorption/adsorption. Finally operational control is obtained by online monitoring/analysis of water vapour concentration in the natural gas as described in the previous chapter.

Gas processing plants will from time to time experience blockages due to freezing in process equipment. The reason for the incidents can be many, but from our experience one or more of the situations in the bullet list below are often seen when unexpected blockages and water condensation have occurred.

- Insufficient drying of processing equipment and pipes before process start-up

- Malfunctioning online water dew point analyser fails to indicate correct water content or fast changes in water content
- Hydrate inhibition system fails (insufficient or no hydrate inhibition)
- Regenerated TEG does not have good enough quality to meet dew point specification
- Adsorption process has been polluted by production chemicals and does not work properly
- Water saturated gas is re-circulated to cold parts of the process
- Water dew point specification is not sufficient for specific parts of the process
- An unwanted aqueous phase is formed even if the gas is far from the water dew point

In the sections below we have selected a few processes where we have experienced operational trouble, condensation or blockages due water in gas. We have tried to discuss the root cause and the preventional work done.

3.1 Ice/hydrate formation and blockages in process related to low temperature propane storage

In Norway, mountain caverns are used for effective storage of large volumes of propane. In such caverns the propane is stored at a pressure slightly higher than atmospheric and at the boiling point temperature of propane (around -40°C). The propane will be in direct contact with the rock walls in the cavern, and because of humidity in the rock, an ice cap will build up on the walls. This ice cap will work as a thermal insulation between the propane product and the mountain, but some heat input will always lead to vaporization of propane. To prevent pressure increase in the cavern, the propane boil off gas is relieved and re-circulated to the cavern via a refrigeration and condensation loop. Due to the ice cap on the rock walls, the propane boil-off gas will be saturated with water at cavern temperature and pressure. The propane boil off gas is mixed with the incoming propane product from the process plant. When this propane product is cooled and condensed there is a high risk that water will precipitate in some form. Blockages due to such precipitation have been experienced at a regular basis in propane storage caverns in Norway. The precipitated ice and hydrate have a tendency to block valves and filters in the propane cooling loop. The blockages normally occur in the coldest part of the cooling loop where the propane has been condensed and the temperature is around -40ºC.

The problem of precipitation of ice and hydrate in low temperature propane can be solved by a number of methods. The most obvious methods would be to remove the water (by e.g. adsorption) from either the full propane stream or from the cavern boil-off gas. Continuous inhibition with methanol or alternatively irregular injection of methanol when blockages start to occur is an alternative problem solutions. These options will have various pros and cons when it comes to cost and operational challenges. Continuous methanol injection is a relatively easy solution, but due to strict specifications for methanol in the propane product, the solution has a high probability of giving an off-spec product. In Figure 5 the results from experimental vapour-liquid-solid (VLS) data from literature and from the laboratory at StatoilHydro Research centre are presented [9]. The figure shows equilibrium methanol concentration in the propane plotted against methanol concentration in the aqueous phase. The figure illustrates that a methanol concentration of about 320 ppm in the propane is needed to enable effective continuous inhibition at -40°C (25 mole% methanol in aqueous phase). Such a high methanol content will in general be unacceptable in the propane product.

Discontinuous methanol injection has proven to be effective to dissolve the solid ice and hydrate to prevent blockage of valves and piping in the cooling loop. By locally injecting high amounts (>300 ppm) of methanol, the ice and hydrate will dissolve, and blockages are removed.

The CPA-EoS model as presented in this work has been useful for estimating the propane-methanol-water vapour-liquid-solid (VLS) phase behaviour. As can be seen in Figure 5, the predictions with the CPA-EoS corresponds well with the experimental data, and shows that the model is well suited for analysis and trouble shooting of such systems.

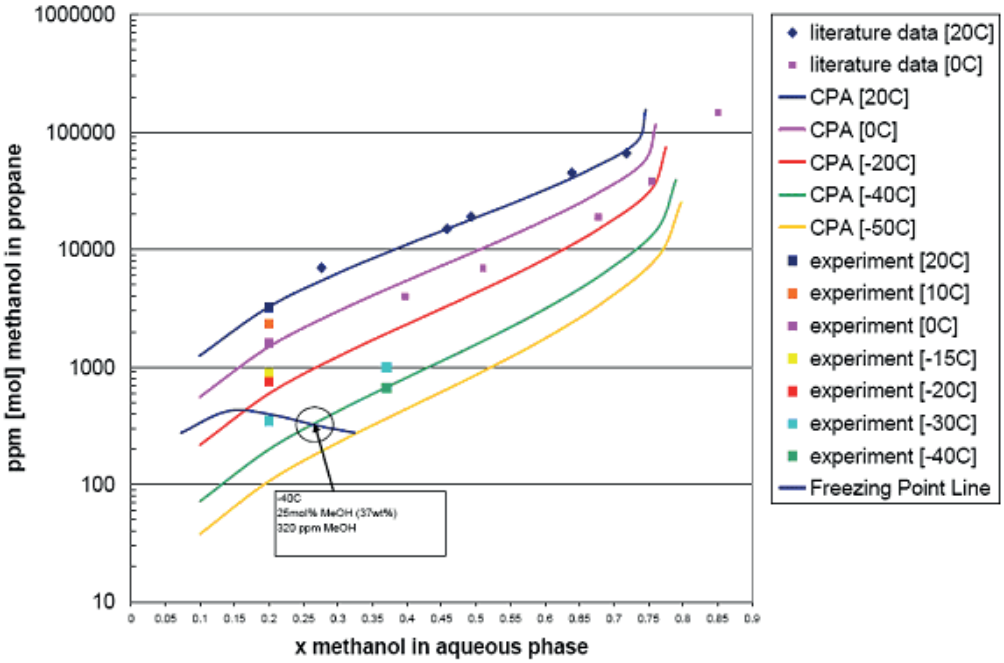

Figure 5: Experimental and modelling results of phase behaviour of propane-methanol-water

3.2 Solid precipitation in cryogenic process equipment

The potential for water precipitation is highest in the low temperature parts of the process. Such low temperature parts are typically in the upper sections of distillation columns such as the de-methanizer or de-ethanizer. It can also be in cryogenic heat exchangers or during expansion through valves or turbines. In many of these processes the water content of the natural gas need to be kept very low to prevent solid precipitation. Even short process upsets in the dehydrating processes can lead to blockages and capacity reduction of such equipment. Precipitation of ice or hydrate is often seen as a steadily decreased capacity of the equipment. Blockages are normally handled by injecting methanol as antifreeze. In some situations a full process shutdown is necessary followed by depressurization and drying of the equipment. Safe and stable operation of water removal processes in combination with accurate and responsive online water analysis is the key for preventing blockages due to water in such cryogenic systems.

In low temperature process equipment we from time to time experience precipitation of solid glycol (TEG and MEG) [10]. It is important to keep in mind that pure glycols form thermodynamic stable solids at relatively high temperatures. Precipitation of solid glycols typically occurs in low temperature equipment handling natural gas saturated with glycol. This

can typically be the case for cryogenic equipment installed downstream of TEG contractors. This type of phase behaviour was illustrated in Figure 2.

Accurate modelling of water, ice, hydrate and solid glycol precipitation is essential for stable operation and trouble shooting of cryogenic equipment. Precipitation and blockages due to precipitation of components naturally present in the gas (e.g. CO_2, benzene) can also occur in cryogenic equipment, and is important to control both in design and operation.

3.3 Challenges related to water dew point analysis

The oil and natural gas industry experiences several challenges connected to water dew point or water vapour concentration analysis:

- Choice of sampling points
- Adequate sampling systems
- Choice of technology and supplier of equipment
- Quality control of the online equipment for water dew point measurements
- Quality control of portable equipment for water dew point measurements
- Calibration routines of equipment for water dew point measurements
- Conversion between dew point or frost point and water vapour concentration (ppm-mole) at high pressures.
- Varying concentrations of production (eg. MEG, TEG and methanol) chemicals in the natural gas

The choice of sampling point is very important, as dew point analysis is easier on a single natural gas phase, free of contaminants such as dust and production chemicals and free of liquid droplets. Dew point measurements close to the gas outlet of glycol contactors are therefore very demanding as this gas will be saturated with glycol and water which can easily condense. At some sites more or less carry-over of liquid glycol from the glycol contactor also will happen with some frequency, giving the sampling systems and analytical instrumentation even worse conditions to work under. Sample points downstream a compressor stage is experienced to always give easier dew point control.

The sampling systems must always be given high attention. It will seldom be helpful to change measurement technique or supplier of technology if the sampling system is inadequate. We have seen examples of lack of communication and understanding between StatoilHydro, the suppliers of the sampling system and the supplier of dew point analyser. This can often result in a situation with disagreements about the cause of suspect dew point analysis. The situation usually ends up with modifications of sampling system before the measuring technique can be evaluated and reliable dew point control can be gained.

Capacitor based humidity determination is widely spread in the oil and natural gas industry. Our experience is that the suggested quality control and calibration routines from most suppliers of these devices are inadequate. This can explain why users often find parallel capacitor sensors, or sensors on parallel gas trains, returning very different levels of dew point readings (10-20°C deviations can often be found).

3.4 Aqueous film condensation in gas transport pipelines

On the Norwegian continental shelf a common way to produce gas is to partly process the gas offshore and transport it to shore for full gas processing. The gas is normally dried in an offshore absorption processing using TEG, and transported to shore in rich gas pipelines (transportation in the hydrocarbon dense phase region above cricondenbar pressure). The partly treated gas from the offshore installation is saturated with TEG at process conditions (at

aqueous dew point). When the temperature and pressure drops in the sub sea pipeline to shore, a liquid film of TEG and water will form. The water content of this film has to be controlled and kept low to keep the corrosion potential in the pipe low. In long distance pipelines (>100 km) flow instabilities with slugs of TEG/water must also be considered and receiving facilities on shore have to be installed (gas scrubbers/filters/slug catchers). Liquid glycol is known to influence the efficiency of down stream gas processing equipment such as H_2S-adsorption and mercury adsorption processes. Glycol coating can result in a considerable reduced life time of the adsorption mass.

It is important to control the amount and composition of the aqueous phase in the pipeline as good as possible. Phase behaviour of natural gas, glycol and water solutions is however challenging to model due to the highly non-ideal system. Much work has been done in our laboratories to obtain experimental data and develop accurate models for such systems [11].

3.5 Water content specifications of natural gas

A number of different water dew point specifications exist for natural gas. The water dew point specification is specified in sales gas contracts or given by requirements for transport, processing or storage. The water dew point specification for gas transported through pipelines to Europe is typically -8°C at 70 bar (EASEE-gas specification [12]). For LNG production the water specification needs to be more stringent, and a specification of <0.1 ppm(mole) water in the gas is normally used. Due to the low solubility of water in hydrocarbon liquids, the water specification for LPG products need to be low. Table 1 summarizes typical water specification used for natural gas products.

Table 1: Typical specification for water in natural gas products

Natural gas type	Water dew point/content specification
Pipeline sales gas	-8°C at 70 bar
LNG	0.1 ppm(mole)
Propane	No free
LPG	No free

As can be seen, specifications are given both as a dew point at a given pressure and as water vapour concentration. Accurate tools are necessary for converting between the various specifications. Online dew point analysers are normally calibrated to report ppm(mole) of water in natural gas.

4 LITERATURE REVIEW

Experimental and modelling work related to equilibrium water content in natural gas have had high focus both in industry and academia for a long time. This chapter gives a short description of the most popular methods used for calculation water content of natural gases. A brief review of previously published experimental data for equilibrium water content of methane and natural gas will also be presented. In chapter 7 results from some of the most widely used estimation methods will be compared to experimental data.

4.1 Methods for calculation of water content and water dew point of natural gas

A large number of methods have been developed for the estimation of water content and water dew point of natural gas. Only a few of them will be examined here. The methods range from simple methods such as generalized charts for direct reading of water content to advanced numerical demanding thermodynamic models (e.g. modern models based on equations of state). We can say that the simple methods will have a limited range of validity when it comes

to gas compositions, pressure- and temperature range. The more advanced models will generally be more accurate and be applicable for a larger span of variables such as gas composition, pressure and temperature.

In this work we differentiate between three types of phase behaviour: vapour–liquid (water and aqueous dew point), vapour–ice (frost-point) and vapour–hydrate (hydrate formation comprising two possible hydrate structures). Most of the simple methods based on charts and empirical correlations are only developed to predict the water dew point, and will not be able to predict hydrate precipitation, ice or the aqueous dew point. Some of the more recently developed models based on fundamental thermodynamics (e.g. CPA-EoS), are developed to predict all mentioned dew points.

4.1.1 Methods based on generalized charts.

The estimation of water content of natural gas based on reading from charts is a common method to use. The charts are generally based on experimental data or thermodynamic models. Normally the water content is plotted on a semi logarithmic scale against the dew point temperature in form of isobaric lines. A large number of such diagrams have been made and published in reference literature in gas processing. The diagrams that are most used in the gas industry are the diagrams from MacCarthy et al. [13] and McKetta and Wehe [14]. These diagrams are based on experimental data measured in the 1940th century [15], [16].

One of the limitations in accuracy of using these methods is that water content of natural gasses is generally dependent on the gas composition, and such composition dependency can in general not easily be implemented in chart based methods. The compositional dependency is normally handled by developing chart for various types of gas mixtures (e.g. sweet gas and sour gas). Another limitation of such methods is that it can not be used to estimate hydrate, ice or the aqueous dew point. The area in the charts where the most stable phase is ice or natural gas hydrate is normally plotted with dotted lines indicating equilibrium water content with meta-stable liquid water. Acid gas components such as CO2 and H2S can have a large influence of water solubility in the gas phase, and generalized charts for such gas mixtures are difficult to develop.

For the chart based method of McKetta and Wehe a correction factor that is a function of relative gas density can be applied to correct for deviations in gas composition [14]. Correction factors for taking in to account the effect of salinity of water have also been presented in this publication. Use of these correction factors is expected to improve the results of the method, but will in general be too simple to expect accurate results.

Even though there are many weaknesses in chart based methods for estimating water content of natural gasses, because of the simplicity of this method, these methods must be expected to be used by the gas industry also in the future. When using such methods it is important to have in mind the weaknesses of the methods, and always look for charts developed for gases with similar compositions.

4.1.2 Methods based on empirical models

Various simple empirical models have been developed for the calculation of water content of natural gas. The simplest models are based on functions fitted to the experimental data for the vapour pressure of pure water. In an ideal gas the water content will be directly given by the vapour pressure of water and the total pressure. However such models will generally be invalid for pressures higher than typically 10 bar. The maximum pressure will depend on how ideal the gas mixture behaves. For gases with high solubility in water (e.g. gases with high CO_2 or H_2S content), the ideal method is not valid even at low pressures.

Some empirical models correct for the non-ideality of the gas by fitting the model to high pressure experimental data. Such models can give reasonable results at higher pressures, but will in general be limited to gases with similar composition as what was as experimental basis. A popular empirical correlation used in the natural gas industry was developed by Bukacek [17]. This method is published as a standard for defining the relation between water content and water dew point of natural gas (ASTM D1142-95) [36]. The equation is on the form

$$W = A/P + B \qquad \textbf{Eq. 1}$$

Where W is the water content, P is the total pressure, A is a constant proportional to the vapour pressure of water and B is a constant depending on temperature and gas composition. The effect of gas composition is indirect corrected for by multiplying the B factor with a term dependent on gas gravity. The B factor has also been estimated based on experimental data for water content in sweet natural gas mixtures and values for the constant are tabulated in the original publication [17].

The accuracy of the Bukacek [17] correlation has been questioned in various publications [19]. One comment is that the model is based on bad experimental data (water content in equilibrium with meta-stable liquid water was measured instead of ice or hydrate). Bukacek's method is fitted to water content in natural gas in equilibrium with liquid water. The method can thus not be expected to be able to estimate water content in equilibrium with hydrate or ice.

In a resent publication [20], an empirical method for calculating the water content of gas in equilibrium with ice and hydrate (and hence hydrate and frost point) has been suggested.

The simple empirical models can not be expected to be as accurate as more advanced thermodynamic models. Extrapolation in gas composition, temperature and pressure must be done with caution. Due to their simplicity and low numerical requirements, such methods are widely used in the industry. Many of the online water dew point analysers use these empirical correlations to estimate water dew point based on water content analysis.

4.1.3 Methods based on equations of state

Thermodynamic models based on equations of state (EoS) for calculating water dew point and water content of natural gas can be relatively complex and computers have to be utilized in doing efficient calculations. However many of the developed models have been shown to give accurate predictions of water dew point for a large number of gas compositions and total pressures. Some of the popular classic equations of state, like the SRK- and PR-EoS often used in the oil and gas industry, have traditionally had problems in handling polar components like water. The traditional way of fixing this limitation of modelling polar components correctly has been to use a modified attractive term in the equation of state to reproduce the vapour pressure of polar components more accurately [42]. Still we have seen a limitation of such models in that the density of the liquid phase was predicted badly and that relatively large and binary interaction parameters between water and hydrocarbons had to be used. Scientific development of equations of state during the last decades [35] has more or less removed this limitation by adding explicit terms for modelling the effect of the hydrogen bonding between polar components.

Most modern equations of state are developed by fitting parameters (e.g. binary interaction parameters) to experimental data for both pure components and mixtures [21]. This is the case for the equation of state used in ISO 18453 [34] which has been developed for converting between water content and water dew point of natural gas. Some of the more recent models have been show to be able to predict mixture properties based on knowledge of only pure component properties. In a recent work [22] it was demonstrated that such a predictive model could be applied for the calculation of the water content of natural gas mixtures with high accuracy. The model was also developed to predict hydrate and ice precipitation from natural gas, and is also suited to estimate the aqueous dew point in gases with traces of production chemicals. This model is normally referred to as the CPA-EoS [35] and is described in more detail in the coming chapters.

The advantages of methods based on fundamental thermodynamic models are that they are expected to cover a larger range of gas compositions, temperatures and pressures. The models used in this work are based on equation of states, and the details of the models are presented in chapter 5. The thermodynamic models can easily be extended to handle undefined components such as oil fractions and has also been shown to be readily extendable to handle electrolyte mixtures (salts).

4.2 Published data for water content and water dew point of methane and natural gas mixtures

Methane is the primary component of natural gas, and is hence the most important component to obtain accurate experimental data. Accurate mathematical models and experimental data for water in methane is a prerequisite for the study of natural gas mixtures. We have therefore focused the literature data collection on finding equilibrium data for water in methane.

A relatively large number of laboratories have published experimental data for equilibrium water vapour concentration in methane. Less experimental data exists for water content of real natural gases. Experimental measurement of water content of methane and natural gas is difficult for a number of reasons:

- Water is generally present in the gas in very low concentrations (ppm level) and analysis is challenging
- Water tend to adsorb to solid surfaces in sampling systems
- Water can be in equilibrium with natural gas in various forms; liquid, ice and hydrate. It is generally difficult to specify exactly what phase we have in the experimental equipment
- The kinetics of ice and hydrate formation can be slow, and it can take long time to obtain stable equilibrium

A lot of published data in the open literature is expected to be error prone due to one or more of the reasons from the list above. As can be understood, experimental data related to water content in gases are often associated with errors, as an inspection of data sets measured at same temperature and pressure conditions indicates. Therefore we have earlier systematically evaluated the available experimental data [1].

Table 2 provides a summary of the experimental data sets published in the literature for water in methane. There exist several sets of experimental data for water in methane, and the measurements have been done in a number of different types of experimental equipments. Data for the equilibrium water content of gases are generally reported without the corresponding value of gas solubility in the liquid, and vice versa. All data considered here are gas phase data. Table 2 includes probably all available data published in the open literature for the binary water–methane system. The experimental data has been compared to predictions with the models used in this work (GERG-water and CPA-EoS as will be presented in chapter 5). We have classified the data according to the type of the precipitated phase that is in equilibrium with the vapour phase: liquid water, ice or hydrate. Since the type of the precipitated phase is generally not reported in the literature sources, we have used experimental temperature and pressure conditions to predict what the thermodynamically stable phase is. The phase with the highest calculated precipitation temperature is considered to be stable, and also assumed to be present during experiments. The experimental points have been classified based on this technique, and compared to prediction with the CPA-EoS. The GERG-water EoS does not distinguish between the natures of the precipitated phases (liquid, ice or hydrate), and we therefore report only one value for the deviation and bias using GERG-water EoS.

We have chosen to report deviation between data and model in terms of dew point temperature, i.e. the difference between the calculated temperature and the experimental temperature for the experimental water content at the experimental pressure. This gives a better overview for the deviation than using water content which varies over several orders of magnitude. It should be pointed out that 1ºC deviation corresponds to around 5–8% change in water content above 0°C and to about 10–11% below. For the experimental data presented in this work, the maximum 5% difference between the largest and smallest value of water content for each of three analyses would then correspond to a variation within each reported value of around 0.3ºC below 0°C and around 0.4ºC above 0°C.

The deviations between calculated and experimental data reported in Table 2 are reported using absolute average deviation (AAD) and bias (BIAS) calculated as,

$$AAD = \frac{\sum_{i=1}^{i=NP} \left| T_{i,calculated} - T_{i,\exp eriment} \right|}{NP} \qquad \textbf{Eq. 2}$$

$$BIAS = \frac{\sum_{i=1}^{i=NP}\left(T_{i,calculated} - T_{i,\exp eriment}\right)}{NP} \qquad \textbf{Eq. 3}$$

where NP is the number of experimental points. The AAD indicates generally how good the model fit to the data. The BIAS indicates if the model has a general tendency to predict to high or too low dew point temperatures. If the AAD and BIAS has the same absolute value, different from zero, it indicates that the model consequently predicts values either higher (positive BIAS) or lower (negative BIAS) than the experimental values.

If several data sets show significant and similar deviations compared to a model, the data set are probably correct and the model probable wrong. If the model describe the data sets well we can consider the model to be fairly accurate as well.

Table 2: Summary of open literature experimental data for equilibrium water vapour concentration in methane gas. Comparison to calculations with the CPA-EoS and the GERG-water EoS

Reference	T [ºC]	P [bar]	CPA-EoS Liquid water			CPA-EoS Ice			CPA-EoS Hydrate			GERG-water EoS	
	min/ max	min/ max	NP Lw	AAD [ºC]	BIAS [ºC]	NP Ice	AAD [ºC]	BIAS [ºC]	NP Hydrate	AAD [ºC]	BIAS [ºC]	AAD ºC]	BIAS [ºC]
Althaus [21]	-20/20	5/100	15	0.4	-0.4	9	0.8	-0.8	26	0.5	-0.3	0.6	0.4
Kosyakov [18]	-40/10	10/101	5	0.8	-0.7	2	1.3	1.0	26	0.5	-0.5	1.1	0.8
Aoyagi [23]	-43/-3	13/103	-	-	-	-	-	-	35	2.3	1.1	3.4	1.8
Chapoy [24][25]	10/45	10/351	39	0.9	0.8	-	-	-	7	2.2	-1.0	1.9[b]	0.9
Bogoya [26]	-15/15	30/60	5	1.4	-1.4	-	-	-	9	1.8	-1.8	1.0	-0.9
Folas [22]	-20/20	15/180	8	1.5	-1.3	2	0.7	-0.1	10	1.4	1.0	1.5	0.7
Olds [15]	37/104	13/206	27	0.9	0.9	-	-	-	-	-	-	0.5[c]	-0.2
Sharma [27]	38/71	15/144	15	1.4	1.4	-	-	-	-	-	-	1.2[d]	0.1
Yarym-Agaev [28]	40/65	25/125	10	1.8	1.2	-	-	-	-	-	-	0.4[e]	-0.3
Yokoyama [29]	25/50	30/80	5	0.5	0.3	-	-	-	-	-	-	0.3[f]	-0.3
Rigby [30]	25/100	23/93	12	0.2	0.0	-	-	-	-	-	-	0.2[g]	0.2
Gillespie [31]	50/75	14/138	6	0.7	0.1	-	-	-	-	-	-	-	-
Culberson [32]	38	52/249	4	2.5	0.6	-	-	-	-	-	-	2.9	-1.8
Mohammadi [20]	-33/3	34/103	-	-	-	-	-	-	12	-	-	-	-
This work[h]	-20/20	100/150	2	1.9	0.9	0	-	-	8	2.2	2.0	3.6	3.6

[a] (NP=nos. of points, Lw=liquid water.

[b] From Chapoy 5 experimental data above 30°C and 300 bar was not included. The corrected data of Chapoy [25] have been used for the evaluations in the table

[c] From Olds 9 experimental data at 37ºC were considered.

[d] From Sharma 5 experimental data at 28ºC were considered.

[e] From Yarym 5 experimental points at 40ºC were considered.

[f] From Yokohama 2 experimental data at 25ºC were considered.

[g] From Rigby 3 experimental points at 25ºC were considered.

[h] Experimental data at 50 bar was not included, high deviations for GERG-water EoS will be discussed in chapter 7

Table 2 is based on our work done earlier on this subject [22]. In this work the various methods used by the authors were discussed. The various experimental equipments used can in principle be divided as static cell experiment and continuous flow experiments. Most of the published

experimental data are reproduced with good accuracy with both the CPA and the GERG-water EoS. Typically the deviation between the calculated and experimental dew point is less than 1-2°C for both models. None of the models show any general tendency to over- or under predict the water precipitation temperature. Only a few authors report data which covers both stable equilibrium with liquid water, ice and hydrate. In the data sets of Althaus [21], Kosyakov [22] and Folas [22] equilibrium water vapour content have been measured with all these. The data set of Althaus shows very low deviations (<1°C AAD and BIAS) to the models in the whole temperature and pressure range.

The data of Althaus [21] have been evaluated as one of the most consistent datasets available in the literature [22]. In his work continuous flow equipment was used. The experimental equipment and techniques used in this work are similar to the one used by Althaus. The advantage of this equipment is that equilibrium with the most thermodynamic stable phase can be relatively easily obtained and controlled. Many of the experimental works published in the literature does not report the form of the condensed phase. In static experiments with relatively large volumes of water in the cell, there is a high probability that water will be a mixture of liquid, ice and hydrate at experimental conditions.

5 THERMODYNAMIC MODELLING USING THE CPA-EOS

In the modelling part of this work we use an equation of state to predict the water content of gases in equilibrium with liquid water, ice or hydrate. The equation of state chosen is the CPA-EoS (Cubic-Plus-Association equation of state) [35], [36]. This model adequately describes LLE or VLLE of water and hydrocarbon systems [37] including also the solubility of hydrocarbons in the aqueous phase, LLE of glycol and hydrocarbon systems [38], VLE and SLE of water and glycol systems [39][40], VLE and SLE of alcohol and water systems [40], and mixtures with methanol or glycol as hydrate inhibitor [36] [41]. For non-associating compounds the model simply reduces to the classical SRK-EoS. The ice and hydrate phase are modelled similar to described in an earlier publication [22], but with a slightly modified thermodynamic model for the hydrate phase.

The CPA-Eos will be compared to a model developed as part of a GERG project on water dew point, which has been accepted as an ISO-standard [34] during recent years. The GERG-water EoS model has a stated working range from -15 to 5°C and from 5 - 100 bar, with a reported uncertainties in estimated dew points of ±2°C. An extended working range, with unspecified uncertainty, is reported to be from -50 to 40°C and 1 to 300 bar. The range of accepted compositions is reported to cover all sales gases found in Europe (e.g. >40mol% methane, <30mol% CO2, <1.5mol% C6+) We have earlier shown that the CPA-EoS is able to describe equilibrium content of water in natural gas with as good or better accuracy as the GERG-water EoS [22]. At the same time predictions in an even large pressure and temperature range have been shown to be good with the CPA-EoS. An advantage of the proposed model is that it can calculate the water dew point, the frost point and the hydrate point. For calculation of the aqueous dew point in gasses with traces of chemicals (eg. MEG, methanol) it is also well applicable.

There are three types of phase equilibrium that must be modelled to cover the actual temperature and pressure range: vapour–liquid, vapour–ice and vapour–hydrate (comprising two possible hydrate structures relevant for this work). Thus, the full model needs to describe the fugacity of four phases. Some models extrapolate equations of state to also describe the solid (ice, hydrate)–vapour equilibrium in an empirical way, by fitting binary interaction parameters to experimental data. This is the case for the GERG-water model which is extended

to solid phases by using a different function for the energy term and fitting (occasionally temperature dependent) binary interaction parameters.

5.1 Description of the GERG-water EoS

The European gas research group GERG [33] has proposed a model to calculate the water content of natural gas (GERG-water EoS [21]), and this model is now an ISO standard [34]. The GERG-water EoS is a model based on the Peng-Robinson equation of state. It uses a modified alpha function with parameters fitted to vapour pressure of liquid water and ice (different parameters in alpha function above and below 0°C). To reproduce the compositional dependency of water in natural gas, temperature dependent binary interaction parameters are fitted to experimental data. The GERG-water EoS is thus a correlative technique based on experimental data.

The GERG-water EoS model extrapolate equations of state to also describe the solid (ice, hydrate)–vapour equilibrium in an empirical way, by fitting binary interaction coefficients to experimental gas-hydrate and gas-ice data. One of the weaknesses of this technique will be the erroneous prediction of the important effect of gas composition on hydrate stability.

5.2 Thermodynamic modelling be combining the CPA-Eos and an ice/hydrate model

Since solid often forms via liquid water, it is an advantage to be able to compute both the real, stable equilibrium and the meta-stable equilibrium involving sub cooled water. In this work separate ice and hydrate models have been combined with the predictive CPA model (having all binary interaction parameters set to 0); in this way both the stable phase and the meta-stable phases can be calculated. The model will also be fully predictive since no binary interaction coefficients between water and hydrocarbons will be used. The applicability of the model to heavier gases (such as rich gas or unprocessed reservoir fluids) is also easy, since interaction parameters between water and heavy hydrocarbon components (or fractions) do not need to be estimated.

5.2.1 The fugacity of vapour and liquid

The gas and liquid phases are both described using the CPA-EoS in the usual manner. Details about CPA have been determined from pure liquid water by Kontogeorgis et al.[35]. The EoS can also be used to calculate the gas solubility in the liquid phase, which may be of interest in other connections.

In this work a modified alpha function based on the work of Mathias and Copeman [42] has been used to improve the prediction of vapour pressure of sub cooled water. The CPA-EoS used in this work was

$$Z^{CPA} = Z^{SRK-EoS} + Z^{association}$$

$$Z^{SRK} = \frac{V}{V-b} + \frac{a}{RT(V+b)} \qquad \textbf{Eq. 4}$$

$$Z^{association} = -\frac{1}{2}\left(1+\rho\frac{\partial \ln g}{\partial \rho}\right)\sum_i \sum_{A_i} x_i\left(1-X^{A_i}\right)$$

where Z^{CPA} is the compressibility factor calculated from the CPA-EoS. It has contributions from physical interaction ($Z^{SRK\text{-}EoS}$) and hydrogen bonding ($Z^{association}$) between molecules. The equation used for describing the influence of hydrogen bonding is dependent on the radial distribution function (g) and the tendency of association sites on a molecule (A_i) to form

hydrogen bonding (X^{Ai}). The equation is further described by Kontogeorgis et al. [35]. The modified function for the a parameter used in this work is given on a form suggested by Mathias et. al. [42] to more accurately estimate the vapour pressure of meta-stable water at temperatures <0°C.

$$a = a_0\left[1 + C_1\left(1-\sqrt{T_r}\right) + C_2\left(1-\sqrt{T_r}\right)^2 + C_3\left(1-\sqrt{T_r}\right)^3\right]^2 \qquad \textbf{Eq. 5}$$

5.2.2 Fugacity of ice

Using standard thermodynamics we write for the water fugacity in the ice phase at the pressure P of the system where f^s_{w,P_0} is the fugacity of water in the ice phase at the reference pressure P_0 (1 atm) and $V^s_{w_0}$ is the molar volume of ice (obtained by the correlation of Avlonitis [12]).

$$\ln\frac{f^s_w}{f^s_{w,P_0}} = \frac{1}{RT}\int_{P_0}^{P} V^s_w dP \qquad \textbf{Eq. 6}$$

The fugacity of ice at reference conditions is calculated by setting it equal to the vapour pressure of ice as estimated by the Antoine equation

$$f^s_{w,P_0} = P_{sat,ice}(T) = \exp\left(A + B/T\right) \qquad \textbf{Eq. 7}$$

Where the constants A and B are the Antoine coefficients fitted to vapour pressure of ice.

5.2.3 Fugacity of hydrate phase

The fugacity of water in the hydrate phase is estimated according to the following equation:

$$f^H_w = f^{EH}_w \exp\left(\frac{\mu^H_w - \mu^{EH}_w}{RT}\right) \qquad \textbf{Eq. 8}$$

where f^{EH}_w is the fugacity of water in the hypothetical empty hydrate phase, and is given by

$$f^{EH}_w = P^{EH}_w \varphi^{EH}_w \exp\int_{P^{EH}_w}^{P} \frac{V^{EH}_w}{RT} dP \qquad \textbf{Eq. 9}$$

The fugacity coefficient φ^{EH}_w of pure water vapour in equilibrium with the empty hydrate at its equilibrium pressure is set to unity. The vapour pressures of hydrate structures I and II, P^{EH}_W are calculated from the equations proposed by Sloan [43]:

$$\ln P^{EH}_w = A - B/T \qquad \textbf{Eq. 10}$$

The parameters A and B are given by Sloan [43] for structure I and II hydrates. The molar volumes of the empty hydrates V^{EH}_w (I and II) are obtained from the correlations proposed by Avlonitis [12]. The chemical potential of the hydrate phase is obtained from the statistical model

by Van der Waals and Platteeuw [44]. The expression for the chemical potential of the hydrate μ_w^H is:

$$\mu_w^H = \mu_w^{EH} + RT\sum_i v_i \ln\left(1 - \sum_{guest\,m}\Theta_{mi}\right) \qquad \textbf{Eq. 11}$$

where R is the gas constant, v_i the number of type i cavities per water molecule (see Sloan [43]. Finally, the occupancy of cavity m by a component i, Θ_{mi}, is calculated using the multi-component Langmouir equation

$$\Theta_{mi} = \frac{C_{mi} f_m}{1 + \sum_{guest\,k} C_{ki} f_k} \qquad \textbf{Eq. 12}$$

where f_k is the fugacity of component k in the equilibrium vapour phase obtained from an equation of state (CPA-EoS in this work), the summation is over all components and C_{mi} are the Langmuir constants. The Langmuir constants are calculated by the approach suggested by Sloan [43] using the Kiahara parameters (ε, σ, a) for guest molecules. These parameters have been fitted to experimental hydrate equilibrium data from the open literature.

5.3 General comparison of the GERG-water EoS and the CPA-EoS for water dew point estimation

The CPA-EoS has been developed as a general purpose equation of state where thermodynamic of polar components and solutions have been in focus. For the CPA-EoS used in this work all binary interaction coefficients between water and hydrocarbons were set to zero. This makes the model purely predictive.

The GERG-water EoS as developed in the work of Althaus [21] can in principle be used for a great variety of gas composition and in a large temperature and pressure range. ISO-18453 [34] is based on the work of Althaus. The validity range of this ISO is limited to temperature between -15 to 5°C and pressures from 5 to 100 bar. An extended temperature and pressure validity range with reduced accuracy is however stated in the ISO.

A summary of important characteristic differences between the GERG-water EoS and the CPA-EoS is presented in Table 3.

Table 3: Summary of characteristics of the equations of state used in this work

	GERG-water EoS	**CPA-EoS***
Accuracy of predicted dew point and water content prediction	Good in limited composition, temperature and pressure range	Generally good
Number of fitted binary interaction parameters	2 (temperature dependent binary interaction parameters)	0
Estimation of water content in equilibrium with sub cooled liquid, ice or hydrate	No	Yes
Estimation of aqueous dew point	No	Yes

*As presented in this work

6 EXPERIMENTAL EQUIPMENT AND METHODS

In this work, the equilibrium water content of methane and real natural gas has been measured in the temperature range -20 to 20°C and pressures from 50 to 150 bar. The experimental equipment used in this work is similar to the equipment used in our previous publication on experimental data on water content of natural gas [22]. For a detailed discussion about pros and cons of the experimental equipment, the reader is referred to this work.

6.1 Experimental equipment

The experimental equipment used in this work consists of continuous flow equipment as shown in Figure 6. Gas is connected to the rig either directly from gas bottles (synthetic gas) or by connecting a variable volume pressure controlled sample cylinder (real natural gas).

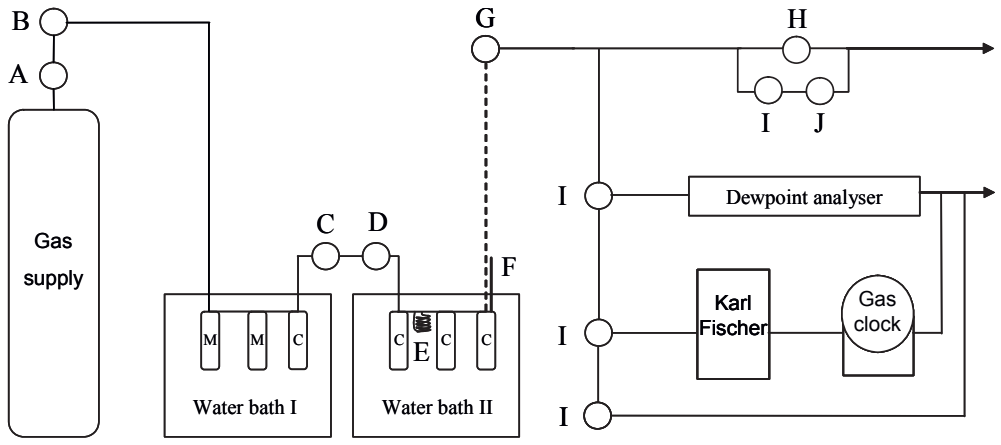

Figure 6: Flow equipment for measurements of water content of natural gas

The gas is saturated when contacted with liquid water between 20-30ºC and high pressure when flowing through a temperature controlled saturator. The saturators and condensers are submerged in Julabo FP-45 baths able to keep the required temperature with a stability of ± 0.01°C, which has been verified by a calibrated reference thermometer. The saturator and condenser baths use a MEG-water solution as cooling and heating medium. The saturator and condenser sections in the baths consists each of three stainless steel cylinders with a volume of about 20 ml. A schematic sketch of the saturators and condensers is given in Figure 7.

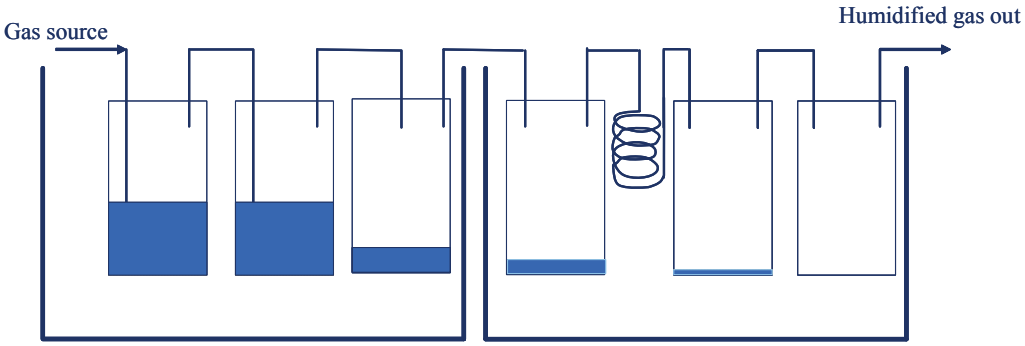

Figure 7: Schematic sketch of the saturators and condensers

The two first cylinders in the saturator bath are filled with water, while the third is initially empty and will work as an entrained droplet collector. In this way a saturated gas free of water droplets are produced in the saturator section of the rig.

Water in the gas is thereafter condensed at a lower temperature but still at high pressure by flowing through piping and cylinders submerged in the condenser baths. To extend the residence time a coil is placed between 2nd and 3rd condenser. Dependent on the composition of the natural gas, temperature and pressure, the water content of the gas from the condenser will be in equilibrium with condensed water, ice or hydrate. The gas flows from the condensation bath via a heated pressure regulator (GO-regulator, HPR-2 Electrical) to the water analysers, after the gas has been depressurized. All piping from the condenser bath to the pressure regulator is heated by a heating cable. The piping from the condensers to the analysers is made of Siltek® tubing (Restek Corporation) to prevent effect of adsorption of water as much as possible. All fittings and seals used in valves and pipe connections are made of stainless steel to prevent effects of adsorption and to ensure that the response time is as fast as possible.

A chilled mirror dew point analyser from Michell Instruments (S4000 Integrale Precision) and a Karl Fischer (KF) coulometric titrator from Metrohm (831 KF Coulometer) are used to measure the water content in the gas from the condenser. The titration routines followed the recommendations given in ISO-10101 [45]. A gas-clock (Ritter TG1 2-120 l/h) connected to the KF titrator measures the total volume of gas of each measured sample.

The experimental equipment, prior to the GO-regulator, can be used up to 200 bar absolute pressure. The maximum dew point temperature is limited by the ambient room temperature. The absolute pressure of the system is measured by a pressure transducer (Keller) with an uncertainty of 0.05 bar. The work presented in this paper is based on an earlier publication covering the same subject [22].

6.2 Gas composition and experimental procedures used

Experiments were done with methane and real natural gas. The temperature range used was from -20 to 20°C and the pressure range was from 50 to 150 bar. For each measurement, the temperature of the condenser is set to control the dew point temperature of the gas. The temperature of the saturator is set 10°C higher than the condenser, but a minimum temperature of 20°C was used to prevent hydrate formation in the saturator section. The

pressure drop through the saturator and condenser sections is very low, and saturation and condensation are in principle done at the same pressure.

The experimental procedure is initiated by filling two of the saturators with water. The third saturator cylinder is emptied. The three condensers are emptied. The temperature of the condenser bath is set to a value automatically controlled by the Julabo bath. The rig is pressurised with gas followed by gas circulation for a limited time. By letting the gas circulate some droplets of water will condense in the saturators. Equilibrium between condensed water, ice or hydrate is obtained by having un-circulated gas in the rig for several hours. For experiments where hydrate formation is expected the gas is kept in the rig for minimum 15 hours without circulation. The pressure in the saturator and condenser did not vary more than ±0.5 bar during an experiment. The experimental values reported in this work are the average of minimum three sample replicates. Samples were taken until the maximum and minimum value did not differ by more than 5 % for three following samples.

If possible, water analysis by the Karl Fischer titrator and the Michell mirror were done simultaneously. Typically one experimental point could be measured per day. The accuracy of the water analysis techniques was verified by using a BOC [46] certified reference gas. The measurement uncertainty of the analysis done in this work is within 10%.

6.3 Chromatographic Gas Analysis

In the natural gas experiments, 1000 ml sample cylinders with 120 bar back pressure are used. The sample cylinder containing high pressure natural gas is heated to 100°C to ensure that only the gas phase is present in the cylinder. Without pre-heating the gas may get into the two-phase area due to cooling when the pressure is reduced. The pressure is reduced through a pressure reduction valve (GO-regulator) installed in a gas injection board directing the gas sample to the injection loop in the gas chromatograph (GC). Both the reduction valve and the tubing are heated to 90°C to prevent condensation of the sample in the injection system. All sample lines are made of Siltek® tubing. The GC used for natural gas analysis is a Hewlett Packard 6890. This GC is equipped with two main channels. One of the channels has a CP-PoraPlot Q-HT column (25 m x 0.32 mm, 10 µm film thickness) for the separation of carbon dioxide, ethane, propane, butanes and pentanes and a CP-Molsieve 5A column (10 m x 0.32 mm, 30 µm film thickness) for the separation of oxygen, nitrogen and methane. A thermal conductivity detector (TCD) is used for this channel. A flame ionization detector (FID) detects the separated hydrocarbons (butanes and higher) from the second channel, separated on an HP PONA column (50 m x 0.20 mm, 0.5 µm film thickness). The loop injection (250 µl for each channel, made of Siltek® tubing) and isolation of the Molsieve channel during carbon dioxide and ethane elution is arranged by two six-port and one ten-port valves from Vici Valco. The valves are located within a heating block on the top of the GC and controlled within the GC software (Chemstation from Agilent Technology).

The method used and the uncertainty in the quantification of the compounds is according to GPA 2286-95 [47] and ASTM D 5131-92 [48].

7 RESULTS AND DISCUSSIONS

The experimental data presented in this paper will be compared to other data sets from open literature where water content of natural gas has been measured. The data sets for methane-water measured by Althaus [21] are known to be consistent and of high reliability [22]. Hence, the data for methane-water of this work will be compared to these data. The thermodynamic models presented in this work, the GERG-water EoS and the CPA-EoS, are compared to the experimental data from this work. The ability to extrapolate calculations from the GERG-water

EoS to pressures higher than 100 bar is tested by comparison to natural gas data obtained at 150 bar total pressure.

7.1 Results and evaluation of the experimental data presented in this work

7.1.1 Results from the methane-water experiments

The methane gas bottles used in the experiments were prepared by Yara Industrial Norway. The purity of methane used in this work was 99.999 %. Both Karl Fischer titration and Michell dew point analyser were used to determine the water content. The measurements have been performed at -20, -10, 0, 10 and 20ºC and at three pressure levels; 50, 100 and 150 bar. The experimental results are presented in Table 4 and Figure 8 to Figure 10. In Table 4, the water content as measured with the Karl Fischer titration technique is reported. In Figure 8 and Figure 9 both Karl Fischer and Michell dew point analyser results are shown.

Experiments with low water content (low temperature and high pressure) generally had poorer repeatability between replicates than experiments with high water content. Due to low water content at -20ºC, the measured water content showed repeatability within 7%.

The water content measurements for methane at 50 bar showed repeatability within 10%. This is considered to be too high and the methane experiments at 50 bar will therefore be repeated. A probable reason for the high relative standard deviation (RSD) at 50 bar was that the experimental procedure used for these experiments involved a shorter time for obtaining thermodynamic equilibrium in the system (5 hours – versus 15-20 hours for the 100 and 150 bar experiments).

Table 4: Gas phase water content ppm(mole) for the binary system water – methane

T/ºC	50 bar	100 bar	150 bar
-20	31	19	19
-10	73	40	35
0	172	80	82
10	273	168	151
20	483	320	297

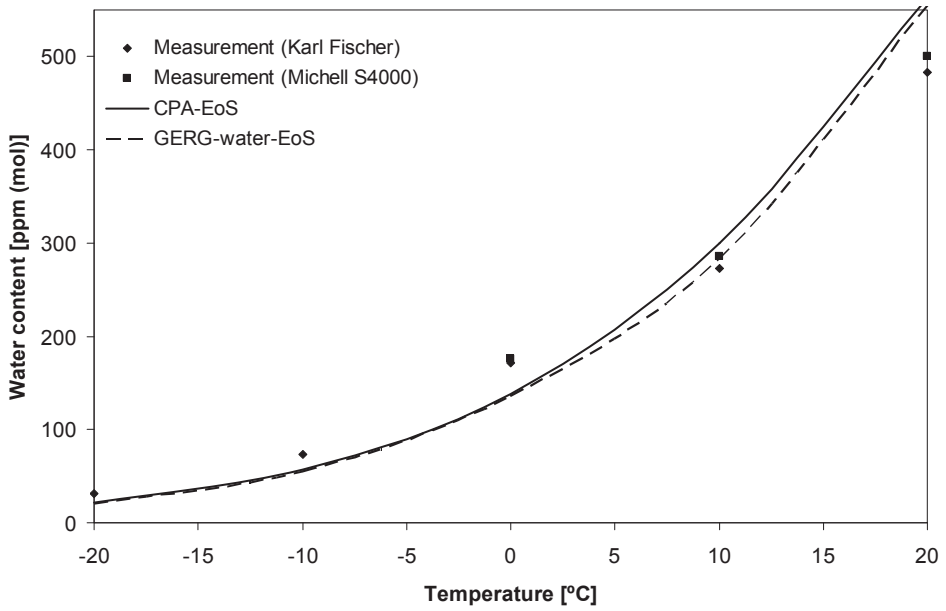

Figure 8: Gas phase water content ppm(mole) for the binary system water – methane at 50 bar

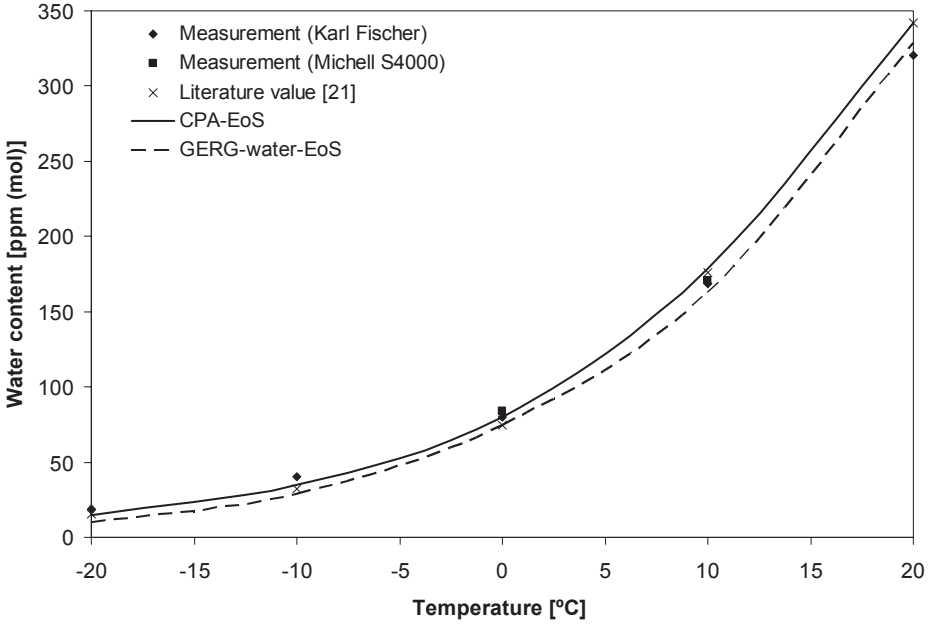

Figure 9: Gas phase water content ppm(mole) for the binary system water – methane at 100 bar

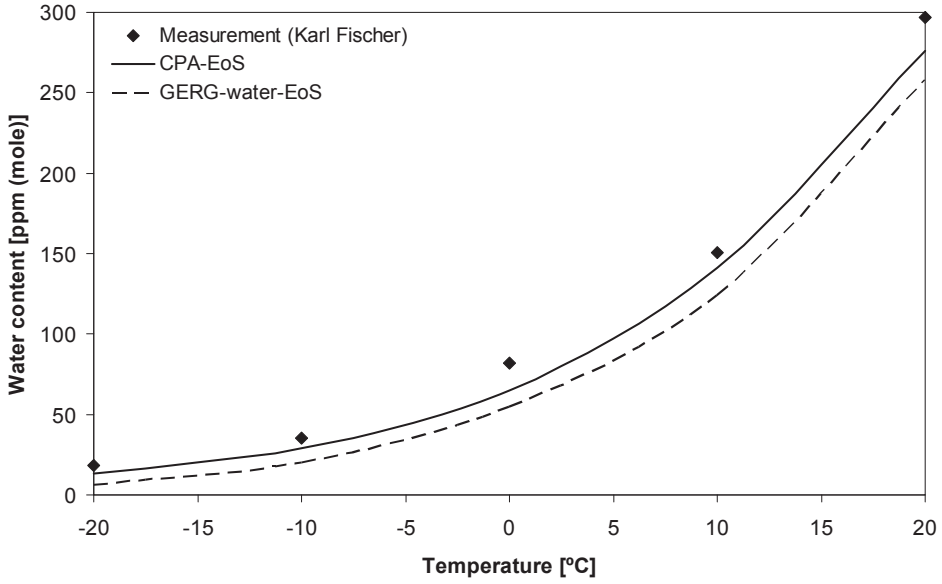

Figure 10: Gas phase water content ppm(mole) for the binary system water – methane at 150 bar

In Figure 8 to Figure 10 the experimental data are compared to predictions with the GERG-water EoS and the CPA-EoS. It should be noted that the results of the CPA-EoS model always show the water content in equilibrium with what is estimated by the model to be the most stable precipitated phase (liquid water, ice or hydrate). As seen from the figures there is good agreement between calculated and experimental data. In Figure 9 the experimental data at 100 bar from this work is compared to the experimental data reported by Althaus [21]. A good mach between the two data sets is obtained. At 50 and 100 bar the CPA and GERG-water models seem to under estimate the water content slightly for temperatures below 0ºC and slightly over estimate at temperatures above 0ºC. At 150 bar the models seem to under estimate in the entire temperature range. At 50 and 100 bar the models seems to have approximately the same deviations to the experimental data, while at 150 bar the CPA-EoS seems to be more accurate. The comparison of CPA and GERG-water to experimental data will be further discussed in chapter 7.1.2.

7.1.2 Measured water content in the natural gas

The natural gas was delivered in 1000 ml piston cylinders with 120 bar pressure. The gas composition was analysed by gas chromatography following the procedures explained in Chapter 6.3. The gas composition is given in Table 5. The molecular mass and density, Table 6, of the fractions/pseudo components (PC) can be calculated based on knowledge or estimation of molecular mass and density of individual components up to C13.

$$M_{PC} = \sum_{fraction} x_i M_i \qquad \textbf{Eq. 13}$$

$$\rho_{PC} = \frac{\sum_{fraction} x_i M_i}{\sum_{fraction} \frac{x_i M_i}{\rho_i}} \qquad \textbf{Eq. 14}$$

where x_i is the mole fraction, M_i is the molecular mass and ρ_i is the density of component i in liquid form at atmospheric pressure and 15ºC.

The calculated molecular mass and density of the pseudo components C7-C13 are given in Table 5. For calculations with the CPA-EoS, necessary critical properties of pseudo components are calculated based on molecular mass and density of fractions using the characterization methods suggested by Pedersen et al. [49]. All components in the GERG-water EoS heavier than C7 are modelled as n-heptane.

The hydrocarbon phase envelope for the natural gas is given in Figure 13. The uncertainties related to prediction of phase envelope from GC analysis are discussed by Rusten et al [50]. The cricondenbar pressure is estimated to be around 100 bar and -10ºC. At pressures lower than 100 bar hydrocarbon condensation might occur in the condenser. Hence the minimum pressure used in these experiments was 100 bar. Some condensation of the natural gas can occur during filling of the rig (when going from atmospheric pressure to test pressure), but this condensate will generally be re-evaporated when the rig has reached its final pressure. The cricondentherm is estimated to be at about 25°C. This phase behaviour is typical for a rich natural gas being transported in the dense phase region in rich gas pipelines on the Norwegian continental shelf.

Table 5: Natural gas composition based on detailed gas composition

Component	GC [mol%]
Nitrogen	0.6032
Carbondioxide	2.6094
Methane	80.1380
Ethane	9.4689
Propane	4.6227
i-Butane	0.6420
n-Butane	1.1427
2,2-dimethylpropane	0.0136
i-Pentane	0.2349
n-Pentane	0.2272
Cyclopentane	0.0121
2,2-dimethylbutane	0.0031
2,3-dimethylbutane	0.0068
2-methylbutanepentane	0.0416
3-methylpentane	0.0216
n-Hexane	0.0535
C7	0.1056
C8	0.0441
C9	0.0074
C10	0.0016
C11	0.00011
C12	0.00004
C13	0.00004
Sum	100

Table 6: Estimated molar mass and density of the heavy fractions based on detailed gas composition

Component	MW [kg/mol]	Liq. Dens. [kg/m3]
C7	89.1	0.75
C8	101.4	0.77
C9	116.2	0.80
C10	134.0	0,80
C11	147.0	0,81
C12	161.0	0,82
C13	175.0	0,83

Natural gas-water experiments have been performed at -20, -10, 0, 10 and 20ºC. Two pressure ranges have been used; 100 and 150 bar. The experimental results are presented in Table 7, Figure 11 and Figure 12. Experiments with low water content (low temperature and high pressure) generally had poorer repeatability than experiments with high water content. Due to low water content at -20ºC, the measured water content showed repeatability within 7%.

Table 7: Gas phase water content ppm(mole) for natural gas

T/ºC	100 bar	150 bar
-20	22	19
-10	41	37
0	86	72
10	178	150
20	341	291

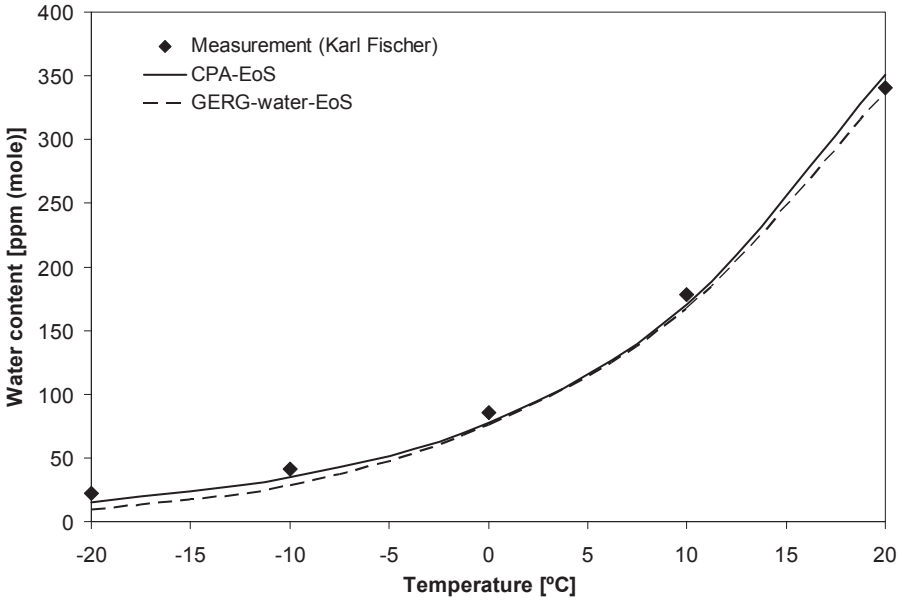

Figure 11: Gas phase water content ppm(mole) in natural gas at 100 bar

As seen from Figure 11 and Figure 12 there is good agreement between calculated and experimental data. At 100 bar the CPA-EoS and GERG-water models seem to slightly under estimate the water content. The measured data are spot on CPA-EoS at 150 bar, while the GERG-water EoS seems to under estimate the water content slightly. The comparison of CPA and GERG-water to experimental data will be further discussed in chapter 7.1.2.

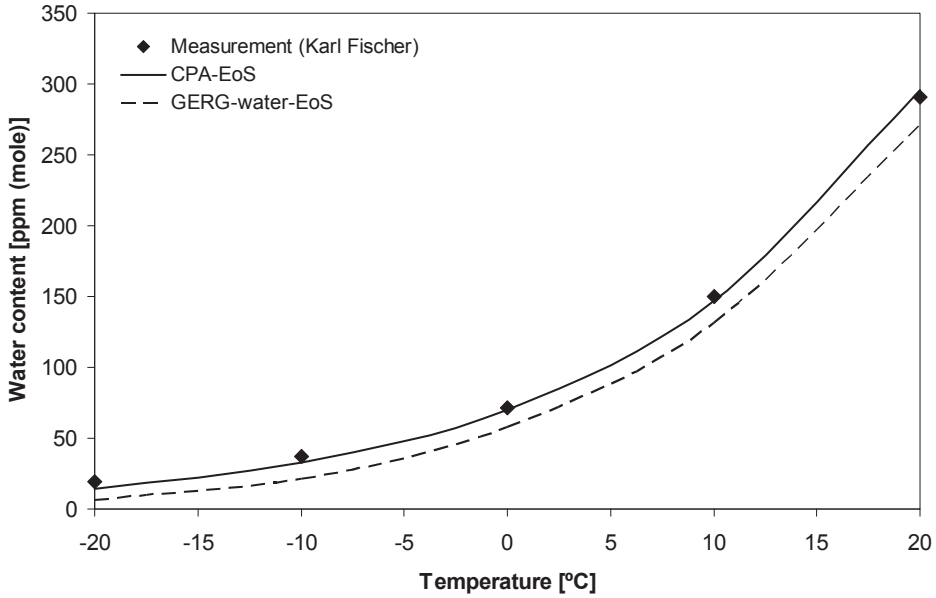

Figure 12: Gas phase water content ppm(mole) in natural gas at 150 bar

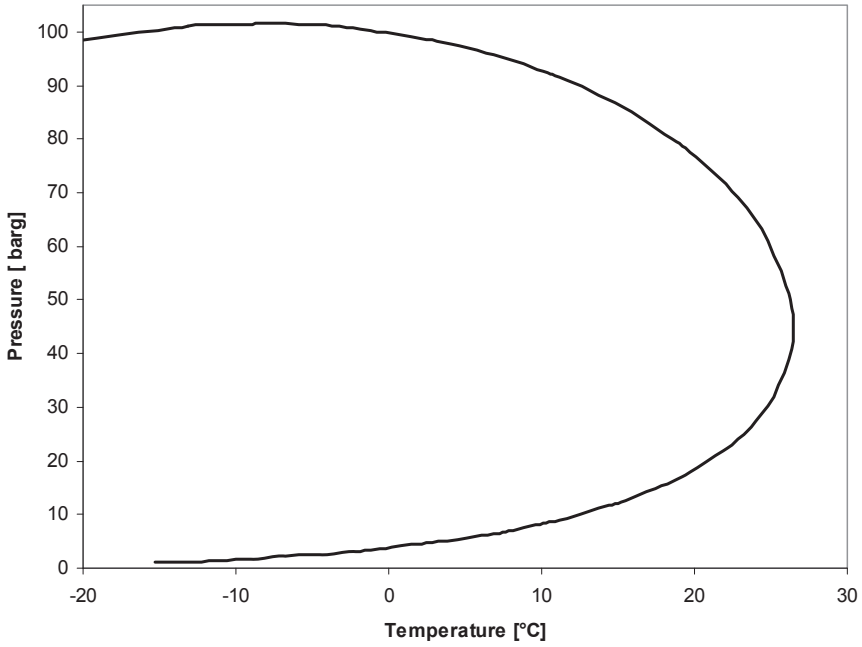

Figure 13: Phase envelope for natural gas used in this work

7.2 Comparison of CPA-EoS and GERG-water EoS to experimental data

As can be seen from Figure 9 both the GERG-water and CPA-EoS estimate water content in methane close to the experimental data at 100 bar in pure methane. The GERG-water model matches these data with good and similar accuracy as the CPA-EoS. Much of the experimental basis of the GERG-water EoS is concentrated in this pressure and temperature range and we would also expect this model to be accurate compared to these data. In Figure 14 the methane-water experimental data has been compared to calculations with the CPA-EoS where also the meta-stable phases have been plotted. As can be seen from the figure the experimental data matches best with the water content in equilibrium with the phase predicted to the stable phase (in this case hydrate for all points lower than about 13°C). This will also be the situation when comparing to the experimental data for methane at 150 bar and for the natural gas data. This is illustrated in Figure 15 where experimental data for natural gas at 150 bar are compared to predicted water content above stable and meta stable phases. This also indicates that the experimental data presented in this work reports water content in equilibrium with the thermodynamic most stable phase at give temperature and pressure.

From Figure 12 we can see that relatively large deviations between experimental data and the GERG-water model are observed at 150 bar, which is outside the defined pressure range for the model. Predictions with the CPA-EoS are very good also at this pressure. This illustrates that the accuracy of the CPA-EoS often seems to be better for an extended composition, temperature and pressure range.

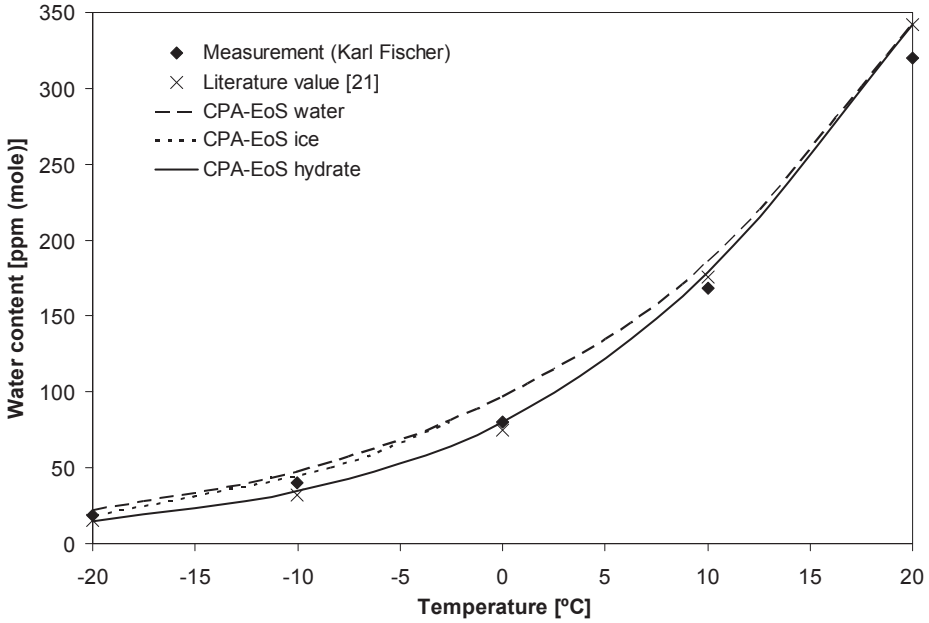

Figure 14: Comparison of experimental data for methane-water at 100 bar to stable and meta-stable phases predicted with the CPA-EoS

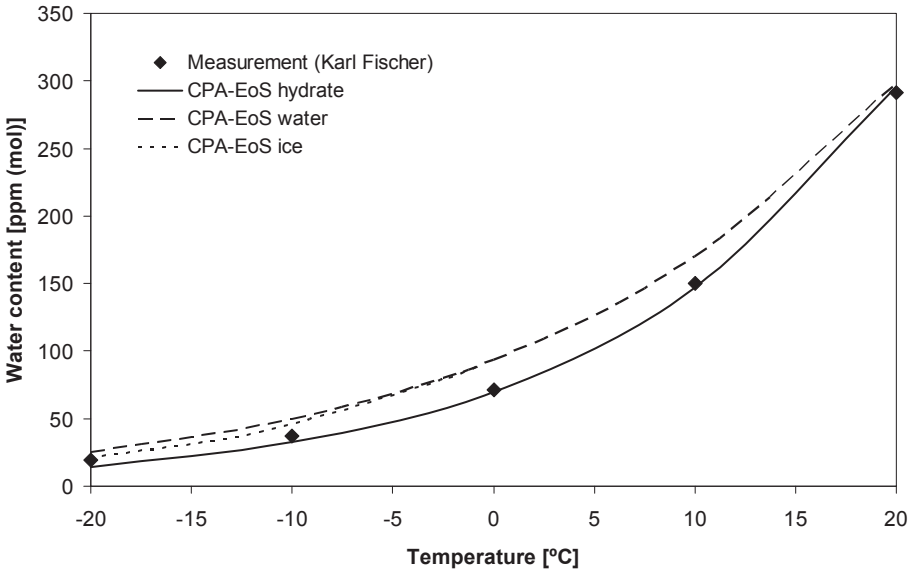

Figure 15: Comparison of experimental data for natural gas - water at 150 bar to stable and meta-stable phases predicted with the CPA-EoS

Table 2 and Table 8 show ADD and BIAS for the comparison of calculated water precipitation values and experimental data for methane–water and natural gas–water, respectively. GERG-

water EoS is applicable in the temperature range -15 to 5ºC and pressure up to 100 bar. In the temperature range -10 to -20ºC the GERG-water EoS showed a large deviation from both experimental results and values obtained from the CPA-EoS. For temperatures above 0ºC the deviation is small.

Table 8: Summary of experimental data for equilibrium water vapour concentration in natural gas. Comparison to calculations with the CPA-EoS and the GERG-water EoS

Reference	T [ºC]	P [bar]	CPA-EoS Liquid water			CPA-EoS Ice			CPA-EoS Hydrate			GERG-water EoS	
	min/max	min/max	NP Lw	AAD [ºC]	BIAS [ºC]	NP Ice	AAD [ºC]	BIAS [ºC]	NP Hydrate	AAD [ºC]	BIAS [ºC]	AAD ºC]	BIAS [ºC]
This work[h]	-20/20	100/150	0	-	-	0	-	-	10	1.5	1.3	6.5	6.5

[a] NP=nos. of points, Lw=liquid water.

Despite being tailor-made for water in gas, the GERG-water EoS does not give any improvement over the CPA model for the data evaluated in this work. The CPA-EoS can be used at higher pressures and temperatures and will also show which precipitated phase is thermodynamically most stable. Natural gas hydrate is often known to be formed from meta-stable liquid water. It is an advantage of the CPA-EoS that it can estimate meta-stable liquid water formation.

7.3 Comparison of the experimental data to empirical correlation and chart based methods

Chart based methods and empirical correlations were discussed in chapter 4.1. In Figure 16 the experimental data from this work are compared to values from the chart published by McKetta and Wehe [14] and to the empirical model of Bukacek [17]. As can be seen the CPA-EoS model used in this work is superior to these models. The water content in the natural gas, estimated by the chart and empirical models, are generally too high. The reason for this is probably that these methods are developed only to estimate the water content in equilibrium with meta-stable liquid water. In Figure 16, most of the readings from the chart of McKetta are done in a region marked as meta-stable equilibrium.

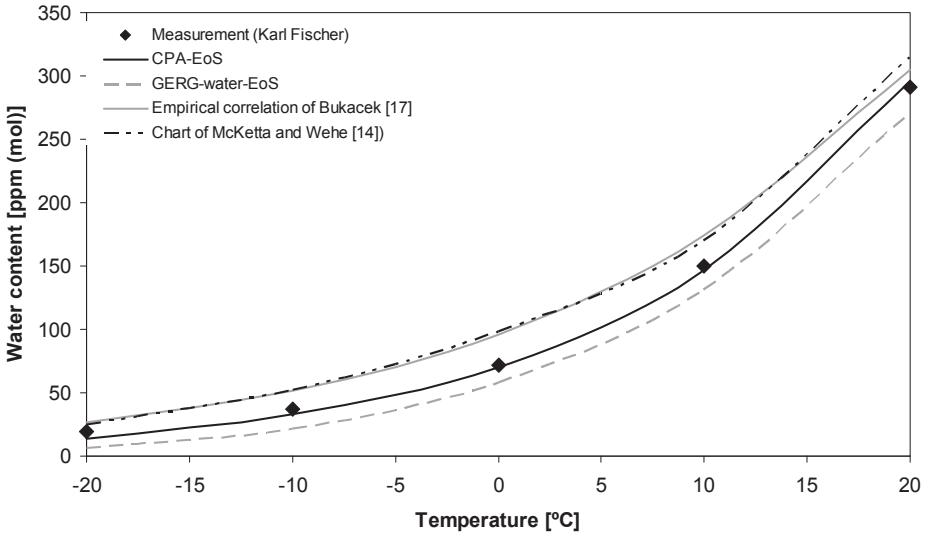

Figure 16: Experimental data of water content in natural gas at 150 bar compared to estimates from the empirical correlation of Bukacek [17] and the chart based method of McKetta and Wehe [14]

7.4 Evaluation of model and data to plant operation data

As illustrated in Figure 16, relatively large errors can be expected when using existing empirical correlations and charts for estimating water content of natural gas in certain pressure and temperature ranges. The largest errors can be expected in regions where the estimated water content of the gas is indicated by the chart to be in equilibrium with the meta-stable phases. In Figure 17 we have the CPA-EoS model described in this work to make a chart for the water content of a natural gas with a composition as given in Table 5. The composition used for making the chart is representative for a sweet natural gas, and the chart can be used also for estimating water content of other sweet gases.

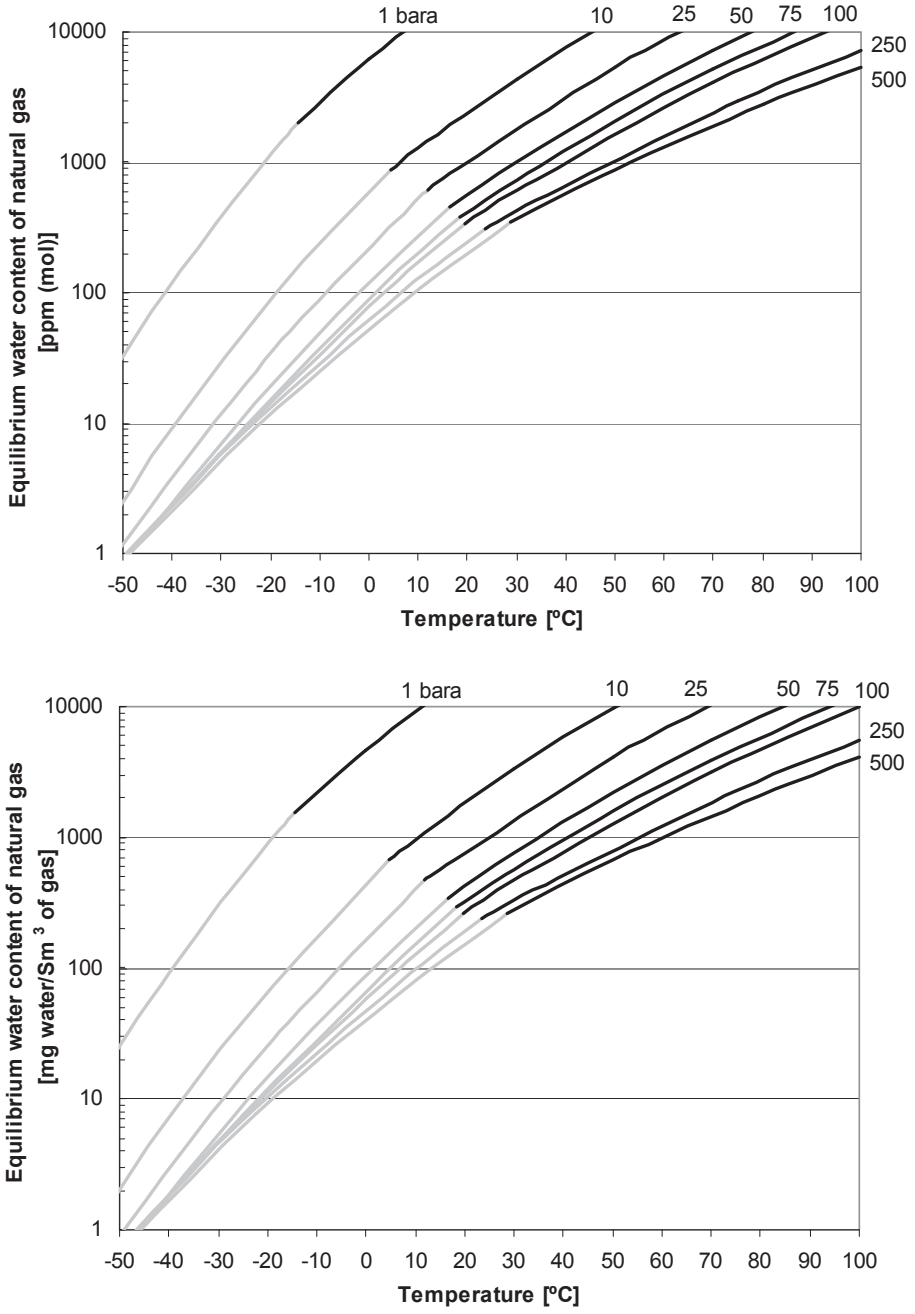

Figure 17: Generalized charts for water content of sweet natural gas. Stable equilibrium with liquid water is plotted with black Lines. Stable equilibrium with natural gas hydrate is plotted with grey lines.

As was explained in chapter 2 and 3 the aqueous dew point of natural gas is important for a number of situations. A typical situation is when the gas has been contacted with TEG for water removal and control of the water dew point. The gas is at its aqueous dew point at glycol absorber conditions. Few experimental studies have been published measuring the solubility of TEG in natural gas have been done. To our knowledge, the only reported TEG solubility data in high pressure gas in the open literature have recently been published by Jerinić et al. [51]. The CPA-model can be used to generate a chart for the aqueous dew point of water and TEG in natural gas. The aqueous dew point plot in Chapter 2 (Figure 7) was made based on predictions with the CPA-EoS model. Further work is being planned by GERG [33] to develop more knowledge, both experimentally and theoretically, regarding the aqueous dew point of natural gas.

8 SUMMARY AND CONCLUSIONS

New data for the equilibrium water content in methane and a natural gas have been presented in the temperature range -20 to 20ºC and pressures up to 150 bar. The experimental data is presented as the water content in equilibrium with the most stable phase (water, ice or hydrate) at the experimental temperature and pressure.

A review of published methods (graphical-, empirical- and thermodynamic models) for the calculation of equilibrium water content in natural gas has been presented. The model used in this work is based on the Cubic Plus Association Equation of State (CPA-EoS) combined with thermodynamic models for the ice and gas hydrate phase. This model is shown to give excellent results, both for the calculation of equilibrium water content of natural gas, water dew point-, natural gas hydrate- and ice precipitation temperature as well as the aqueous dew points. The model is compared to the ISO 18453 developed for water dew point calculation of natural gas, and shown to be superior when it comes to extrapolation of pressure, temperature and gas composition. An accurate chart for graphical reading of water content of a sweet natural gas is presented.

This work presents and discusses experiences from selected StatoilHydro and Gassco operated plants where condensation of water, ice formation or hydrate formation has created operational disturbances in the gas processing plants. The experience from these situations is compared to the results from the experimental and modelling work.

The methods and data presented in this paper can be used in design of water removal processes.

9 ACKNOWLEDGEMENTS

The authors are thankful to Gassco and StatoilHydro for financial support and for letting us publish this work.

REFERENCE LIST

[1] Home page on web: http://twisterbv.com/
[2] Knight, H.S., Weiss, F.T., Analytical Chemistry, 34 (1962) 749-751.
[3] Funke, H.H., et al., of Scientific Instruments, 74 (2003) 3909-3933.
[4] McAndrew, J.J., D. Boucheron, Solid State Technology, 35 (1992) 52-60.
[5] Wiederhold, P.R., Water Vapor Measurement. 1997, New York: Marcel Dekker.
[6] Mychajliw, B.J., International School of Hydrocarbon Measurement. 2002. Oklahoma City.
[7] Mehrhoff, T.K., Rev. Sci. Instrum., 56(1985) 1930-1933.
[8] Løkken, T.V., Water vapour determination - Assessment of equipment and measurements in the presence of methanol and glycols, IFEA On-Line Analyse, Conference presentation April 2006.
[9] Water Vapor Content of Gaseous Fuels be Measurement of Dew Point Temperature, American National Standard, ASTM D 1142-95
[10] Nordstad, K., Gjertsen, L.H., A New Approach to the Use of Glycol in Low Temperature, High-Pressure Gas Processing Applications, GPA annual conference 1999
[11] CBP 2005-001-01 Gas Quality Harmonisation, Web page: http://www.easee-gas.org/
[12] Avlonitis, V., Chem. Eng. Sci. 49 (1994) 1161–1173.
[13] McCarthy, E.L., Boyd, W.L., Reid, L.S., AIME, 189 (1950)
[14] McKetta, J.J, Wehe, A.H., Petroleum Refiner 37 (1958) 153-154
[15] Olds, R.H., Sage, B.H., Lacey, W.N., Ind. Eng. Chem., 34 (1942)
[16] Skinner, W., M.S. Thesis in Chem. Eng., U. of Uklahoma, 1948
[17] Bukacec, R.F., Equilibrium moisture content of natural gases, Institute of gas technology, Research bulletin 8 (1955)
[18] Kosyakov, H.E., Ivchenko, B.I., Krishtopa, P.P. Vopr.Khim.Khim.Tekhnol.47 (1982) 33-36.
[19] Sloan, E.D., Khoury, F.M., Kobayashi, R., Ind. Eng. Chem.Fundam, 15 (1976), 318-323
[20] Mohammadi, A.M., Richon, D., AIChe Journal, 53 (2007), 1601-1607
[21] Althaus, K. Fortschritt-berichte VDI, Reihe 3, nr 590, 1999.
[22] Folas, G.K., Froyna, E.W., Lovland, J., Kontogeorgis, G.M., Solbraa, E., Fluid Phase Equilibr. 252 (2007) 162–174.
[23] Aoyagi, K., Song, K.Y., Kobayashi, R., Sloan, E.D., Dharmawardhana, P.B., GPA RR-45, Tulsa, Okla (1980).
[24] Chapoy, A., Coquelet, C., Richon, D., Fluid Phase Equilib. 214 (2003) 101-117.
[25] Chapoy, A., Coquelet, C., Richon, D., Fluid Phase Equilbri., 230 (2005) 210-214
[26] Bogoya, D., Müller, C., Oellrich, L.R., Wiss.Abschlussber. 28. Internat. Seminar Univ. Karlsruhe (1993) 54-63.
[27] Sharma, S.C. PhD-thesis, University of Oklahoma, Norman, OK (1969).
[28] Yarym-Agaev, N.L., Sinyavskaya, R.P., Koliushko, I.I., Levinton, L.Ya., J. Appl. Chem. USSR 58 (1985)154-157.
[29] Yokoyama, C., Wakana, S., Kaminishi, G., Takahashi, S., J.Chem.Eng.Data 33 (1988) 274-276.
[30] Rigby, M., Prausnitz, J.M., J.Phys.Chem. 72 (1968) 330-334.
[31] Gillespie, P.C., Wilson, G.M., GPA RR-48, Tulsa, OK (1982).
[32] Culberson, O.L., McKetta Jr, J.J., Petr.Trans.AIME 192 (1951) 297-300.
[33] GERG – The European Gas Research Group. http://www.gerg.info/
[34] ISO 18453:2004, Natural gas - Correlation between water content and water dew point

[35] Kontogeorgis, G.M., Voutsas, E.C., Yakoumis, I.V., Tassios, D.P., Ind. Eng. Chem. Res. 35 (1996) 4310–4318.
[36] Kontogeorgis, G.M., Yakoumis, I.V., Meijer, H., Hendriks, E.M., Moorwood, T., Fluid Phase Equilibr. 158–160 (1999) 201–209.
[37] Folas, G.K., Michelsen, M.L., Kontogeorgis, G.M., Stenby, E.H., Ind. Eng. Chem. Res. 45 (2006) 1527–1538.
[38] Derawi, S.O., Michelsen, M.L., Kontogeorgis, G.M., Stenby, E.H., Fluid Phase Equilibr. 209 (2003) 163–184.
[39] Derawi, S.O., Kontogeorgis, G.M., Michelsen, M.L., Stenby, E.H., Ind. Eng. Chem. Res. 42 (2003) 1470–1477.
[40] Folas, G.K., Gabrielsen, J., Michelsen, M.L., Stenby, E.H., Kontogeorgis, G.M. Ind. Eng. Chem. Res. 44 (2005) 3823–3833.
[41] Folas, G.K., Kontogeorgis, G.M., Michelsen, M.L., Stenby, E.H., Fluid Phase Equilibr. 249 (2006) 67–74.
[42] Mathias, P.M., Copeman, T. , Fluid Phase Equilib. 13 (1983) 91–108.
[43] Sloan, E.D., Clathrate Hydrates of Natural Gases, Second Edition, 1998
[44] Van der Waals, J.H., Platteeuw, J.C., Adv. Chem. Phys. 2 (1959) 1–57.
[45] ISO 10101, Natural Gas – Determination of water by the Karl – Fischer method
[46] BOC, web page: http://www.boc-gases.com/
[47] GPA 2286-95 – "Extended Analysis for Natural Gas and Similar Gaseous Mixtures"
[48] ASTM D 5134-92 – "Detailed Analysis of Petroleum Naphta through n-Nonane by Capillary GC"
[49] Pedersen, K.S., Blilie, A.L., Meisingset, K.K., I&EC Research, 31 (1992), 1378-1384
[50] Rusten, B.H., Gjertsen, L.H., Solbraa, E., Kirkerød, T., Haugum, T., Puntervol, S. GPA conference (2008) Texas.
[51] Jerinić, D., Schmidt, J., Fischer, K., Friedel, L., *Fluid Phase Equilibria, 264 (2008), 253-258*
[52] Sloan, E.D., Khoury, F.M., Kobayashi, R., Ind. Eng. Chem.Fundam, 15 (1976), 318-323

SYMBOLS AND ABBREVIATIONS

f_w^s	Fugacity of water in ice phase
$V_{w_0}^s$	Molar volume of ice
f_w^H	Fugacity of water in hydrate phase
f_w^{EH}	Fugacity of water in hypo theoretical empty hydrate phase
μ_w^H	Chemical potential of hydrate
μ_w^{EH}	Chemical potential of empty hydrate
φ_w^{EH}	Fugacity coefficient of pure water vapour in equilibrium with the empty hydrate
P_W^{EH}	Vapour pressures of hydrate structures
V_w^{EH}	Molar volume of empty hydrate
$V_{w_0}^s$	Molar volume of ice
$P_{sat,ice}$	Vapour pressure of ice
P_W^{EH}	Vapour pressure of hydrate structures
v_i	Number of type i cavities per water molecule
Θ_{mi}	Occupancy of cavity m by a component i
f_k	Fugacity of component k
ρ	Molecular density
ρ_i	Density for component i
A	Constant proportional to the vapour pressure of water
a	Attractive parameter in SRK
AAD	Absolute average deviation
ASTM	American Society for Testing and Materials
B	Constant depending on temperature and gas composition
b	Co-volume in SRK
C	Mathias Copeman parameter
C_{ki}	Langmuir constant
C_{mi}	Langmuir constant
CPA	Cubic Plus Association
EASEE	European Association for the Streamlining of Energy Exchange
EoS	Equation of State
Eq	Equation
FID	Flame ionization detector
g	Radial distribution function
GC	Gas chromatograph
GERG	The European Gas Research Group
HPHR	High pressure, high temperature
ISO	International Organization for Standardization
KF	Karl Ficsher
LNG	Liquefied natural gas
MEG	Monoethylene glycol
M_i	Molecular mas of component i

M_{PC}	Molecular mas of pseudo components
NG	Natural gas
NP	Number of points
P	Total pressure
P_0	Reference pressure
R	Gas constant
RSD	Relative standard deviation
SRK	Soave Redlich Kwong
T	Temperature
TCD	Thermal conductivity detector
T_{dew}	Dew point temperature
TEG	Triethylene glycol
VLE	Vapour-liquid equilibrium
VLLE	Vapour-liquid-liquid equilibrium
VLS	Vapour-liquid-solid
W	Water content
X	Mole fraction not forming hydrogen bonding
x_i	Mole fraction
Z	Compressibility factor

LIST OF TABLES

LIST OF FIGURES